Aquaglyceroporine aus *Trypanosoma brucei* ein potentielles chemotherapeutisches Target: Klonierung, heterologe Expression, biochemische Charakterisierung und Lokalisierung

Aquaglyceroporins of *Trypanosoma brucei* a potential target for chemotherapy: Cloning, heterologous expression, biochemical characterization and localization

DISSERTATION

der Fakultät für Chemie und Pharmazie
der Eberhard-Karls-Universität Tübingen

zur Erlangung des Grades eines Doktors
der Naturwissenschaften

2006

vorgelegt von
Néstor Luis Uzcátegui Araujo

Tag der mündlichen Prüfung:	27 Juli 2006
Dekan:	Prof. Dr. S. Laufer
1. Berichterstatter:	Prof. Dr. M. Duszenko
2. Berichterstatter:	Prof. Dr. D. Mecke

Acknowledgement

This work was carried out at the Interfakultäres Institut für Biochemie at Eberhard-Karls University of Tübingen under the direction of Prof. Dr. M. Duszenko.

I would like to thank the Deutscher Akademischer Austausch Dienst (DAAD) and the Consejo de Desarrollo Científico y Humanístico de la Universidad Central de Venezuela (CDCH-UCV) for granting Fellowships for the German language and funding for the Ph.D., respectively.

I would like to thank my supervisor, Prof. Dr. M. Duszenko, for providing all his support throughout this work as well as for his suggestions and discussions.

I am grateful to Professors: G. Dodt, F. Lang, D. Mecke and E. Beitz, for kindly accepting to serve on the evaluation committee.

Many thanks to Prof. Rita Mukhopadhyay for her suggestions concerning the “results” and “discussion” sections of my thesis and, once again to Prof. D Mecke, for correction of the final version of the thesis.

I thank my wife, Katherine, for her invaluable and timely suggestions and unconditional support, not only in my Ph.D. but also during our lives together. Most importantly of all, thank you for making my life special…

I am indebted to Prof. D. Simarro for his friendship, his constant encouragement and for his fundamental support in each phase of my academic life. I would also like to thank my friend, Prof R. Cordero, for his concern and his constant help.

I wish to thank those who somehow contributed to this thesis including Alexandra Thor and Caroline Schönfeld for their help with Trypanosoma cultures, Björn Bassarak and Rudolf Koopmann for their computer support, Martin Schmidt for transmission electron microscopy images, Prof. Bardele for scanning electron microscopy images and Professor F. Land and E. Beitz along with their co-workers for their support with *Xenopus* oocytes experiments.

I would like to say a big 'thank-you' to all the members of Prof. Duszenko´s lab for their help and for the good times. Each of you, particularly with your different cultures, made the time in the lab very interesting and enjoyable.

I am grateful to all my family for their continuous help and an invaluable moral support during my stay in Germany and, of course, during my whole life.

Table of Contents

Abbreviations

AQP	Aquaporin
BSA	Bovine serum albumin
CGA	Citrate glucose anticoagulant
CNS	Central nervous system
DCFH-DA	Dichlorofluorescin diacetate
DHA	Dihydroxyacetone
DMSO	Dimethylsulfoxid
DTT	1,4-Dithiothreitol
EDTA	Ethylendiamin-tetraacetat-dinatriumsalzdihydrate
EGTA	Ethylenglycol-bis(2-aminoethylether)-N,N,N',N'-tetraacetate
FACS	Fluorescent activated cell sorting
FRD	Fumarate reductase
GFP	Green fluorescent protein
GAPDH	Glyceraldehyde-3-phosphate dehydrogenase
GLP	Aquaglyceroporin
GPO	Glycerophosphate oxidase
HEPES	N-(2-hydroxyethyl)piperazin-N'-(2-ethansulfonic acid)
IC_{50}	Concentration, which cause 50% inhibition
IgY	Gamma immunoglobin from egg-yolk
IPTG	Isopropyl-beta-D-thiogalactopyranoside
kb	Kilo base
kDa	Kilo Dalton
LS	Long slender
MDH	Malate dehydrogenase
MG	Methylglyoxal
MIP	Major intrinsic protein
MITat	Molteno institute trypanozoon antigenic type
PBS	Phosphate buffered saline
PC	Procyclic trypomastigotes
PCR	Polymerase chain reaction
PEG	Polyethylene glycol

PPDK	Pyruvate phosphate dikinase
PYK	Pyruvate kinase
RNase	Ribonuclease
SDS-PAGE	Polyacrylamid gel electrophoresis with sodium dodecyl sulphate
SF	Selective filter
SHAM	Salicylhydroxamic acid
SS	Short stumpy
TBS	Tris buffered saline
TCA	Trichloro acetic acid
TEMED	N,N,N',N'-tetramethylethylendiamine
Tris	Tris(hydroxymethyl)aminomethane
VSG	Variant surface glycoprotein
WHO	World Health Organization

1. Introduction

1.1. *Trypanosoma brucei* and the disease

1.1.1. Epidemiology

Trypanosoma brucei is the causative agent of sleeping sickness in Africa. According to the report of the World Health Organization (WHO), about 60 million people living in 36 sub-Saharan countries are at risk of acquiring sleeping sickness. The real prevalence is estimated to be between 300 000 and 500 000 cases (WHO, 2001) and the mortality is about 100% if the disease is untreated. It is estimated that the number of annual deaths is close to 66 000 (Gelb and Hol, 2001).

Since the parasite is transmitted by the bite of the tsetse fly, *Glossina sp*., the geographical distribution of the disease is defined by the habitat of the vector. The disease is only endemic in areas where tsetse flies are found, i. e. the zone between the latitudes 14°N and 20°S of sub-Saharan Africa (Pentreath *et al*., 1996) (Fig. 1.1). In humans the disease occurs in two distinct forms: the chronic form due to *T. b. gambiense* that is confined to Central and Western Africa and the more acute *T. b. rhodesiense* form that is prevalent in Eastern Africa (http://www.who.int/tdr/diseases/tryp/diseaseinfo.htm) (Fig. 1.1).

The gambiense reservoir is almost entirely human, whereas *T.b. rhodesiense* is only occasionally transmitted to people. It has an important zoonotic component, different species of wild animals and domestic cattle are reservoirs (http://www.who.int/tdr/diseases/tryp/diseaseinfo.htm). Due to that, along with long disease progression, most of the cases reported are *T. b. gambiense* forms and only relative few cases are diagnosed as *T. b. rhodesiense* forms (Schmid *et al*., 2004).

The subspecies known as *T.b. brucei* infects a wide range of mammals but is unable to infect humans because this subspecies is lysed by the trypanosome lytic factor present in normal human serum, the HDL-bound apolipoprotein L-I (Perez-Morga *et al*., 2005).

Sleeping sickness affects mainly the poor, rural African population, and the socio-economic impact is very high. Most of the economic loss is due to the reduction of working force, family disruption and trypanosomiasis in animal ("nagana") husbandry. In this sense, it is necessary to eradicate sleeping sickness in order to give the people the

opportunity to lead a normal live. In general, this would represent a strong impulse to improve the live standard in affected African countries.

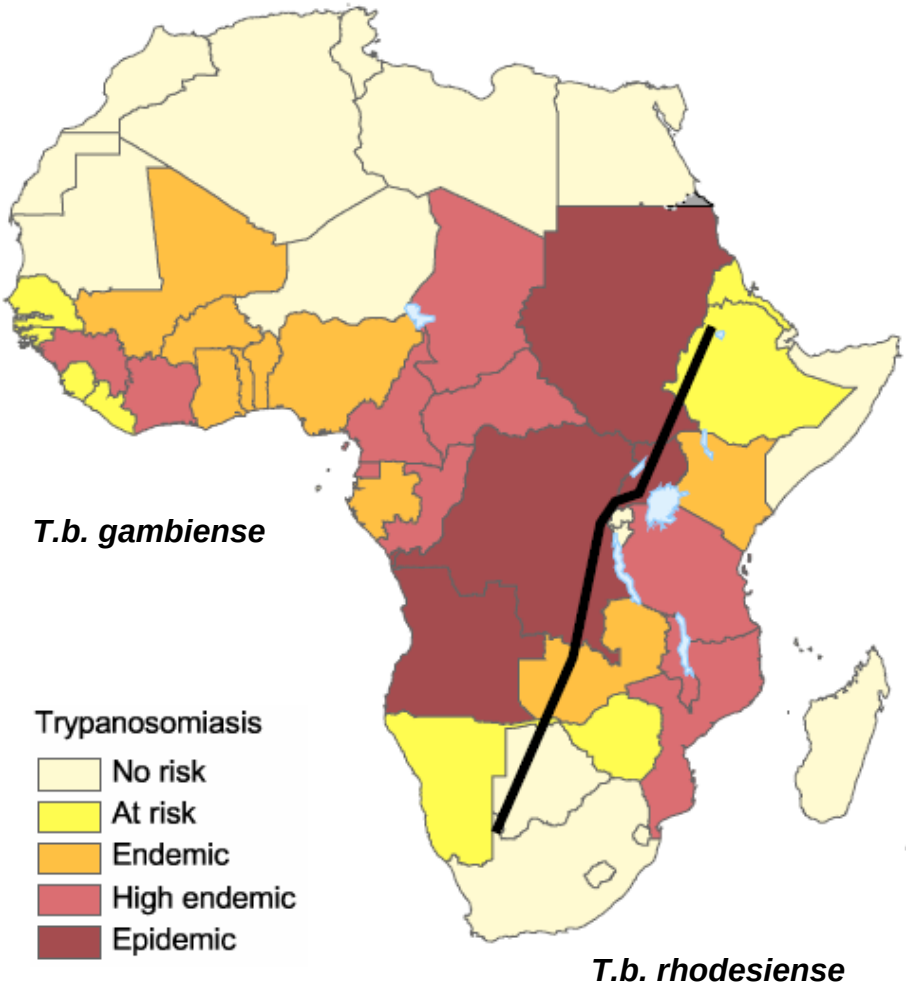

Figure 1.1. Sleeping sickness in Africa: Distribution and endemicity status (WHO, 2004)

1.1.2. Biology of *Trypanosoma brucei*

1.1.2.1. Taxonomy and Phylogeny

Trypanosomes are protozoa belonging to the order of *Kinetoplastida*. This order is one of the earliest branching in the history of eukaryotic evolution. In the eukaryotic tree, the amitochondriate diplomonads appeared first, then microsporidia and parabasalids. After them, the mitochondriate protist lineages follow with *Kinetoplastidae* as the first eukaryotes containing a mitochondrion (Dacks and Doolittle, 2001)(Fig 1.2a). The Kinetoplastida are subdivided into two groups: Bodonina and Trypanosomatina (Fig.1.2b). Organisms of the first group are characterized by the presence of two flagella and a quite

large kinetoplast. This group is formed by both free-living organisms and parasites of fish and snails. Trypanosomatina have only a single flagellum and a smaller kinetoplast than the Bodonina. The former comprise only one family, the Trypanosomatidae, of which all members are parasites of invertebrates, all classes of vertebrates or plants (Fig 1.2b). The genus *trypanosoma* is divided into two sections, according to the place where the parasite develops in the insect hosts: Salivaria develop in the anterior portion of the digestive tract and within the salivary gland, while stercocaria develop in the hindgut (Levine *et al*., 1980). *T. brucei* belongs to the *salivaria* section (Levine *et al*., 1980):

Phylum	Protozoa
Subphylum	Sarcomastigophora
Class	Mastigophora
Subclass	Zoomastigophora
Order	Kinetoplastida
Family	Trypanosomatidae
Genus	Trypanosoma
Section	Salivaria
Sub-genus	Trypanozoon
Species	*Trypanosoma brucei*
Subspecies	*T. brucei brucei ,T. brucei gambiense, T. brucei rhodesiense*

1.1.2.2. Morphology

Trypanosoma brucei is a unicellular organism, approximately 18-20 µm long and 3 µm thick, with a clearly visible flagellum running along the length of the cell body (Fig. 1.3). The flagellum emerges from the cell body at some point close to the cell's posterior end. The nucleus is approximately 1.5 µm in diameter and contains a large central nucleolus (karyosome). The nucleus is a clear oval in the procyclic form, but rather more flattened in the BSF (Rout and Field, 2001). *Trypanosoma* is also characterized by a single large mitochondrion containing a structure which, as a nucleus, acquires intensive color by DNA staining because it possesses up to 25% of the total cell DNA. This structure is known as kinetoplast, from which the order name Kinetoplastida is derived. The kinetoplast is located close to the flagellar basal body and the flagellar pocket, and depending on the developmental stage, the relative position of kinetoplast and nucleus change. In the procyclic form, the kinetoplast is closer to the posterior end of the parasite than the nucleus, but in bloodstream form occurs the opposite (Hoare, 1972).

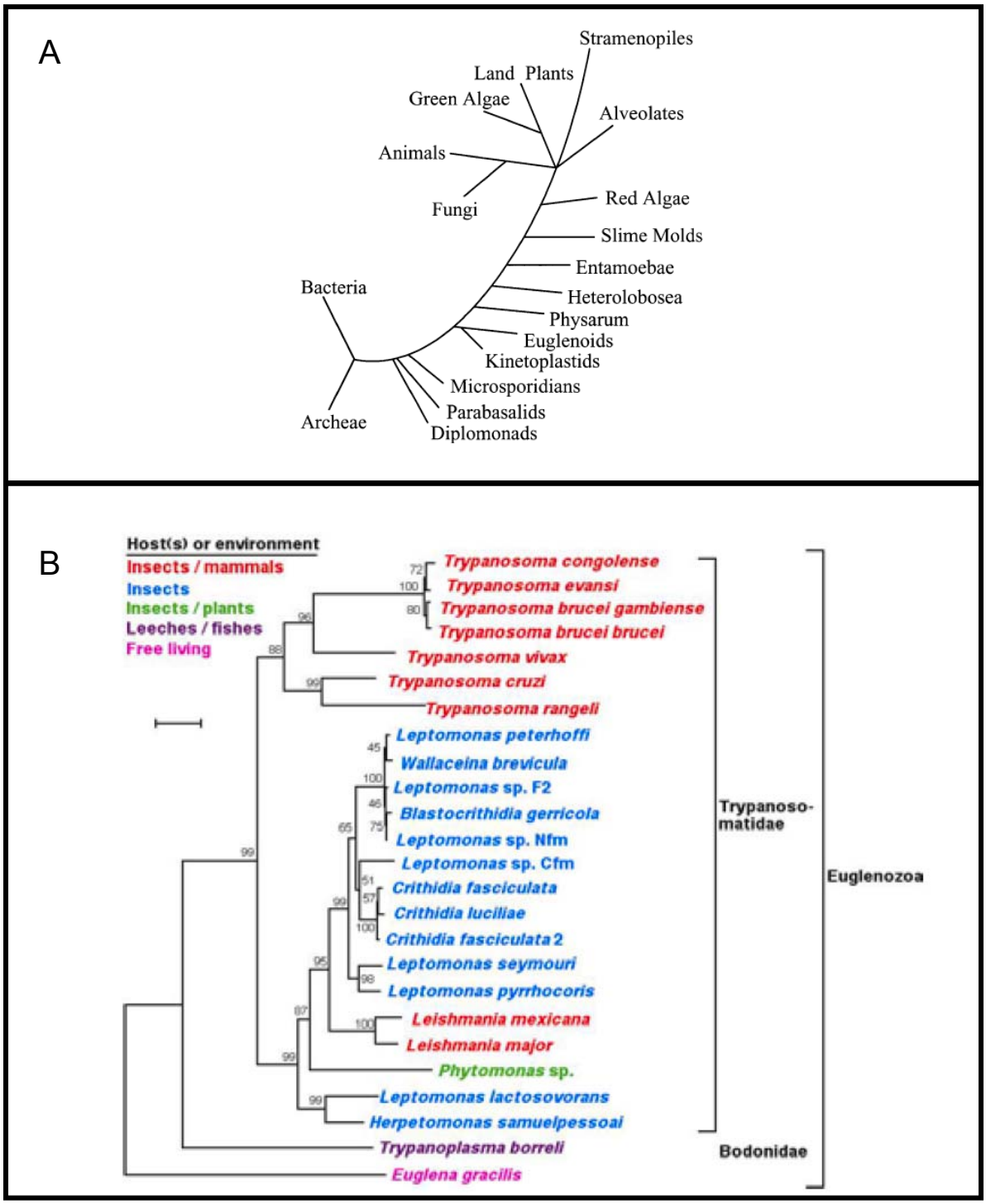

Figure 1.2. Phylogenetic relationships of *T. brucei*. A) The tree of eukaryotes including Kinetoplastida based on Small subunit ribosomal RNA gene sequences (Dacks and Doolittle 2001). B) Tree of the Kinetoplastida based on GAPDH–gene sequences. The Kinetoplastida are subdivided into two groups: Bodonina and Trypanosomatina (Hannaert *et al.*, 2003)

On the other hand, the majority of the endomembrane system is placed between nucleus and kinetoplast, which reflects the role of the flagellar pocket in both endocytosis and secretion as well as the polarity of the cytoskeleton (Morgan *et al.*, 2002a; 2002b). The Golgi complex, the lysosome and the endosomes are located in this posterior region of the

cell (Field *et al*., 2004). By contrast, the endoplasmic reticulum (ER), the mitochondrion and the glycosomes are all dispersed thoughout the cell. Acidocalcisomes are also distributed throughout the cytoplasm, with no apparent polarity (Docampo and Moreno, 1999). Whilst there is no contractile vacuole, and *T. brucei* appears unable to osmoregulate, recent evidence points to an evolutionary relationship between the contractile vacuole and acidocalcisomes (Marchesini *et al*., 2002).

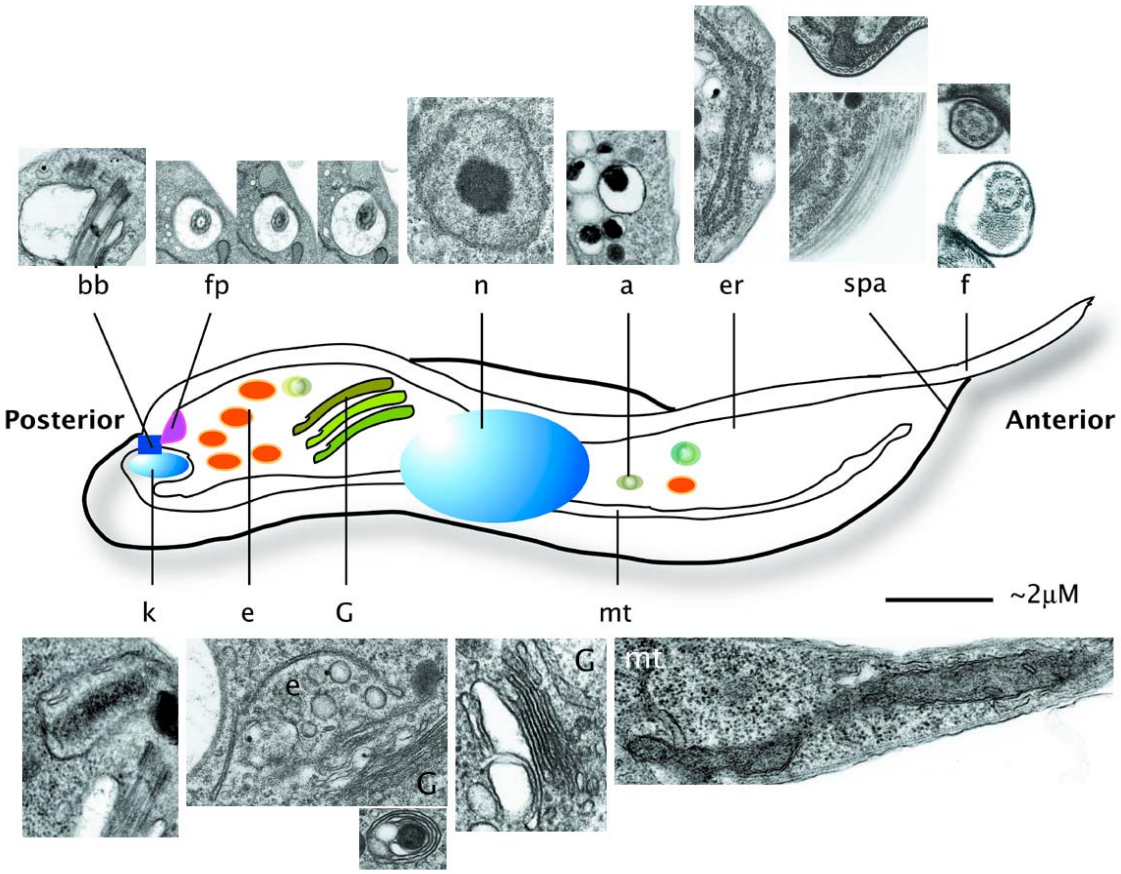

Figure 1.3. Morphology of *Trypanosoma brucei.* The central image is a cartoon showing the locations of the major organelles and structures. The endoplasmic reticulum (er) has been omitted for clarity as this structure extends throughout the cell and also forms the nuclear envelope. Structures shown are: fp, flagellar pocket; bb, basal body; n, nucleus; spa, subpellicular microtubule array; f, flagellum; k, kinetoplast (mtDNA); e, endosomes; G, Golgi complex; mt, mitochondrion; er, endoplasmic reticulum and a, acidocalcisomes. The insets show examples of these structures as seen by thin section transmission electron microscopy (Field *et al*., 2004).

1.1.2.3. Life Cycle

The biological characteristics of the two forms of sleeping sickness, caused by *T. b. gambiense* and *T. b. rhodesiense*, respectively, are so similar that the following description applies to both.

The life cycle of trypanosomes involves two hosts: a mammal and an intermediate insect vector which transmits the infection to a new mammalian host. African trypanosomes are extracellular parasites, both in the mammalian and the insect host. Infection in the human host begins when the infective stage of mammals, the metacyclic stage, is injected intradermally by the tsetse fly (Fig. 1.4). The form develops into blood-stage trypomastigotes (BSF), the so called “long slender form” (LS), i.e. the proliferative form in the mammalian host. This form of the parasite divides by binary fission in the interstitial spaces at the site of the bite. The production of cell debris and metabolic degradation products leads to the formation of a chancre. The parasite enters the bloodstream and divides further, originating a parasitemia. Due to the oscillating population density in the blood, diagnosis by microscopic examination may become difficult. At some point of the disease, the trypanosomes cross the blood-brain barrier and enter the central nervous system. During this stage of the disease, the patient shows the characteristic features of ‘sleeping sickness'. Some slender parasites transform into a non-dividing form pre-adapted to the vector, the so called “short stumpy” (SS) form. Its metabolism is very similar to that of the long slender form but is pre-adapted to transform into the insect procyclic form, because some TCA enzymes and cytochromes exist, although the complete metabolic pathways are still absent.

The tsetse fly is infected when the insect ingests a blood meal from an infected mammalian host. In the midgut of the fly, the trypanosomes transform into procyclic trypomastigotes (PC), and continue to divide for approximately 10 days. Here, they show a fully functional cytochrome system and a TCA cycle. Procyclic forms migrate to the salivary glands where, attached to the epithelial cells, they multiply as a distinct morphological stage, the epimastigote. In this parasite form, the kinetoplast is anterior to the nucleus. After cessation of division, the epimastigote starts to express a dense variable surface glycoprotein coat (VSG coat), and this expression leads to detachment and maturation as non-dividing, infective metacyclic trypanomastigotes, the infective stage for humans and reservoir hosts. It is important to note that the life cycle is a dynamic process. *T. brucei* is pleomorphic, i.e. different morphological stages exist within the mammalian and the insect hosts.

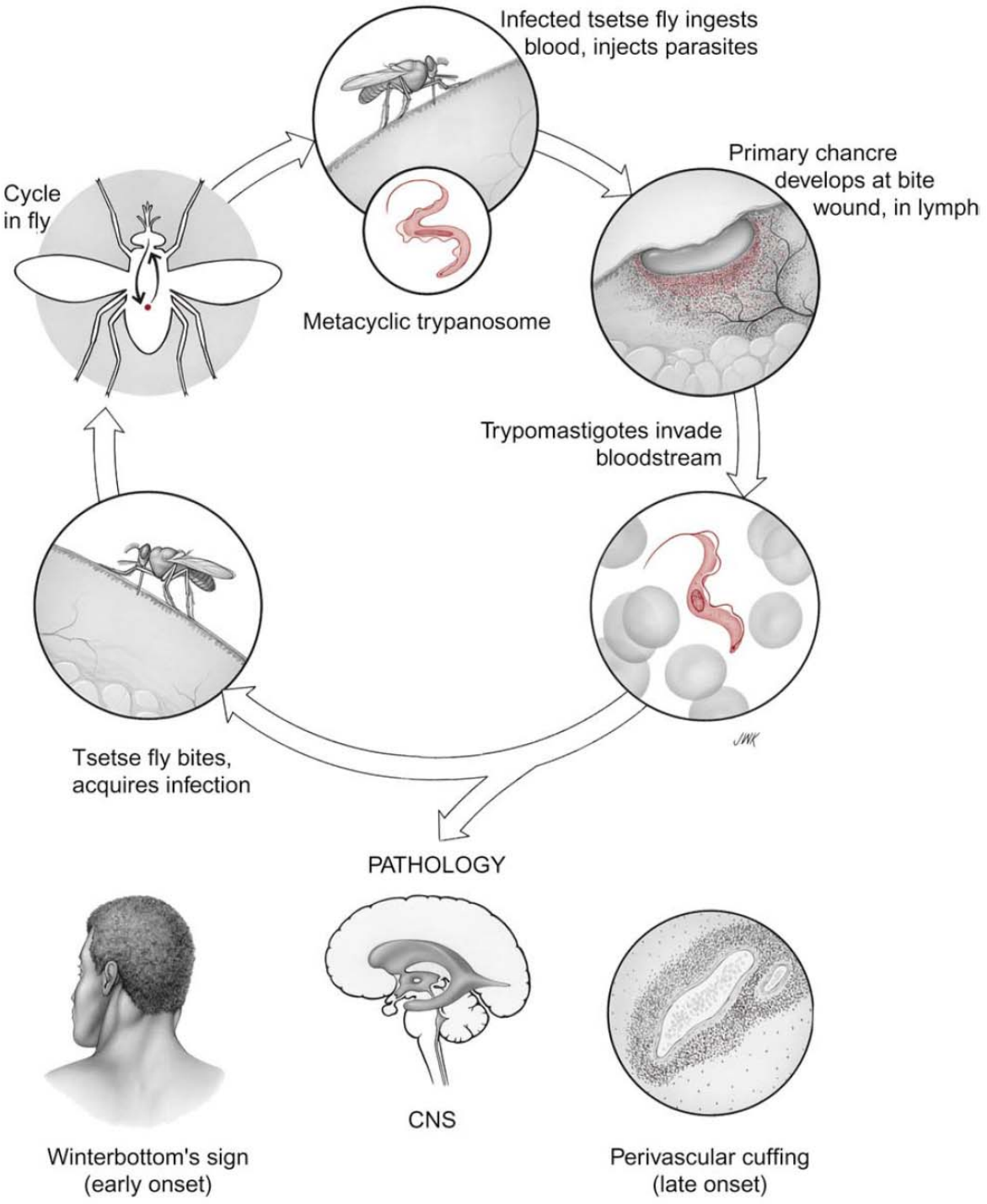

Figure 1.4. Life cycle of *Trypanosoma brucei*. The figure depicts the life cycle of the parasite joint to the more relevant signs observed in the infected human (Despommier *et al*., 2000)

The cycle in the insect takes 25-50 days, depending upon different factors: the species of the fly, the strain of the trypanosome, and ambient temperature. Flies remain infected for their whole life (2-3 months) and inject over 40,000 metacyclic trypanosomes when they take a blood meal. The minimum infective dose for most hosts is 300-500 organisms, although it has been reported that experimental animals have been infected with a single organism (Despommier *et al*., 2000).

1.1.2.4. Glycolysis overview and glycerol importance in *T. brucei* metabolism

The bloodstream forms depend solely on glycolysis for ATP production, with glucose as the main energy source and glycerol as an alternative substrate. It is a consequence of the lack of a functional Krebs cycle and oxidative phosphorylation capability. In many respects, glycolysis in trypanosomes and in other members of the order Kinetoplastida differs markedly from the corresponding pathway in higher eukaryotes. The most striking peculiarity is in fact that the first seven glycolytic reactions occur in a peroxisome-like organelle called glycosome (Michels *et al.*, 2000)

Under aerobic conditions, glucose is converted into pyruvate, which is disposed by facilitated diffusion (Wiemer *et al*., 1995). The enzymes that convert glucose into 3-phosphoglycerate are all inside the organelle, whereas the last three enzymes are present in the cytosol (Fig. 1.5). As a consequence, no net changes in ATP/ADP ratio occur within the glycosome. Net ATP production occurs in the cytosol, in the reaction catalyzed by pyruvate kinase (PYK).

Similarly, the NADH produced by glyceraldehyde-3-phosphate dehydrogenase (GAPDH) is reoxidized to maintain the redox balance. NADH cannot leave the glycosome and is reoxidized during the formation of glycerol-3-phosphate from dihydroxyacetone phosphate. Glycerol-3-phosphat goes into the mitochondrion, in which it is oxidized by glycerophosphate oxidase (GPO). This enzyme uses molecular oxygen (alternative respiration) and is inhibited by salicylhydroxamic acid (SHAM). Finally, the newly formed dihydroxyacetone phosphate re-enters the glycosome and can be glycolytically converted. Obviously, suppression of glycolysis by blocking the release of pyruvate or glycerol is a potential therapeutic approach against sleeping sickness (Wiemer *et al*., 1995, Bakker *et al*., 1997; 2000; Eisenthal and Cornish-Bowden, 1998). Under anaerobic conditions or in the presence of SHAM, glucose degradation results in equimolar amounts of pyruvate and glycerol to maintain the redox balance within the glycosome (Clayton and Michels, 1996). In this case, glycerol is formed from glycerol-3-phosphate by glycerokinase, which in trypanosomes leads to the formation of ATP (Steinborn *et al*., 2000). To drive this reaction to ATP formation, glycerol has to be readily released. Consequently, in the presence of SHAM, the addition of 5 mM glycerol to the parasite culture reverses the glycerol diffusion gradient across the membrane and results in cell death (Wille *et al.*, 1998). However, a therapeutic exploitation of the glycerol sensitivity of the parasite has not yet been successful (Brohn and Clarkson, 1978; Bakker *et al*., 2000).

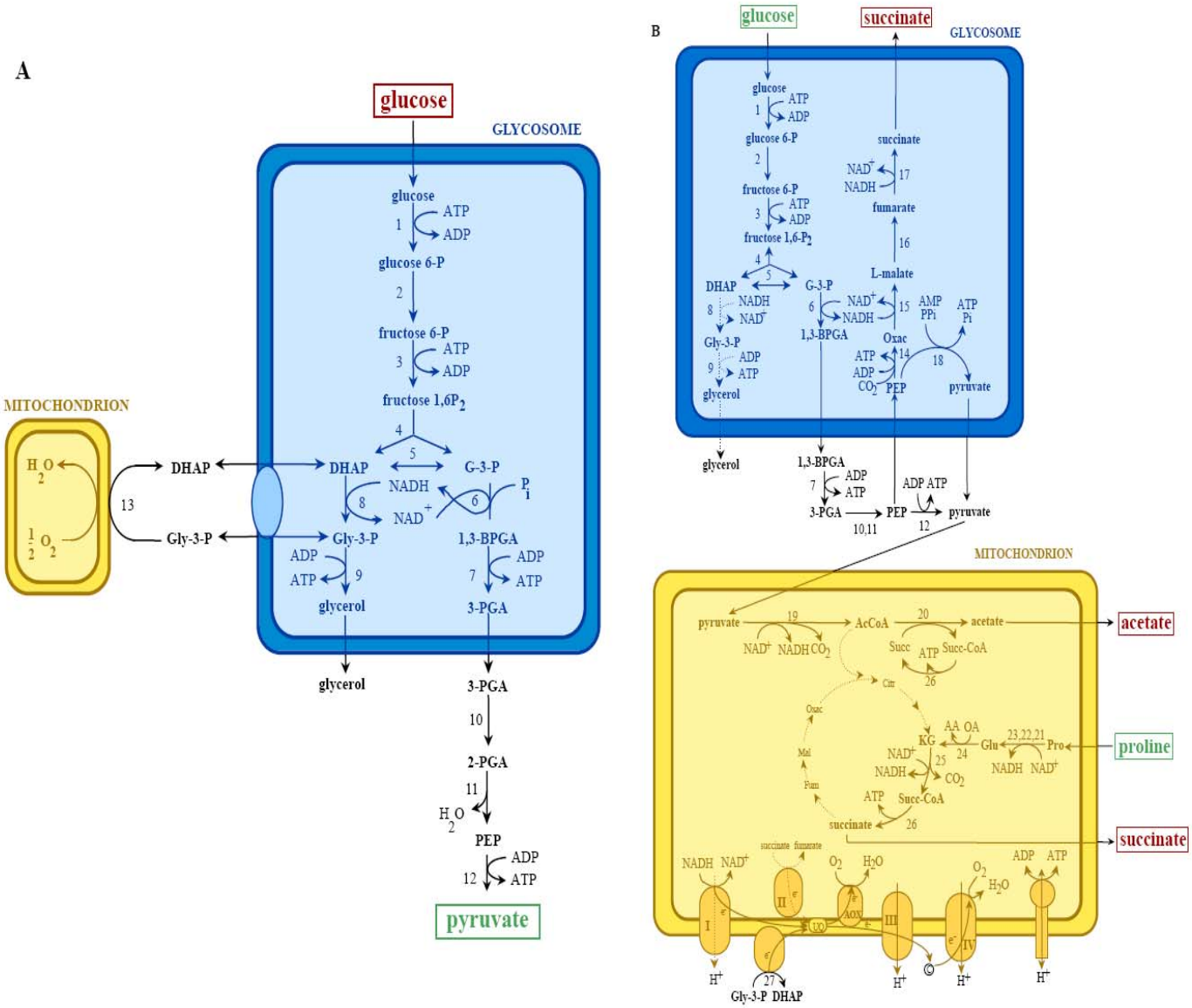

Figure 1.5. The energy metabolism of bloodstream-form (A) and procyclic *T. brucei* (B). Enzymes: 1, hexokinase; 2, glucose-6-phosphate isomerase; 3, phosphofructokinase; 4, aldolase; 5, triosephosphate isomerase; 6, glyceraldehyde-3-phosphate dehydrogenase;7, phosphoglycerate kinase; 8, glycerol-3-phosphate dehydrogenase; 9, glycerol kinase; 10, phosphoglyceratemutase; 11, enolase; 12, pyruvate kinase; 13, glycerol-3-phosphate oxidase; 14, phospho*enol*pyruvate carboxykinase; 15, Lmalate dehydrogenase; 16, fumarase; 17, fumarate reductase; 18, pyruvate phosphate dikinase; 19, pyruvate dehydrogenasecomplex; 20, acetate:succinate CoA transferase; 21, proline oxidase; 22, Δ'-pyrroline-5-carboxylate reductase; 23, glutamate semialdehyde dehydrogenase; 24, glutamate dehydrogenase; 25, α-ketoglutarate dehydrogenase; 26, succinyl CoA synthetase; 27, FAD-dependent glycerol-3-phosphate dehydrogenase. Abbreviations: AA, amino acid; AcCoA, acetyl-CoA; 1,3-BPGA, 1,3-bisphosphoglycerate; c, cytochrome c; Citr, citrate; DHAP, dihydroxyacetone phosphate; Fum, fumarate; G-3-P, glyceraldehydes 3-phosphate; Glu, glutamate; Gly-3-P, glycerol 3-phosphate; KG, α-ketoglutarate; Mal, malate; OA, 2-oxoacid; Oxaloxaloacetate; PEP, phospho*enol*pyruvate; 3-PGA, 3-phosphoglycerate; Succ, succinate; Succ-CoA, succinyl-CoA; UQ, ubiquinone. (Hannaert et al., 2003)

Procyclic, insect-stage *T. brucei* have a more elaborate energy- and carbohydrate metabolic network that also involves the mitochondrial Krebs' cycle enzymes and a respiratory chain with coupled transmembrane proton-translocating activity (Norbeck and Blomberg, 1997; Sun *et al*., 2003)(Fig. 1.5). In these cells, two other ATP-dependent kinases (phospho*enol*pyruvate carboxykinase and pyruvate phosphate dikinase (PPDK) are found in the glycosome, whereas PGK is relocated to the cytosol, with the consequence that the glycosomal ATP/ADP balance is maintained (Fig. 1.5). Similarly, the presence of a glycosomal NAD^+-dependent malate dehydrogenase (MDH) and NADH-dependent fumarate reductase (FRD) in these cells is accompanied by a significant drop in the activity of GPDH, so that the NAD^+/NADH balance is also maintained (Hannaert *et al*., 2003).

However, the metabolism of insect-stage *T. brucei* is very complex and, at the moment, the classical view of this process is changing rapidly with the appearance of new data (see Besteiro *et al.*, 2005 for details)

1.1.3. Pathogenesis

T. b. gambiense and *T. b. rhodesiense* cause the same type of clinical disease, with only few particularities in each disease. The relevant difference is the time scale of their development; the classical chronic form is due to *T. b. gambiense* and the more acute forms is caused by *T. b. rhodesiense*.

The initial acute inflammation at the site of the inoculation of metacyclics, the chancre, is the first sign of infection. The lesion is more frequently observed in *T.b. rhodesiense* infections, it resolved spontaneously between one and four weeks. From this place, the parasite enters the lymph channels and blood circulation producing disseminated lesions. This is the first stage of the sickness named haematolymphatic stage, which is associated with irregular intermittent fever, generalized lymphadenopathy and splenomegaly (Despommier *et al*., 2000). Frequent symptoms are headache, weight loss, joint pains, skin rashes, and pruritus. An enlargement of lymph nodes is often seen, especially at the posterior cervical lymph nodes (Winterbottom's sign, fig. 1.4). Sometimes the symptoms are minor and may not alert the patients about sleeping sickness (WHO, 2001).

The parasite is able to remain in the blood and to escape from the host's immune response because of its ability to change its surface coat covering the complete plasma membrane, thus resulting in antigenic variability. The host develops specific antibodies against a determined variant surface antigen (VSG), which is no longer effective against

any other one. This VSG change every 8 ~ 10 days, leading to a oscillating parasitemia that is characteristic of the disease (Despommier *et al*., 2000) (Fig. 1.6).

When parasites invade the central nervous system (CNS), the second stage of the sickness or the meningoencephalitic stage begins. The involvement of the CNS may occur within a few weeks, as seen in *T.b. rhodesiense* infections, or may not occur until years later (*T.b. gambiense* infections). The organisms penetrate into the brain tissue and produce inflammatory lesions. Early changes and symptoms involve abnormal body movements, tremors, irritability, and alterations in mood. Indifference or the reversal of sleep rhythm with daytime somnolence and night insomnia is the prominent symptom and is responsible for the name "sleeping sickness". As the disease progresses, the neurologic abnormalties become more significant. Epileptiform seizures may occur as well as local paralysis, total indifference and somnolence. The brain shows evidence of inflammation with perivascular cuffing consisting of infiltrates of glial cells, lymphocytes, and plasma cells (Fig. 1.4). Due to the long duration of *T.b. gambiense* infections, extensive neurological changes might be observed, which lead next to acute infections or malnutrition to death. In the acute form of the disease caused by *T. b*. *rhodesiense*, death often occurs before CNS involvement because of cardiac failures, pneumonia or superimposed infectious diseases (Pentreath *et al.*, 1996).

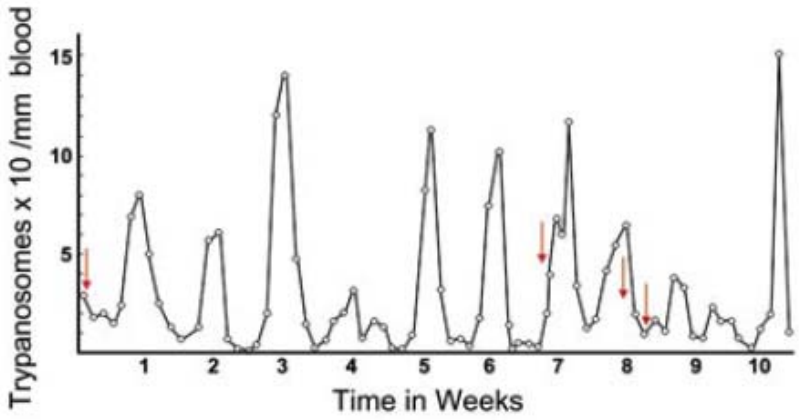

Figure 1.6. ***T. brucei* parasitemia** Fluctuating load of parasites in the blood of a patient with sleeping sickness (Despommier *et al*., 2000).

1.1.4. Diagnosis

Definitive diagnosis depends upon finding the organisms in blood smears stained with either Wright's stain or Giemsa stain, or in the cerebrospinal fluid. Aspirates of lymph nodes may also contain organisms. However, the parasites might not be found in such preparations, even in a patient dying from the disease, because of the fluctuating parasitemia (Despommier *et al*., 2000). In order to improve the sensitivity of diagnosis, examination of the buffy coat and the centrifuged sediment of the CSF is recommended

(Despommier *et al*., 2000). Moreover, ELISA and PCR are useful diagnostic tools. The World Health Organization (WHO) has developed an agglutination test that detects antibodies to common antigens and has been adapted for use in the field.

History of travel in an endemic area, recalling a painful fly bite, and the presence of a chancre is suggestive of trypanosomiasis. The differential diagnosis includes syphilis, leishmaniasis, and malaria. Finding malarial parasites in the blood of a patient with trypanosomiasis is not unusual, and can mislead the clinician, diverting their attention from the diagnosis of trypanosomiasis.

1.1.5. Treatment

There are only a few active drugs available for the treatment of trypanosomiasis, and most of them are practically identical with the ones developed 50 years ago. These drugs can not be used throughout all stages of the disease, have many adverse effects, are expensive and not readily available. They have limited efficacy and the parasite can develop resistance (Croft, 1997).

Four drugs are currently approved for the treatment of human trypanosomiasis, namely suramin (1922), pentamidine (1937), melarsoprol (1949), eflornithine (1981) and nifurtimox (1960), a drug which is registered for Chagas disease. There is also one used in veterinary medicine, a pentamidine analog called diminazeneaceturate (1960) or berenil (Bouteille *et al*., 2003).

Early-stage disease is treated with suramin (Germanin®, Bayer) in rhodesiense infection and with pentamidine (Lomidine®, Aventis) in gambiense disease; both drugs are ineffective in treating the late stage (WHO 2001). Melarsoprol (Arsobal®, Aventis), a trivalent organic derivative of arsenic, is effective for treatment of the late meningoencephalitic stage of the disease and is the only effective drug for both *T.b. rhodesiense* and *T.b.gambiense*. Eflornithine (Ornidyl®, Aventis) is also effective against the final stage of the disease and is less toxic than melarsoprol. However, it is largely ineffective in *rhodesiense* infections (Bouteille *et al*., 2003). Nifurtimox (Lampit®, Bayer) is the only other potential alternative treatment for late-stage disease, but there is not yet well-documented evidence of efficacy and safety for the treatment. Its use is more likely to be in the context of a combination therapy for melarsoprol refractory cases or when eflornithine is not available.

Due to the difficulty of treatment of the disease, its endemic character, and the socio-economic consequences, it is imperative to search for new biochemical targets,

which allows to develop new drugs closer to the ideal medicament; more efficient, the low cost and easy administration.

1.2. Aquaporins

1.2.1. General feature

Water constitutes about 70% of the body mass; the appropriate distribution of this huge water volume is required to maintain fluid balance within different anatomic compartments. Therefore, the regulation of water permeability of cell membranes is a fundamental requirement for life (Yasui, 2004).

With the discovery of the lipid bilayer in the 1920s appeared an explanation for how cells maintain their optimal intracellular environment despite of being bathed in an extracellular fluid of lower or higher pH or containing toxic concentrations of Ca^{2+} or other solutes. Exchangers and transporters were discovered by 1950s and provided a molecular basis for transmembrane movements of solutes (Agre *et al*., 2002). Nevertheless, since water is a small uncharged molecule and is considered the "universal solvent" with a huge concentration in life systems, it was long assumed that the transport of water is owing to simple diffusion through the lipid bilayer. Although water can diffuse through lipid bilayers, diffusion is not sufficiently rapid for many physiological processes (Kozono *et al.*, 2002). Observations from multiple experimental systems with high membrane water permeabilities, such as kidney, urinary bladder, and erythrocytes, suggested that simple diffusion through lipid bilayers is not the only pathway for water to cross the membrane (Verkman, 1989). Finally, in 1992 with the discovery of human aquaporin 1 (hAQP 1), Agre´s group demonstrated the existence of water-specific transport proteins (Preston *et al.*, 1992). It is now known that both simple diffusion and channel-mediated water movements occur in cellular membranes (Agre *et al*., 2002). Water diffusion through biological membranes is a process that occurs with a relatively low velocity, and the presence of AQP in this structure increases the capacity for water transport between 10- and 1000 fold. For many AQPs, the activation energy required to allow the water passage is about 5 Kcal mol^{-1}, which is very close to the diffusion of water in solution (Borgnia *et al.*, 1999).

The identification of AQP3, in the year 1994, a homologue of AQP1 permeated by water, glycerol, some polyols and urea, contradicted the statement that all members of the aquaporin family are selectively permeated only by water (Echevarria *et al.*, 1994a; 1994b;

Ishibashi *et al.*, 1994; Ma *et al.*, 1994). AQPs are also permeable for other compound, e.g. ammonia and CO_2 (Tyerman *et al.*, 2002; Jahn *et al*., 2004). Apart of those, other solutes are very likely to be discovered. These new reports indicate the growing fundamental importance of these proteins in animal and plant physiology.

These "aquaporins" (AQP) are members of the superfamily of major intrinsic proteins and fall into the aquaporin branch. The aquaporin family is divided by functionality into two groups: orthodox aquaporins (AQP), which facilitate permeation of water, and aquaglyceroporins (GLP), permeable for small non-ionic solutes, such as glycerol and urea. These membrane proteins are found in all life forms, including archaea, eubacteria, fungi, plants, and all phyla of animals (Agre *et al*., 2002).

1.2.2. Phylogeny

Sequence analyses indicate that the so called MIP (major intrinsic proteins) can be divided into two closely related halves that may have arisen by gene duplication. According to phylogenetic analyses, the main difference of substrate selectivity (AQPs and GLPs) was acquired early in the history of the family by gene duplication and functional shift. The great diversification of the protein family occurred in vertebrates and higher plants (Zardoya and Villalba, 2001; Zardoya *et al*., 2002). Up to 11 putative members of the MIP family have been described in human (AQP0 to AQP10), eight of which are orthodox AQPs (AQP0, 1, 2, 4, 5, 6, and 8) and four (AQP3, 7, 9, and 10) are permeable to glycerol (Fig.1.7) (Zardoya, 2005). Recently, AQP11 and 12 have been reported, but so far there is scarce information about them.

In plants exists a great variety of AQPs. In *Arabidopsis* for example up to 35 different AQP genes have been described (Johanson *et al*., 2001), and at least 31 MIPs in corn (Chaumont *et al*., 2001). AQPs from plant are classified into four subfamilies. The first group is called tonoplast intrinsic proteins (TIP), with for subclasses (α-TIP, β-TIP, γ-TIP, δ-TIP). The second, the plasma membrane intrinsic proteins (PIP) possess two subgroups correlating with high (PIP2) and low (PIP1) water channel activity. The third one was named small basic intrinsic proteins (SIP); these proteins are quite divergent from the other plant MIPs and show significant sequence differences in loop B where the NPA box consists of NPT or NPL. Because of the importance of amino acid residues in loop B for transport characteristics, it is possible that the SIPs could display quite different transport selectivity (Tyerman *et al*., 2002). NOD26-like intrinsic proteins (three subgroups NIP1, NIP2 and NIP3) form a fourth distinct group. Members belonging to this

classification are unique in conferring the ability to transport glycerol in plants (Wallace and Roberts, 2004). It has been shown that NIPs are AQPs that were recruited to transport glycerol in plants. There are no real aquaglyceroporins from plants, thus it was suggested that NIPs were acquired from a single event of horizontal gene transfer from bacteria at the origin of plants, this phenomenon could have occurred about 1,200 million years ago (Zardoya, 2002).

Interestingly, out of the 463 non-redundant sequences known so far, only 20 have a non-canonical NPA box in loop B, and around 30 have changes in the NPA box of loop E. On the other hand, three putative paralogs of AQPs in insects, two in plants, and vertebrate's AQP11 and 12 possess highly divergent sequences. However, the absence of various conserved motifs in the insect AQPs, as well as in AQP11 and 12, suggests that these proteins may be only distantly related or may not belong to this family at all (Zardoya, 2005).

1.2.3. Structure

1.2.3.1. Molecular features of aquaporins deduced from structure and sequence alignments

The quaternary structure of the protein is a homotetramer. Each MIP monomer contains six hydrophobic membrane-spanning helices connected by five loops (A-E, Fig. 1.8a) that delimit a polar channel with two wide periplasmic vestibules and one central pore (hourglass model) (Fig. 1.8a). The loops B (cytoplasmic) and E (extracellular) interact with each other from opposite sides through two highly conserved NPA (Asn-Pro-Ala) boxes forming one of the narrowest region of the pore. A single N-glycosylation site is present in the extracellular loop C, and a cysteine residue in loop E is known to be responsible for mercurial sensitivity of most MIPs (Preston *et al*., 1993). The most conserved feature is the NPA motif in loops B and E (at positions 76-78 and 192-194 of hAQP1, respectively) (Fig.1.8b). However, amino acid residues highly conserved are also found close to this position. A consensus sequence for the first NPA box could be S-G-x-H-x-N-P-A-V-T (Fig. 1.8b). Similarly, for the second box, a consensus sequence could be G-x-x-x-N-P-A-R-(S/D)-x-G (Fig. 1.8b)(Heymann and Engel, 2000; Zardoya and Villalba, 2001).

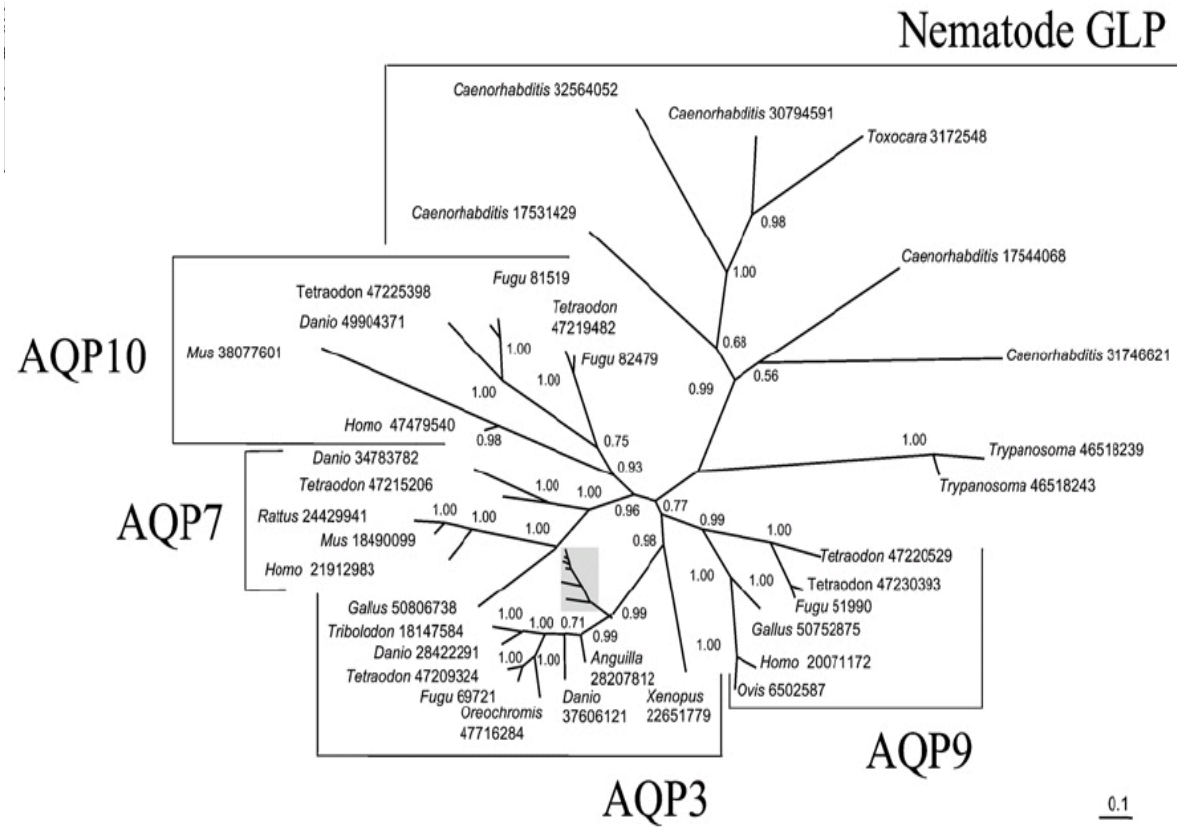

Figure 1.7. Phylogenetic tree showing evolutionary relationships of animal GLPs, including trypanosomes (from Zardoya, 2005).

Other conserved motifs in the first half of the polypeptide are: A) a glutamate in transmembrane helix 1 (at position 17 of hAQP1), forming the conserved box A-E-F-x-x-T; B) a glycine in helix 2 (at position 57 of hAQP1), and C) three almost contiguous residues in helix 3, tyrosine, glutamine and glycine (at positions 97, 101, and 104 of hAQP1, respectively) (Fig. 1.8b). On the other hand, in the second one half: D) glutamate, threonine and leucine in helix 4 (at positions 142, 146, and 149 of hAQP1, respectively); E) glycine in helix 5 (at position 173 of hAQP1), and F) tryptophan, proline, glycine, and tyrosine in helix 6 (at positions 210, 216, 219, and 227 of hAQP1, respectively) (Fig. 1.8b). Finally, no conserved residues are found in loops A, C, and D neither in the amino nor the carboxy ends. Deduced conserved boxes were mapped onto the crystal structure of hAQP1. (Murata *et al*., 2000)

In a three-dimensional view of the fourfold symmetry axis of the protein, it is observed that conserved boxes are localized in the center of the protein, close to the

narrowest part of the pore. All face inside the protein except phenylalanine of helix 1 and tryptophan of helix 6. These two residues might be involved in oligomerization of the tetramer. A view from the cytoplasmic side trough the channel shows that all conserved boxes are in one side of the pore except the conserved glycine from helices 2 and 5, which are found on the opposite side (Fig. 1.8c) (Zardoya, 2005).

1.2.3.2. Molecular characteristic features of aquaporins associated to the permeability of water and glycerol

The mechanism of water and glycerol permeability across the different members of the aquaporin family has gradually become clearer. The growing information about the selectivity of aquaporins for their substrate is based on different approaches: sequence analysis (Froger *et al*., 1998; Zardoya and Villalba, 2001; Zardoya *et al*., 2002; Zardoya, 2005; Wallace and Roberts, 2004), simulation (de Groot and Grubmüller, 2001; Tajkhorshid *et al*., 2002; Lee *et al*., 2004), site-directed mutagenesis (Lagree *et al*., 1999; Hansen *et al*., 2002; Beitz *et al*., 2004; Liu *et al*., 2005) and crystal structure (Braum *et al*., 2000; Savage *et al*., 2003; Stroud *et al*., 2003).

Several residues have been proposed to be involved in selectivity towards water or glycerol. By direct comparison among sequences known to be AQP and GLP, Froger and collaborators (1998) identified five positions (P1-P5) corresponding to amino acid residues conserved with typical physico-chemical properties in each group. P1 is located at the end of helix 3, (at position 116 of hAQP1); it is an aromatic residue in the GlpF sequences. P2 and P3 are located in loop E, just downstream the second NPA motif (at positions 196, and 200 of hAQP1, respectively). They correspond to a basic following an acidic residue (D, then R or K) in the GLPs cluster and to two small uncharged residues in the AQP cluster. P4 and P5 correspond to two consecutive amino acids located in the last transmembrane domain (at positions 212, and 213 of hAQP1, respectively). These positions can be defined as two aromatic residues in the AQP cluster (usually F, Y then W) compared with a proline followed by a nonaromatic residue in the GLP sequences. In summary, for GLPs the couples P2-P3 possess charges of opposite sign associated with nonaromatic residues in P4-P5, whereas for AQPs uncharged residues in P2-P3 are associated with aromatic residues in P4-P5. P1 is generally the counterpart of P4-P5 (aromatic/nonaromatic) between the two clusters. In this study, only about 5% of key residues analysed did not obey to these rules (Froger *et al*., 1998).

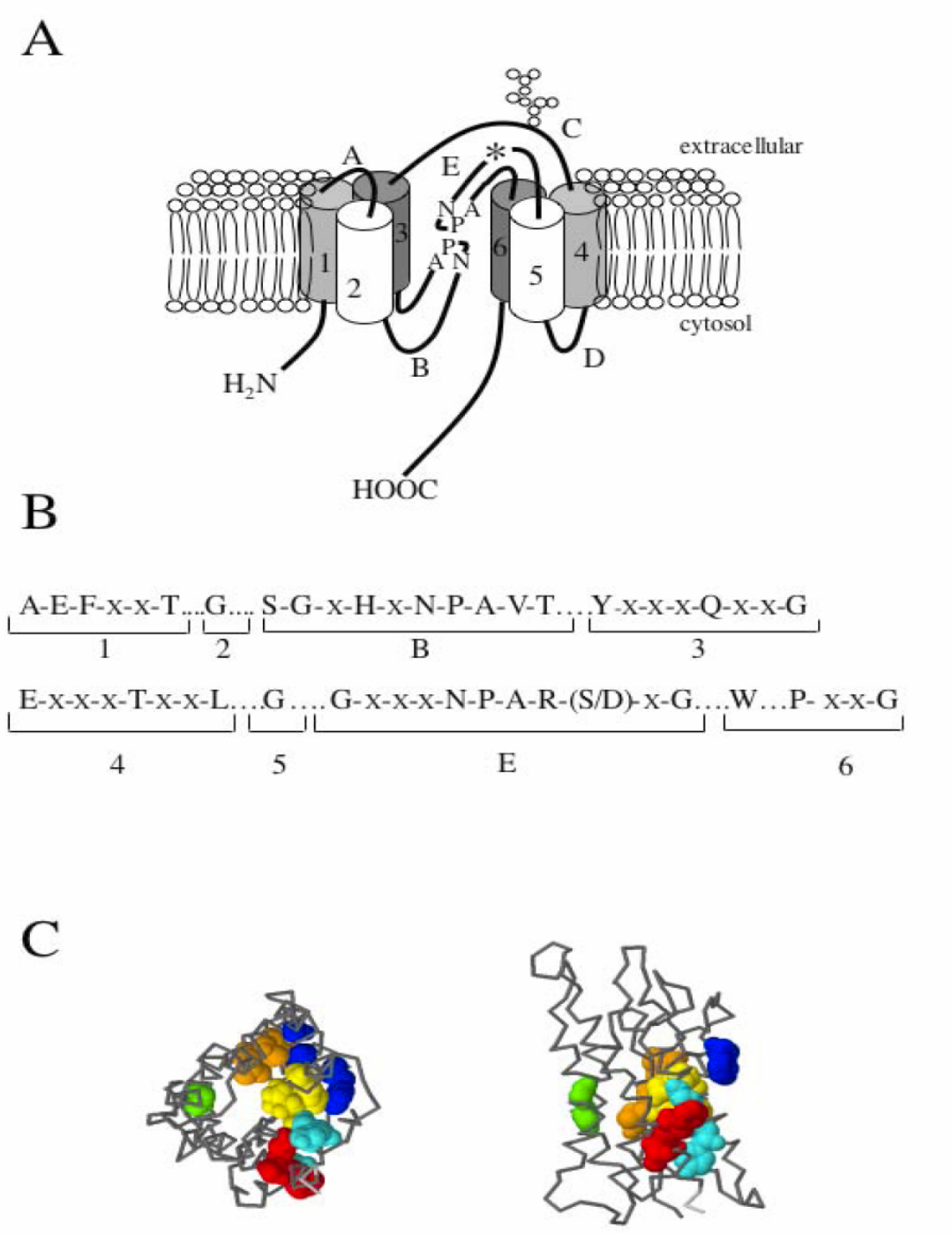

Figure1.8. Molecular features of AQP A) Cartoon showing the structural organization of AQPs B) Conserved signatures of the AQP molecule deduced from comparative analysis of the multiple alignments. C) Views of the human AQP1 crystal structure along and perpendicular to the pore. Conserved signatures of helix 1, 3, 4, and 6 are shown in red, cyan, orange, and blue, respectively. NPA motifs are depicted in yellow. Gly residues of helices 2 and 5 are shown in green (From Nielsen *et al.* 2002 and Zardoya 2005).

Evidence for the function of particular amino acid residues has been obtained from site-directed mutagenesis experiments. By use of this approach, the importance of the P4-P5 position in the substrate specificity was clearly demonstrated (Lagree *et al*., 1999). Changes of amino acid residues according to the rules described above at P4-P5 positions, like in AQP from Cicadella viridis (AQPcic) and GLP from *Escherichia coli* (GlpF), lead to a switch in the selectivity of the channels, from water to glycerol (AQPcic) and *vice versa* (GlpF). The unique bi-functional aquaglyceroporin present in Plasmodia is permeated by glycerol as well as water at about the same rate as described for the classical AQP 1 (Hansen *et al*., 2002). It has been demonstrated by mutation experiments that this extraordinary water conduction relies on E at position 125 in the extracellular C-loop (Beitz *et al*., 2004). Recently it has been shown that the substitution of an N residue at position 60, present in all known mammalian orthologs of AQP6, by G (highly conserved residues in AQPs) totally eliminates the particular anion permeability of AQP6 and exhibits a significantly higher osmotic water permeability (Liu *et al*., 2005).

The structure determination of AQP1 and GlpF, along with 3-D modelling and simulation of solute permeability, has further allowed improving our understanding of water and glycerol uptake mechanisms. For instance, the aromatic/R region found in the narrowest part of the pore was proposed to be involved in substrate selectivity by direct comparison of AQP and GLP crystal structures. This region is formed by F 58 (helix 2), H 182, C 191 (loop E), and R 197 (loop E) of hAQP1 (Murata *et al*., 2000). In *E. coli* GLP (Fu *et al*., 2000), these positions correspond to W 48, G 191, F 200, and R 206, respectively.

1.2.4. Model of permeability mechanisms

Water selectivity of AQP1 is basically due to a simple size exclusion effect. AQP1 has a constriction of about 2.8 Å in diameter in the aromatic/R region, which represents the size of water, so that solutes larger than a water molecule can not pass the AQP 1 pore (Murata *et al*., 2000; Unger, 2000). However, it is not obvious why protons are so effectively blocked. Murata *et al.* (2000) proposed a model to explain this phenomenon (Fig. 1.9). The idea is that hydrogen interchange can be inhibited by breaking the hydrogen bonding pattern along a single file column of water molecules. The reduced size of the pore forces the bulk solution to a single file column of about seven water molecules, and the two conserved N of the NPA motifs stabilize the central water, aligned perpendicular to the channel axis. This conformation converts the central water molecule in a hydrogen

bond donor to its neighbouring water molecules. Therefore, an organization of two opposite water orientation in the two halves of the channel occurs. This bi-orientational ordering of the water-wire prevents the contiguous hydrogen-bonded water chains trough the channel, a necessary condition for proton conductance (Murata *et al*., 2000; Unger, 2000; Groot and Grubmüller 2001).

The selectivity in GlpF depends on the spatial structure of its pore. The diameter of the channel opening measures about 3.5 Å at its narrowest point, and the constriction region of the channel is approximately 28 Å long. Due to this geometric constraint, the substrates can only pass in single file, exactly three glycerol molecules at a time (Fu *et al*., 2000). Although the conserved N in the NPA motifs in GlpF provides hydrogen bonds during glycerol passage, they are not involved in the initial discrimination of glycerol from other solutes. In the GlpF this role falls on a region called selective filter (SF), which is strongly amphipathic with a strip of polar residues opposing a hydrophobic wall (Unger, 2000). The hydrophobic backbone of glycerol is oriented toward apolar residues, it is particularly tightly packed against two hydrophobic amino acids, W 48 and F 200, whereas two of hydroxyl groups of glycerol form hydrogen bonds with R 206.

GlpF has a much lower conductivity for water than glycerol. It is thought that the water conductivity may be impaired by the more hydrophobic wall of the channel (Fu *et al*., 2000). In AQP1, W 48 and F 200 of GlpF are replaced by F 58 and C 191, respectively. In this ambient, water would need a "fully hydrated" state in order to satisfy hydrogen bonding requirements. However, because of the pore restriction size, water could only pass this filter in a single file. In this situation, water could retain only two water molecules as neighbours, and not 4 or 5 coordinate water molecules as it typically occurs. The high energetic barrier for such dehydration leads to low water conductivity (Fu *et al*., 2000; Unger, 2000; de Groot and Grubmuller, 2001).

1.2.5. Aquaporin in mammals

The organization of water within biological compartments is fundamental for life, and the aquaporins serve as the plumbing systems for cells. Aquaporins explain several physiological phenomena related with water movement: Brain secretion and absorption of spinal fluid, generation of the aqueous humor within eyes, secretion of tears, saliva, sweat, and bile, and the efficient urine concentration in kidneys.

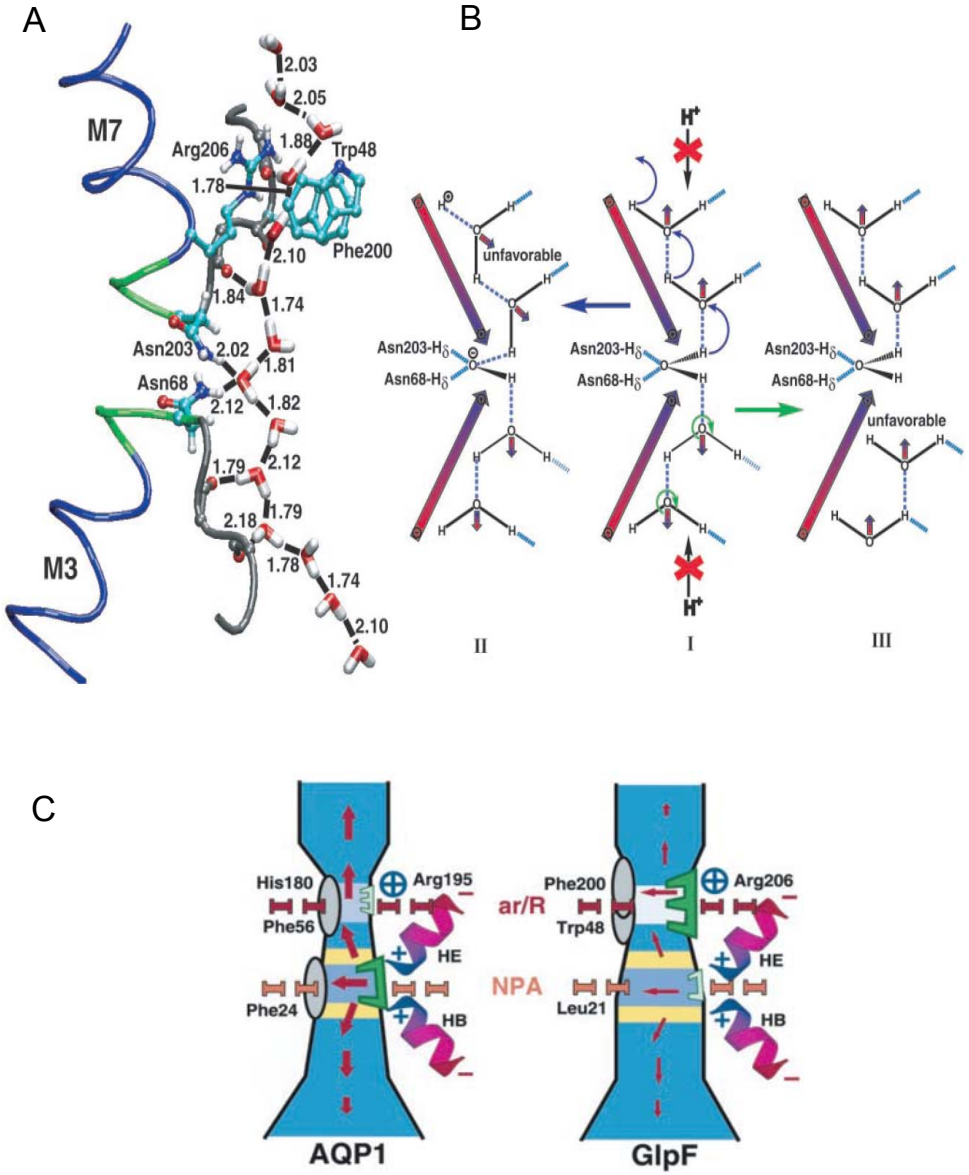

Figure 1.9. Model of water and glycerol permeability by GlpF, comparation with AQP1. A) water permeation by GlpF showing the F 200 and W 48 amino acid residues, which create a SF region more hydrophobic. Water repulsion by the aromatic W 48 and F 200 causes a low occupancy of water molecules in the SF region, resulting in a lower capacity of water permeability for GlpF than that observed for AQP1. B) cartoon of the proton preclusion. The cartoon shows three possibilities where proton transport is blocked. C) Permeation mechanism for AQP1 and GlpF. In both proteins the ar/R region is the narrowest part of the pore and forms the upper filter (red), this region together with the positive charge of the conserved R 195 and R 206 renders a proton filter. In GlpF, the region harboring the aromatic W 48 and F 200 (gray ellipses) is responsible of the specificity for glycerol permeation. Further down, the second stage of the filter (orange) is located at the conserved NPA motifs and is mainly a size-exclusion selectivity filter. In both proteins, the dipoles of water molecules passing the pore (red arrows) undergo a rotation during passage. (From Tajkhorshid *et al*., 2002 and de Groot and Grubmuller 2001)

Since AQP1 was identified as a molecular water channel, hundreds of homologous proteins have been recognized in plants, microbes, invertebrates, and vertebrates. Thirteen mammalian aquaporins have now been identified and at least partially characterized (Yasui, 2004). Functional measurements indicate that mammalian aquaporins 0, 1, 2, 4, 5, and 8 are water-selective, whereas aquaporins 3, 7, 9, and 10 (called 'aquaglyceroporins') also transport glycerol and other small solutes. AQP6 has been proposed to function in kidney endosomes as a pH-sensitive chloride channel (Verkman, 2002).

1.2.5.1. AQP0

AQP0 is the major intrinsic protein of lens fiber cells (Fig. 1.10). Unlike the majority of water-selective aquaporins, the permeability of AQP0 is relatively low, conferring a modest four- to fivefold increase in water permeability over the intrinsic permeability of lipid bilayers. It is resistant to inhibition by mercurials. The physiological importance of this protein may lie in facilitating cell-to-cell adherence between lens fiber cells via interactions between AQP0 molecules in adjacent cells (Kozono *et al*., 2002). Two kindreds with dominantly inherited congenital cataracts were recently identified with AQP0 mutations: E-134→G or T-138→R (Agre *et al*., 2002). Both mutations interrupt trafficking of the nascent polypeptide to the plasma membrane. The phenotypes of the cataracts are distinct: Patients with the E-134→G mutation have single lamellar opacities, whereas those with the T-138→R mutation have multifocal opacities throughout the lens (Kozono *et al*., 2002).

1.2.5.2. AQP1

AQP1 protein was demonstrated in red cells as well as other tissues with important secretory roles including choroid plexus (cerebrospinal fluid), non-pigment epithelium in anterior compartment of eye (aqueous humour), cholangiocytes (bile), and capillary endothelium in many organs including bronchial circulation of the lung (Agre *et al*., 2002) (Fig. 1.10).

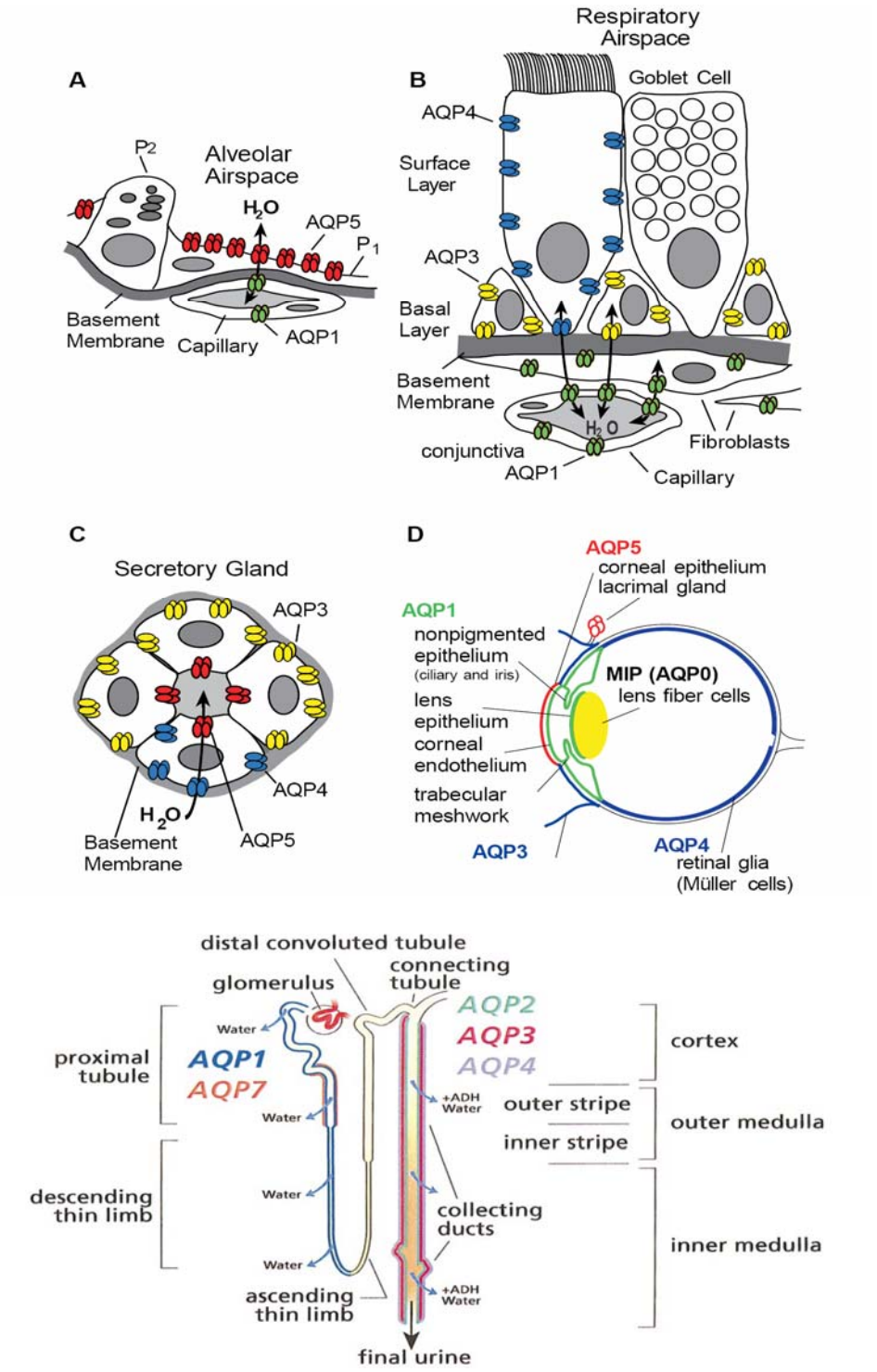

Figure 1.10. Diagrammatic representation of the localization of different aquaporins in several tissues. *A*) Alveolus. *B*) Airway. *C*) Secretory gland. *D*) Eye and E) Nephron and collecting duct system (from Borgnia *et al.*, 1999 and Nielsen *et al.*, 2002).

AQP1 is highly abundant in both apical and basolateral plasma membranes in proximal tubules and descending thin limbs, and it constitutes almost 1% of total membrane protein in kidney cortex. AQP1 is absent in other nephron segments and absent from the collecting duct and is thus exclusively expressed in segments of the kidney

nephron that are constitutively, and highly, water permeable and is not involved in the vasopressin regulation of kidney water transport (Nielsen *et al*., 2002).

AQP1-deficient mice are polyuric and unable to concentrate urine more than 700 mosmol/kgH_2O even in response to water deprivation. Thus AQP1 is required for the formation of concentrated urine (Nielsen *et al*., 2002). However, "AQP1-null" patients with inherited mutations in the gene for AQP1 and thus unable to express the protein, are not symptomatic in the unstressed state, although careful clinical testing shows that they have renal concentration defects and reduced water permeability in the peribronchiolar capillary plexus. Either of these abnormalties could be of great clinical significance if the individuals should be deprived of water or sustain fluid overload from any cause (Kozono *et al*., 2002).

1.2.5.3. AQP2

AQP2 is abundant in the apical plasma membrane and apical vesicles in the collecting duct principal cells and at lower abundance in connecting tubules (Fig. 1.10). Likewise, at low abundance, AQP2 has also been found to be associated with the basolateral plasma membrane, especially in the inner medullary collecting duct principal cells.

AQP2 is the primary target for vasopressin regulation of collecting duct water permeability (Nielsen *et al*., 2002). It was shown that AQP2 is largely restricted to intracellular vesicles in the basal state, but vasopressin induces redistribution to the apical membrane of collecting duct cells accompanied by a fivefold increase in water permeability. When vasopressin is removed, AQP2 is reinternalized and the water permeability returns to baseline. This traffic is due to the regulation of AQP2 by exocytosis by receptor-activated adenylyl cyclase-protein kinase A phosphorylation of S-256 in the C-terminal cytoplasmic domain of the protein (Agre *et al*., 2002).

Unlike patients with AQP1 mutations, AQP2 homozygotes and heterozygotes are severely affected clinically. Altered expression levels of AQP2 have been identified in most known defects of urine concentration or fluid retention. For example, AQP2 is underexpressed in diabetes insipidus and nocturnal enuresis, and AQP2 is overexpressed in congestive heart failure and pregnancy (Kozono *et al*., 2002).

1.2.5.4. AQP3

AQP3 is an aquaglyceroporin principally present in kidney collecting ducts, epidermis, urinary, respiratory, and digestive tracts (Takata *et al*., 2004) (Fig. 1.10). AQP3 appears to be regulated at a biosynthetic level, similar to AQP2. No humans have yet been identified with AQP3 deficiency, and the physiological role as well as the clinical importance of this molecule remains to be established. Mice lacking AQP3 are remarkably polyuric but, however, are able to generate partly concentrated urine after water deprivation. These mice also have an abnormally dry stratum corneum in skin as a result of defective epidermal cell barrier/transport function (Verkman, 2000).

1.2.5.5. AQP4

AQP4 is the most abundant aquaporin in brain, located principally at the perivascular margin of astroglial cells (Fig. 1.10). Its function may be to serve as an exit for excess brain water which can be lethal in cerebral edema. AQP4 is also present in glial lamellae surrounding vasopressin secretory neurons, where it has been suggested to function as an osmoreceptor, and in ependymal cells lining the cerebrospinal fluid-filled cavities. AQP4 is also present in the basolateral membranes of collecting duct principal cells in the inner medulla in kidney. The protein presumably provides the exit pore from these cells during vasopressin-dependent water reabsorption (Agre, 2000).

In addition, the distribution of AQP4 has been defined in retina and optic nerve. Recently, AQP4 has been demonstrated in fast-twitch skeletal muscle in rats. Because fast-twitch fibers accumulate high concentrations of lactate, the presence of AQP4 may permit the rapid water flux needed to restore the osmotic equilibrium (Borgnia *et al*., 1999).

Unlike the other aquaporins, AQP4 exists in two forms owing to the alternate use of two translation initiation sites. Also unlike most aquaporins, AQP4 is not inhibited by mercury and was reported to have higher unit permeability. Disruption of the mouse AQP4 gene has been reported to result in a defect in renal concentration (Borgnia *et al*., 1999).

1.2.5.6. AQP5

The alveolar epithelium is composed mainly of type I cells which express AQP5 at their apical membrane, and the microvascular endothelium expresses AQP1 (Verkman, 2002) (Fig. 1.10). AQP1 and AQP5 provide the major pathways for osmotically driven water transport across the serial endothelial and epithelial barriers. However, as shown by deletion of these genes in mice, they are not required for physiologically important lung

functions. AQP5 resides also in a subset of salivary and lachrymal glands where it presumably regulates the release of saliva and tears (Borgnia *et al*., 1999). Support of this idea was obtained form AQP5 null mice, their saliva secretion was remarkably reduced (Verkman, 2002).

1.2.5.7. AQP6

AQP6 has been shown to reside in intracellular vesicles at three sites in rat kidney: within foot processes of glomerular podocytes, in subapical vesicles of proximal tubules, and in alpha-intercalated cells of the collecting duct (Yasui *et al*., 2000) (Fig. 1.10). AQP6 was observed to colocalize with H1-ATPase in alphaintercalated cells of the collecting duct, suggesting that low pH may be the natural activator of the protein. AQP6 is not a simple water channel, it exhibits minimal water permeability. AQP6 functions as a pH-regulated anion channel with greatest selectivity for nitrate (the halide permeability sequence: $NO_3^- > I^- > Br^- > Cl^- > F^-$) (Liu *et al*., 2005). This aquaporin has been proposed to function in kidney endosomes as a pH-sensitive chloride channel, contributing to the secretion of acid (Agre *et al*., 2002). However, the precise role of AQP6 is still unclear.

1.2.5.8. AQP7

AQP7, an aquaglyceroporin that is permeated by water, glycerol and urea, is highly abundant in spermatocytes (Ishibashi *et al*., 1997). It also is present in other tissues. AQP7 is expressed in the proximal tubule brush border, especially in the segment 3 proximal tubule, and it is likely to be involved in proximal tubule water reabsorption (Nielsen, 2002). AQP7 was also identified in adipose tissue, where it may provide the exit route for glycerol in fasting states (Agre *et al*., 2002). However, little is known about its function**.**

1.2.5.9. AQP8

AQP8 is present mainly in intracellular domains of proximal tubule and collecting duct cells (Nielsen, 2002), in addition to being present in many other organs: kidney, liver, testis, epididymis, jejunum, colon, principal bronchi, and salivary glands (Elkjaer *et al*., 2001). As for other AQPs, the physiological function of this channel remains undefined**.**

1.2.5.10. AQP9

AQP9 was identified in hepatocytes and was shown to be permeated by water, glycerol and a variety of other small uncharged solutes (Tsukaguchi *et al*., 1998). AQP9

could provide the entry into hepatocytes for glycerol, so that the latter could be used as substrate for gluconeogenesis. (Agre *et al*., 2002)

1.2.5.11. AQP10, AQP11 and AQP12

New members of the aquaporin family have recently been identified. AQP10 is an aquaglyceroporin expressed in the human duodenum and jejunum (Hatakeyama *et al*., 2001), in the apical membrane domain of epithelial cells. This suggests that this protein may represent an entry pathway for water and small solutes from the lumen across the mucosal side (Mobasheri et *al*., 2004).

AQP11 has been identified with unusual NPA boxes, but its function is unknown. AQP11 was localized intracellularly in the proximal tubule. AQP11 is essential for the proximal tubular function because AQP11-null mice showed cyst formation of the proximal tubule and early death due to advanced renal failure with polycystic kidneys (Morishita *et al*., 2005).

AQP12 is specifically expressed in the pancreas, selectively localized in the acinar cells of the pancreas, but not targeted to the plasma membrane. Due to the localization, a role of AQP12 in digestive enzyme secretion could be believed (Itoh *et al*., 2005).

The information about this new AQP is scarce, and, therefore, not conclusive about their physiological roles or potential implication in disease. More investigation is required in order to define the importance of this AQP homolog**.**

1.2.6. Aquaporins in protozoa

So far only few protozoan MIPs have been described, and there is not enough information yet to perform separate phylogenetic analyses with them, therefore they are placed in phylogenetic analyses together with animal GLPs and AQPs (Zardoya, 2005). In general, protozoan AQPs are of normal length (277± 28 amino acids), but their sequences are found to be relatively divergent and produced long branches in phylogenetic trees, assuring its unambiguous phylogenetic position (Fig. 1.7). Phylogenetic analyses indicated that protozoan AQP homologues are located generally at the base of animal GLP and AQP trees (Fig. 1.7) and that the GLP and the AQP genes underwent one duplication event in *Trypanosoma* and *Dictyostelium*, respectively (Zardoya, 2005).

It is possible that in the protein repertoire of protozoans there is at least one AQP and one GLP. However, according to phylogenic studies, some protozoans do not show sequences with similarity to GLPs. It is likely that they have highly divergent amino acid

sequences that are difficult to identify by similarity searches (Zardoya, 2005). For example, *Plasmodium falciparum* has only one AQP, which is a bi-functional AQP (PfAQP). It is highly permeable for water and glycerol, as well as other polyols (Hansen *et al*., 2002). *Toxoplasma gondii* has only an AQP (TgAQP) sequence which is closely related to TIP, a water-specific orthodox AQP of plant (47% similarity). However, it is highly permeable to glycerol, implicating that after the transfer of this gene to the parasite, the glycerol conductance appeared (Pavlovic-Juranovic *et al*., 2003). Therefore, comparative sequence analysis is a good approach to find out the protein function, but it is not a conclusive tool.

So far there are only few AQPs from protozoa investigated: *Toxoplasma* (Pavlovic-Juranivic *et al*., 2003), *Plasmodium* (Beitz *et al*., 2004), *Leishmania* (Gourbal *et al*., 2004), *Trypanozoma cruzi* (Montalvetti *et al*., 2004) and *Dyctiostelium* (Flick *et al*., 1997). Likewise, only the AQPs from *Toxoplasma* and *Plasmodium* have completely been biochemically characterized, while *Leishmania* and *T. cruzi* AQPs are only partly characterized.

PfAQP is a highly water and glycerol permeable aquaglyceroporin. Its water permeability is about 300 μm s^{-1} and therefore comparable to that of classical AQP1, whereas the TgAQP value of water permeability is about 100 μm s^{-1}, 3fold lower than that of PfAQP but 8fold higher than that of control oocytes (injected with water); its water conductance is comparable to the renal AQP2. In the case of the TcAQPs, there is only one characterized and this was identified as orthodox AQP, although its water permeability is very low, 30 μm s^{-1}, and thus hardly different from that reported for plain lipid membranes (typically between 10-30 μm.s^{-1}) (Beitz, 2005). Glycerol conductance is high and comparable between these channels, but the permeability for other polyols is quite different. PfAQP allows passing of sugar alcohols with up to 5 carbon atoms in the backbone, whereas TgAQP has a narrower pore resulting in 1/3 of polyol transport capacity than that of PfAQP (Beitz, 2005). From the few protozoan aquaporins reported, one can conclude that they are divergent and also possess differential properties from of rest of the AQPs. It makes sense to characterize these groups of proteins in order to improve the understanding of the physiology and evolution of AQPs as well as permeability mechanisms that AQPs use to selectively transport such a huge diversity of non-charged molecules.

1.3. Aim of this study

Water and glycerol are known to diffuse through membranes. However, the permeability rate is not high enough for most of the biological functions, thus requiring proteins that facilitate rapidly the movement of water and glycerol. On the other hand, many biological membranes represent a real barrier for water and, especially, for glycerol. For example, the defence mechanism of yeast against imbalances of osmolarity is based on both the low permeability of its membrane for glycerol and the existence of aquaglyceroporins. Now it is known that the AQP family is widely distributed throughout nature, and it is also believed that life would be hardly possible if this family was absent. There is few information about AQPs in protozoans, and only recently the first characterizations of some AQPs from protozoan pathogens have been published (Hansen *et al*., 2002; Pavlovic-Juranic *et al*., 2003; Gourbal *et al*., 2004; Montalvetti *et al*., 2004,).

In its life cycle, *Trypanosoma brucei* is submitted to sudden changes in osmolarity, e.g. during the course of transmission from mammals to insects, the renal transit and the whole life within the insect form. Notably, under anaerobic conditions or in a diminution of oxygen supply, the bloodstream form of *T. brucei*, due to its unique organization of glycolysis, requires production of glycerol as an essential intermediate for homeostasis of the redox balance. Under this condition, exogenously added glycerol inhibits glycolysis resulting in cell death. Thus the existence of aquaglyceroporins should play an important role, making it a suitable subject to look for AQP members in this parasite.

The first evidence of AQP presence has been reported by Wille *et al*. (1998). By transport experiments using bloodstream and procyclic *T brucei* forms, they demonstrated that glycerol uptake is linear and temperature independent, which is consistent with facilitated diffusion through a channel protein. These results together with the physiological importance of the putative existence of AQPs in the parasite were the basis of this investigation.

The object of this work was to identify, clone, and characterize protein members of the AQP family from *T. brucei*. The functional expression and biochemical characterization of these proteins was carried out in two different heterologous expression systems, *Saccharomyces cerevisiae* and *Xenopus laevis* oocytes. The selectivity profile for substrates was evaluated not only for classical solutes such as water, glycerol and other polyols, but also for non-conventional solutes which exhibited pharmacological relevance, e.g. arsenic, antimony and dihydroxyacetone. Furthermore, the first results of localization of these proteins in the parasite are also reported and discussed.

The results of this study define the molecular basis of water and glycerol movements across membranes mediated by proteins in *T brucei* and give clues about the importance of this process in glycerol metabolism and in physiological phenomena such as osmoregulation. Likewise, the data indicate that aquaglyceroporins from *T. brucei* could be a target candidate for chemotherapy, mainly as entry pathway for drugs.

2. Materials and Methods

2.1. Materials

2.1.1. Primers and Peptide

Primers for cloning

TbAQP1

Sense: ATG TCT GAC GAA AAA ATT AAC G

Anti sense: TTA GTA GGG AAC AAA GTA TTT G

TbAQP2

Sense: ATG CAG AGC CAA CCA GAC AAT G

Anti-sense: TTA GTG TGG AAG AAA ATA TTT G

TbAQP3

Sense: ATG CAG AGC CAA CCA GAC AAT G

Anti-sense TTA GTG TGG CAC AAA ATA TTT G

Primers against the spliced leader sequence

CGC TAT TAT TAG AAC AGT TTC TG

Primer against the poly-A tail

CCC GGG $T_{(20)}$VNN

GFP

Sense: ATG GTG AGC AAG GGC GAG GAG

Anti-sense: TCT AGA TCC GGT GGA TCC AAG

All primers represent only sequences without cut site. The restriction sites were chosen depending on plasmids and the specific task. GFP was placed at N-terminus of TbAQPs. Therefore, the GFP sense primer was made with initiation codon and the anti-sense primer was synthesized without termination codon.

Primer for probe production (Northen blotting)

ß-tubuline

Sense: ATG CGC GAA ATC GTC TGC GTT CAG

Antisense: CGG AGC CAG TAC CAC CAC CAA

Amplified region (438):

ATGCGCGAAATCGTCTGCGTTCAGGCTGGCCAATGCGGTAACCAGATCGGCTCAAAGTTCT
GGGAGGTGATCAGTGACGAGCACGGTGTGGACCCCACAGGTACCTACCAGGGTGACTCTGA
CCTGCAGCTGGAGCGCATCAATGTGTACTTTGATGAGGCAACGGGAGGTCGCTATGTGCCC
CGCTCCGTGCTGATTGATCTGGAGCCAGGTACAATGGACTCCGTACGTGCTGGCCCCTATG
GTCAGATCTTCCGCCCCGACAACTTCATCTTTGGACAGTCTGGCGCCGGCAACAACTGGGC
AAAGGGCCACTACACGGAGGGTGCGGAACTGATCGACTCTGTGCTCGATGTGTGCTGCAAG
GAGGCGGAGAGCTGTGACTGCCTCCAAGGCTTCCAGATCTGCCACTCCCTTGGTGGTGGTA
CTGGCTCCG

TbAQP1

Sense: TAC CCG GTT ACA TCG CAG CAC A

Antisense: GGA TAA ACA ACG GCA CCC AAA AGT

Amplified region (438):

TACCCGGTTACATCGCAGCACAAATGCTCGGTGCTTTTGTTGGTGCGGCATGTGCTTATGG
TGTTTATGCTGATCTTCTGAAGCAACACAGCGGTGGGTTGGTTGGTTTTGGTGATAAGGGT
TTTGCCGGTATGTTCAGCACGTACCCACGCGAAGGGAATCGTCTCTTTTACTGCATCTTTT
CCGAGTTTATCTGCACAGCAATTCTTCTCTTTTGCGTCGGTGGCATATTTGATCCCAATAA
CTCACCTGCCAAAGGGCATGAACCGCTGGCAGTTGGTGCTCTTGTGTTTGCTATTGGAAAC
AACATTGGTTATGCATCCGGTTATGCGATTAATCCGGCTCGTGATTTTGGTCCAAGAGTTT
TCTCCGCTATTCTCTTCGGTTCCGAGGTGTTTACGACGGGAAATTATTACTTTTGGGTGCC
GTTGTTTATCC

TbAQP2

Sense: CCT CAC TAC TTG TTC CAG ATT TTG

Antisense: GAT TCA TCG CAA GGG GAG ACG CTA

Amplified region (504bp):

CCTCACTACTTGTTCCAGATTTTGGGCTTCTCGGTCTTACGATTGGTATTGGTGTGGCTGT
CACGATGGCTCTGTATGTTTCACTGGGCATCTCCGGTGGCCATCTCAACTCTGCCGTCACC
GTTGGCAATGCGGTTTTCGGTGATTTCCCTTGGAGAAAAGTCCCCGGCTACATCGCGGCGC
AGATGCTCGGCACTTTCCTTGGTGCTGCCTGCGCTTACGGAGTGTTTGCTGATCTCCTGAA
GGCGCATGGTGGTGGTGAGTTGATTGCCTTCGGTGAAAAGGGGATTGCGTGGGTGTTTGCC
ATGTACCCCGCGGAAGGAAATGGTATATTTTATCCAATTTTTGCTGAACTCATTTCCACCG
CAGTGCTACTGCTCTGTGTCTGCGGTATCTTTGACCCCAATAACTCTCCTGCCAAGGGGTA
CGAAACGGTAGCTATTGGTGCTCTTGTCTTCGTCATGGTCAACAACTTCGGCTTAGCGTCT
CCCCTTGCGATGAATC

TbAQP3

Sense: GGT TAT CAT TGA TGG GAA ACT GG

Antisense: GGA TTT ATT GCG TAA CCC GTT G

Amplified region (504bp):

GGTTATCATTGATGGGAAACTGGGGTTCCTCAGCATTACGCTTGGTTGGGGCATTGCCGTC
ACGATGGCTCTGTATGTTTCATTGGGTATCTCGAGCGGCCACCTTAATCCCGCCGTCACCG
TTGGCAATGCGGTTTTCGGTGATTTCCCTTGGAGAAAAGTCCCCGGCTACATCGCGGCGCA
GATGCTCGGTGCCTTTCTTGGTGCTGCCTGCGCTTACGGAGTGTTTGCTGATCTCCTGAAG
GCGCATGGTGGTGGTGAGTTGATTGCCTTCGGTGAAAAGGGGACCGCAGGTGTGTTCAGCA
CCTACCCAAGGGATTCAAATGGTCTATTTTCTTGTATCTTTGGTGAGTTTATATGTACGGC
GATGCTATTGTTCTGTGTCTGCGGTATCTTCGACCCCAATAACTCTCCTGCCAAGGGACAC
GAGCCGTTGGCAGTTGGTGCTCTTGTCTTCGCCATTGGCAATAACATCGGTTACTCAACGG
GTTACGCAATAAATCC

Peptides Sequences for antibodies production:

Peptide-TbAQP1: KINVHQYPSEADVRGLKARC

Peptide-TbAQP2: CDVQKHEVAEAQEKPV

Peptide-TbAQP3: CEKGTAGVFSTYPRDSN

2.1.2. General Chemicals

Adenosine5´(α-^{32}P) trphosphate	Amarsham Biosciences, Freiburg
Acrylamide (Rotiphorese Gel 30)	ROTH, Karlsruhe
Agar-Agar	ROTH, Karlsruhe
Agarose	FMC
alk. phosphatase (CIP)	NEB GmbH Schwalbach/Taurus
Ampicillin	ROTH, Karlsruhe
Albumin, Bovine (BSA)	Sigma, Deisenhofen
3-aminobenzoic acid ethyl ester	Sigma, Deisenhofen
Ammonium persulphate (APS)	Merck, Eurolab GmbH Germany
Annexin-V	Roche, Mannheim
ATP	Sigma, Deisenhofen
Bradford	BioRad Laboratories GmbH, München
Bisbenzimide	Sigma, Deisenhofen
Bromophenol blue	ROTH, Karlsruhe
Dimethyl sulfoxide (DMSO)	Sigma, Deisenhofen
1kb DNA ladder	NEB GmbH Schwalbach/Taurus
100 bp DNA ladder	NEB GmbH Schwalbach/Taurus
dNTPs	Sigma, Deisenhofen
DTT	ROTH, Karlsruhe
EDTA	ROTH, Karlsruhe
Ethidium bromide	ROTH, Karlsruhe
Formaldehyde (37%)	Sigma, Deisenhofen
G-418	Sigma, Deisenhofen
Glass bead	Sigma, Deisenhofen
Glycerol (100%)	Sigma, Deisenhofen
Glycerol (87%)	Merck, Eurolab GmbH Germany
[^{14}C]Glycerol	Amarsham Biosciences, Freiburg
Glycine	Merck, Eurolab GmbH Germany
GTP	Sigma, Deisenhofen

Haemin	Sigma, Deisenhofen
HEPES	Sigma, Deisenhofen
Hygromycin B	Invitrogen GmbH, Karlsruhe
isopropanol	Merck, Eurolab, GmbH germany
Imidazol	Merck, Eurolab GmbH Germany
Isopropanol	Merck, Eurolab GmbH Germany
L-Isoleucine	Sigma, Deisenhofen
Leupeptin	Sigma, Deisenhofen
MEM vitamine solution	Sigma, Deisenhofen
Mowiol,®	Calbiochem, Schwalbach
Protein molecular marker	Sigma, Deisenhofen
Prestained protein ladder, BenchMark™	Gibco BRL, Karlsruhe
Pepstatin A	Sigma, Deisenhofen
Pfu-polymerase	Stratagene Europe Netherland
Pwo polymerase	Roche, Mannhein
Phenol	ROTH, Karlsruhe
Polyethylene glycol 4000 (PEG 4000)	ROTH, Karlsruhe
Restriction enzyme and buffers	NEB GmbH Schwalbach-Taurus / Fermentas
RNasin®ribonuclease inhibitor, 40U/ml	Promega, Madison, USA
Salmon perm	Sigma, Deisenhofen
Sodium acetate	Sigma, Deisenhofen
Sodium dodecyl sulfate (SDS)	Serva, Heidelberg
SuperSignal® West Pico Chemiluminescent substrate	Pierce, Illinois, USA
Taq-polymerase	Sigma, Deisenhofen
T4 polynucleotide kinase	NEB GmbH Schwalbach/Taurus
T4-DNA-ligase	NEB GmbH Schwalbach/Taurus
Tetracycline	Sigma, Deisenhofen
TEMED	ROTH, Karlsruhe
Tris-hydroxymethyl-aminomethane (Tris)	Serva, Heidelberg

Triton X-100	Sigma, Deisenhofen
Tween 20	ROTH, Karlsruhe
Ultima Gold^{TM} Scintillation cocktail	Packard, Frankfurt a.M.
Urea	Merck, Eurolab GmbH Germany
Yeast extract	ROTH, Karlsruhe

2.1.3. Plasmids

pBSKS^{+}	Stratagene, La Jolla, Ca, USA
p416MET25	Mumberg *et al.*, 1994
pLew100	http://tryps.rockefeller.edu/
pT7T5	Paul Krieg, Center for Developmental Biology, University of Texas, USA

2.1.4. Kits

Agarose gel elution kit	Qiagen GmbH, Hilden
Hot Star Taq® PCR	Qiagen GmbH, Hilden
HexaLabel DNA labeling Kit	Fermentas GmbH, St. Leon-Rot
Ligation	Qiagen GmbH, Hilden
Mini, midi prep	Qiagen GmbH, Hilden
Omniscript reverse Transcription	Qiagen GmbH, Hilden
RNeasy-mini kit	Qiagen GmbH, Hilden

2.1.5. Antibodies

Anti-chicken IgG phosphatase conjugate	Sigma, Deisenhofen
Anti-chicken IgY FITC conjugate	Sigma, Deisenhofen
Anti-TbAQPs	Biogenes, Berlin

2.1.6. Equipments

Biofuge A	Heraeus, Osterode
Electrophoresis Minigel System 'Mighty Small II' SE 250	Hoefer Scientific Instrument, San Francisco, USA

ELISA reader	MRX II, Dynex Technologies, England
FACS Calibur®	Becton Dickinson & Co., NJ, USA
Incubator	Heraeus, Osterode
Labor Centrifuge 302K	Sigma, Deisenhofen
Liquid Scintillation Counter LSC 1600 CA	Packard, Frankfurt a.M
Microfuge E	Beckmann, München
Microscope Olympus BH2 fluorescent	Zeiss, München
Microscope	Zeiss, München
Nanoliter 2.000	World Precision Instruments, USA
Minicicler TM	MJ Research, Inc. USA
Puller-universal	Zeitz Instrumente München
Semi-Dry Electrophoretic transfer Cell	BioRad, München

2.1.7. Experimental organisms

2.1.7.1. *Escherichia coli* XL-1 Blue: Bacteria strains were purchased from Stratagene, Heidelberg

2.1.7.2. *Saccharomyces cerevisiae*: Yeast strains used in this study were W303-1A (MAT a Leu2-3/112 ura3-1 trp1-1 his3-11/15 adec2-1 can1-100 gal SUC2) and YSH295 (MATa Leu2-3/112 ura3-1 trp1-1 his3-11/15 adec2-1 can1-100 gal SUC2 fps1Δ:LEU2), kindly provided by Dr. Stefan Hohmann (Goteborg University, Sweden). Other yeast strain used was BY4742 (MAT a; his3D1 leu2D0 lys2D0 ura3D0 YLL043w::kanMX4) from Euroscarf, Frankfurt.

2.1.7.3. *Trypanosoma brucei*: in this work were used a monomorphic strains of Trypanosoma *brucei* bloodstream forms known as strain EATRO 427; clone MITat 1.2 (**M**olteno **I**nstitute **T**rypanozoon **a**ntigenic **t**ype, Cambridge) with the VSG antigen variant 221. Procyclic forms were obtained from MITat 1.2 using a standard transformation protocol (Overath *et al*., 1986). Transfected Procyclic form *T. brucei* cells (strain 29:13; a gift from G.A.M. Cross), constitutively expressing T7RNAP and TETR were also used in this study.

2.1.7.4. Animals: *Xenopus laevis*, the South African clawed frog, were purchased from *Xenopus Express* (USA) or *Nasco* (USA). The frogs were housed in the veterinarian animal facility at the Physiological Institute, University of Tuebingen. The animals were maintained in covered tanks containing 200 mosm/kg salt solution, under controlled lighting conditions (Light-dark cycle, 12h) and a constant ambient temperature 22 °C. Sprague-Dawley rats were purchased from Interfauna, Tuttlingen and housed in the veterinarian facility at the Biochemical Institute, University of Tuebingen.

2.1.8. Media, buffers and solutions for the different organisms

2.1.8.1. Bacteria

Luria-Bertani medium (LB-medium) pH 7.0

Peptone	1%
Yeast extract	0.5%
NaCl	0.5%

Adjusted to pH 7.0 using 1 M NaOH.

Ampicillin stock solution (1000 x)

Ampicillin in 70 % ethanol	50 mg/ml

Culture plates

Agar-Agar in LB medium	2%

Transformation medium for *E. coli* (TSS)

In LB medium:

DMSO	5%
$MgCl_2$	50 mM
PEG6000	10%

2.1.8.2. Yeast

YPD medium (Rich medium)

Yeast extract	1%
Peptone	2%
Glucose	2%

Adjusted to pH 5.5 using 1 M NaOH.

Glucose was prepared as a 20% (10X) solution and autoclaved separately.

Complete minimal (CM) dropout medium

- 0.2% of "dropout" powder. The constitution of this powder in percentage is:

  0.59% of P-aminobenzoic acid and 5.85% of following compounds: L-alanine, L-arginine, L-asparagine, L-aspartate, L-cysteine, L-glutamine, L-glutamate, L-glycine, L-myo-inositol, L-isoleucine, L-methionine, L-phenylalanine, L-proline, L-serine, L-threonine, L-tyrosine, L-valine.
- 0.67% of yeast nitrogen base (YNB) without amino acids, Difco, Hamburg
- 0.5% of ammonium sulphate
- 2% of Glucose (or another carbon source)

Note: the following compound, which represent autotrophic marker, were added to the end concentration indicated according to the required selection: L-histidine (300 μM), L-leucine (1.7 mM), L-lysine (1 mM), L-tryptophan (400 μM), adenine (300 μM) and uracil (200 μM). In this study usually uracil was used as marker, it means, all compounds were added except uracil. CM media without methionine and cysteine (CM-S) were prepared as induction media when the pRS416-plasmid was used.

Culture plates for yeast

Agar-agar in YDP (either CM or CM-S)	2%

Transformation solutions for *Saccharomyces cerevisiae*

Litium-acetate washing solution

Litium-acetate (in 1X TE)	100 mM

Autoclaved

10x TE buffer pH:7.5

Tris-HCl	100 mM
EDTA	10 mM

Adjusted to pH 7.5 using 1 N HCl and sterile filtrated or autoclaved

10X Litium-acetate transforming solution

Litium-acetate	1 M

Adjusted to pH 7.5 using 1 N HCl and autoclaved

PGE solution

PEG (4000)	50%

DNA carrier solution

DNA from salmon testes (in TE buffer)	2 mg/ml

Preparation: High weight molecular DNA from salmon testes (Sigma D-1626) was added to TE buffer to reach 2mg/ml concentrations. It was dispersed repeated pipetting and vigorous stirring on magnetic stirrer. The procedure was stopped when the viscosity of the solution had greatly been decreased. Aliquots were stored at -20 °C. Before to use it was heat-denature in boiling water for 5min and then chilled quickly on ice.

Mix-transformation solution:

For each transformation:

30 µl 10X TE buffer

30 µl 10X lithium-acetate transforming solution

240 µl PEG (4000) solution

10 µl DNA carrier

1-4 µl plasmid DNA

Buffer for yeast lysis

Breaking buffer:

Tris-HCl	25 mM
EDTA	5 mM

Adjusted to pH 7.5 using 1 N HCl.

Storage Buffer

Potassium phosphate (KPi) (pH: 6.3)	50 mM
$MgSO_4$	1 mM
Glycerol	20%

2.1.8.3. Trypanosoma

Citrat-Glucose-Anticoagulant (CGA) pH 7.7

Na_3-citrate x $2H_2O$	100 mM
Glucose	40 mM

Separation buffer, pH 8.0 (Lanham and Godfrey, 1970)

Na_2HPO_4 x $2H_2O$	57 mM
KH_2PO_4	3 mM
NaCl	44 mM
Glucose	55 mM

Basic medium, pH 7.4

(According to Eagle, 1959; modified by Duszenko *et al*., 1985, 1992)

	[mg/l]
$CaCl_2$ x H_2O	265
KCl	400
$MgSO_4$ x $7H_2O$	200
NaH_2PO_4 x H_2O	140
NaCl	6800
HEPES	7140
Phenol Red	10

These chemicals were dissolved in water and the pH was adjusted to 7.4.

L-Arginine/HCl	126
L-Cysteine	24
L-Histidine/HCl x H_2O	42
L-Isoleucine	52

L-Leucine	52
L-Lysine	73
L-Methionine	15
L-Phenylalanine	100
L-Threonine	48
L-Tryptophan	10
L-Tyrosine	100
L-Valine	46
L-Ornithine/HCl	10
Adenosine	12

These amino acids and adenosine were dissolved separately, mixed together and then added to following stock solutions:

	[ml/l]
MEM nonessential amino acids solution	10
MEM vitamine solution	10

This so-called basic medium was sterilized and stored at 4°C. It can be used for up to 3 months.

Complete culture bloodstream medium

For preparation of a complete culture medium the following stock solutions were added to the basic medium:

		[ml/l]
$NaHCO_3$	(750mg/10ml distilled water)	30
L-Cysteine	(30.3mg/10ml distilled water)	10
Bathocuproindi-sulfonate (BCS)	(5.6mg/10ml distilled water)	1
Hypoxanthine	(13.6mg/10ml 0.1 N NaOH)	10
2'-Desoxythymidine	(3.9mg/10ml distilled water)	10
L-Glutamine	(292mg/10ml distilled water)	10
Myristic acid linked on defatted BSA (50 x)		20
Fetal calf serum	(heat inactivated: 30min. 56°C)	150
Penicillin-Streptomycin-solution		5
Glucose		5.4 g

Preparation of the myristic acid linked to defatted BSA (Ferguson and Cross, 1984):
24 mg myristic acid was dissolved in 100 µl ethanol (95%). This myristic acid was then gradually added to a BSA solution (1 g defatted BSA/20ml distilled water). The medium was sterilized and stored at 4°C for about 4 weeks.

Procyclic culture medium pH 7.4

The following stock solutions were added to the basic medium to cultivate of procyclic parasites:

		[ml/l]
Glutamine	(5.6mg/10ml distilled water)	10
Haemin	(25mg/10ml distilled water)	3
Pyruvate	(220mg/10ml distilled water)	10
Proline	(600mg/10ml distilled water)	10
Fetal calf serum	(heat inactivated: 30min. 56°C)	100
Penicillin-Streptomycin-solution		5

The culture medium was sterilized and stored at 4°C for up to 4 weeks.

Trypanosome dilution buffer (TDB); pH 7.7 (Cross, 1975)

KCl	5 mM
NaCl	80 mM
$MgSO_4$ x $7H_2O$	1 mM
Na_2HPO_4 x $2H_2O$	20 mM
NaH_2PO_4 x H_2O	2 mM
D-Glucose	20 mM

Freezing medium

77 ml TDB and 23 ml Glycerin (87%). Sterile filtrated

10 mM buffer (PBS) for trypanosoma lysis, pH 7.4

Na_2HPO_4	7.7 mM
KH_2PO_4	2.3 mM
NaCl	120 mM
KCl	8.7 mM

Protease inhibitor mix (1000 x)

Pepstatin	1 mM
Chymostatin	1 mM
Leupeptin	1 mM

The 3 inhibitors were dissolved in DMSO and stored as aliquots at -20°C.

Lysis buffer

PBS	10 mM
Protease-Inhibitor-Mix	1X
Triton X100	0.1%

Zimmerman Post-Fusion medium

NaCl	132 mM
Na_2HPO_4	8 mM
KH_2PO_4	1.5 mM
Mg acetate,	0.5 mM
Calcium acetate	90 µM
Glucose	1% (w/v)

Adjusted to pH 7.0 and autoclaved.

2.1.9. Buffers and solutions for SDS-PAGE (according to Laemmli, 1970)

Running gel (2.6% C)	(10% T)	(12% T)
Rotiphorese gel 30	15.2 ml	18.2 ml
1 M Tris-HCl pH 8.8	17.2 ml	17.2 ml
Distilled water	13.2 ml	10.2 ml
10% SDS	456 µl	456 µl
10% Ammonium peroxodisulfat	156 µl	156 µl
TEMED	48 µl	48 µl

Stacking gel

Rotiphorese Gel 30	4.0 ml
1 M Tris-HCl pH 6.8	3.0 ml
Distilled water	16.8 ml
10% SDS	240 µl
10% Ammonium peroxodisulfat	120 µl
TEMED	24 µl

Sample buffer (2X)

Tris-HCl pH 6.8	180 mM
SDS	4.4%
Glycerol	19.4%

DTT/BPB (20X)

DTT	1 M
Bromophenolblue	0.2%

Running buffer

Tris/HCl	25 mM
Glycine	192 mM
SDS	0.1%

Coomassie Staining

Staining solution

Coomassie Brilliant Blue R	0.1%
Methanol	40% (v/v)
Acetic acid	10% (v/v)

Distaining solution

Acetic acid	10% (v/v)
Methanol	40% (v/v)

2.1.10. Buffers and solutions for Western Blot

Transfer buffer, pH 9.2 (Bjerrum and Schafer-Nielsen, 1986)

Tris/HCl	48 mM
Glycine	39 mM
SDS	0.00375%
Methanol	20%

Blocking buffer

Defatted milk power in 2fold-PBS (or in PBST)	10 %

PBS

Na_2HPO_4	80 mM
NaH_2PO_4	20 mM
NaCl	100 mM
KCl	0.2g/l

PBS-Tween

Tween 20 in PBS	0.1%

Developing buffer for alkaline phosphatase (AP buffer), pH 8.9

Tris/HCl	20 mM
NaCl	150 mM
MgCl2	10 mM

Stain Solutions

BCIP	0.38 mM
NBT	0.4 mM

BCIP and NBT were dissolved in 100% and 70% DMSO, respectively.

BCIP: Bromo-chloro-indol-phosphate. NBT: nitro blue tetrazolium. The end developing solution was prepared mixing 0.5: 1: 97.5 from BCIP, NBT and AP buffer, respectively.

2.1.11. Buffers and solutions for molecular biology

TE-buffer, pH 7.5

Tris/HCl	10 mM
EDTA	1 mM

DNA gel electrophoresis

DNA sample buffer, pH 8.0

Glycerol	5%
Bromophenol blue	0.025%
EDTA	0.1 M

TAE- buffer, pH 8.0

Tris-HCl	0.04 M
EDTA	0.001 M

Adjusted to pH 8.0 with HCl.

RNA gel electrophoresis

RNAase-Free water was used as dissolvent in all solutions

FA (10X) Gel Buffer

MOPS	200 mM
Sodium Acetate	50 mM
EDTA	10 mM

RNA loading buffer (5x)

Bromophenolblue	0.16%
EDTA (pH: 8.00)	4 mM
Formaldehyde	2.7%
Glycerol	20%
Formamid	30%
FA (10X) gel Buffer	40%

FA Running Buffer

FA (10X) gel Buffer	10%
Formaldehyde	0.74%

Gel preparation: 0.5 g agarose were dissolved in 50 ml of FA (1X) gel buffer using microwave. Thereafter, 0.9 ml of 37% formaldehyde and 0.5 µl of ethidium bromide were added.

2.1.12. Solutions for FACS analysis

Tetramethylrhodamine ester (TMRE) solution

TMRE (in H_2O dest.)	25 µM

Dichlorodihydrofluorescein diacetate (DCFH-DA) stock solution

DCFH-DA (in DMSO)	10 mM

Lysis buffer for DNA content analysis

Na_2HPO_4	7.7 mM
KH_2PO_4	2.3 mM

Digitonin stock solution

Digitonin (in H_2O dest.)	6.4 mM

Staining solution for DNA content analysis

PBS	2 ml
Propidium iodide (10 mg/ml)	4 µl

Annexin-V-buffer, pH 7.4

Hepes	10 mM
NaCl	140 mM
$CaCl_2$	5 mM

Staining solution for phosphatidylserine determination (for each sample)

Annexin-V-Puffer	48 µl
Annexin-solution (commercial)	1 µl
Propidium iodide (50 µg/ml in H_2O dest.)	1 µl

2.1.13. Immunofluorescence

Hank's buffered saline (HBS) pH 7.3

NaCl	0.85%
HEPES	25 mM

Fix-solution

Paraformaldehyde in HBS (or PBS)	4%
Glutaraldehyde	0.1%

The paraformaldehyde in HBS (or PBS) was dissolved using microwave avoiding boiling. The solution was cooled on ice and then glutaraldehyde (25% stock solution) was added to obtain 0.1% final concentration. This fix-solution was always used fresh.

BSA solution

BSA (in PBS)	1%

Na-glycine buffer pH 7.2

Na_2HPO_4	100 mM
Glycine	100 mM

2.1.14. Solutions for oocytes

(ND96), pH 7.4

NaCl	96 mM
KCl	2 mM
$CaCl_2$	1.8 mM
$MgCl_2$	1 mM

HEPES	5 mM

The solution is about of 214 mosm./Kg. It was autoclaved for sterilization

ND96 storage solution

The ND 96 storage solution is the same ND96 complemented after sterilisation with 5 mM pyruvate, 50 µg/ml gentamycin and 0.5 mM theophylline.

Homogenization buffer for preparation of *Xenopus* oocytes crude extract:

Tris-HCl	20 mM
NaCl	100 mM
Triton X-100	1%

Adjusted to pH 7.6 with HCl

Lysis buffer for preparation of *Xenopus* oocytes membranes

Na_2HPO_4 (pH 7.4)	7.5 mM
EDTA	1 mM

Note: Prior use, protease inhibitors were added to the above indicated solutions according to recommendation of the manufacture company.

2.1.15. Electron microscopy

EM-buffer, pH 7.4 (Glauert, 1975; Langreth and Balber, 1975)

Sodium cacodylate x 3 H_2O	0.1 M
Sucrose	0.12 M

Glutaraldehyde solution (Glauert, 1975)

Glutaraldehyde in EM-buffer	2%

Uranyl acetate solution

Uranyl acetate in distilled water	5%

This solution was stored at RT in dark.

Osmiumtetroxide solution

Osmiumtetroxide in distilled water	3%

Epon-Mix (Luft, 1961)

Epon 812	16.8 g
DDSA	8.0 g
MNA	8.7 g
DMP-30	0.3 g

Must be prepared fresh before use.

2.1.16. Cytotoxicity buffer

p-nitrophenyl phosphate (in 1M sodium acetate, pH 5.5)	20 mg/ml
Triton X-100	1%

2.2. Methods

2.2.1. General methods

2.2.1.1. Glycerol, ammonia, and protein determination

The glycerol concentration was determined enzymatically using the glycerol kinase/ glycerol-3-phosphate dehydrogenase method (Bergmeyer, 1984). Protein concentrations were estimated using the Bradford method (Bradford, 1976) with serum albumin as a standard.

For determination of ammonia concentration, the glutamate dehydrogenase enzyme-assay was used according to the Bergmeyer and Beutler (1990) with some modification. A reaction mix containing 607 µl buffer TEA-HCl (pH 8, 155 mM), 217 µl ADP (3,6 mM), 50 µl of NADPH (6 mM), 217 µl of α-oxoglutarate (71 mM) (all compounds were dissolved in TEA-HCl buffer) and 300 µl of standard (NH_4Cl) or sample was measured at 340 nm after the stabilization of base line (OD1). Thereafter, 14 µl of glutamate dehydrogenase (0.74 U/µl, in TEA-HCl buffer) was added and then the decay of OD was monitored until a constant value was obtained (OD2). The data were analysed plotting the standards concentration vs. delta OD.

2.2.1.2. SDS-PAGE

Preparation of sample:

Trypanosomes: the parasites grown in exponential and stationary were lysed in a hypo-osmotic buffer (PBS) containing a protease inhibitor mix.

Yeast extract and isolation of yeast total membrane: Usually 40-50 ml of grown cells on selective medium to mid-logarithmic phase (about 2 OD) were harvested by centrifugation at 4000 rpm for 10 min in a table centrifuge. Supernatant was discarded, the pellet washed once with 20 ml water and once with breaking buffer (0°C). The cells were resuspended in 200 µl of breaking buffer (0°C) with protease inhibitor mix, and transferred to a microcentrifuge tube containing 0.5 g of glass bead pre-washed with diluted HCl and then pre-cooled on ice. The cells were broken by five cycles of 45 sec vortexing and 45 sec resting on ice (to reach maximal agitation, the vortex mixer should be set to permanent operation). To store by -20°C, glass bead were discarded by centrifugation after adding adequate among of storage buffer and inhibitor mix (yeast extract). For isolation of yeast total membrane, it was added 1 ml of breaking buffer containing protease inhibitor mix to

the broken cell after vortex cycles. Thereafter, the sample was vortexed and glass bead were removed by centrifugation at 3,000 g for 2 min at 4°C. The supernatant (membranes and soluble proteins) was centrifuged at 75,000 g or 30 min at 4°C. The supernatant was discarded and the pellet was resuspended in 100 µl of storage buffer containing protease inhibitor mix and stored by -20°C.

Xenopus oocytes, crude extract and total membrane preparation: Due to the excessive amounts of egg yolk in the cytosol of the oocytes, it is not possible to prepare samples by direct homogenisation of oocytes with a buffer (Wagner *et al*., 2000). The simplest method to obtain an extract was as following: Oocytes were homogenized in ice-cold homogenisation-buffer (10 µl per each oocyte) with proteases inhibitor using a 1 ml pipette to break open the cells by pipetting up and down 20-30 times. The homogenate is subsequently centrifuged at 10,000 g and then the supernatant was used directly used for gel electrophoresis. For isolation of total oocytes membrane, oocytes were mixed with cold lysis buffer (10 µl per each oocyte) containing proteases inhibitor and the cells were broken as above described. The homogenate was centrifuged at 500 g for 5 min at 4°C. The supernatant was transferred to an ultracentrifuge tube and centrifuged at 16,000 g for 30 min at 4°C. The membrane pellet obtained was washed twice with 2 ml aliquots of ice-cold lysis buffer containing proteases inhibitor. Thereafter, this pellet was resuspended in the same buffer and stored at -20°C.

After samples preparation of trypanosomes, yeast and oocytes, the protein concentration was determined.

SDS-polyacrylamide gel electrophoresis (SDS-PAGE)

Samples were mixed with sample buffer (1:1) and heat-denatured by either boiling for 3 min or incubation at 4°C for at least 40 min (to prevent membrane protein aggregation). SDS-PAGE was performed according to the method of Laemmli (1970). The gel contain two part; resolving gel (10%) and stacking gel (5%) and was prepared according to the follow schema:

For 4 Mini-Gele (10%)(8x10 cm)	Resolving gel (ml)	Stacking gel (ml)
30% acrylamide mix	7.6	2
H_2O	6.6	8.4
10% SDS in H_2O	0.228	0.12

1M Tris/Hcl buffer. pH 8.8	8.6	-
1M Tris/Hcl buffer. pH 6.8	-	1.5
10% ammonium persulfate	0.078	0.06
TEMED	0.024	0.012

After polymerization was completed (~30 min for each gel) 10-30 µg of protein of the prepared samples were loaded into the pocket bottom in the gel. At the beginning a voltage of 100 V was applied to the gel. After the dye front has moved into the resolving gel, the voltage was increased to 200 V and the gel was run until the bromophenol blue reaches the bottom of the resolving gel. For determination of the molecular mass of proteins, molecular markers were run.

2.2.1.3. Western blot analysis

Semi-Dry-Apparatus was used to perform Western blotting, according to the manufacture's instructions. Three filter papers were laid on the anode plate. Then nitrocellulose membrane, gel and 3 filter papers were added one after another. All the materials were soaked with transfer buffer before use. The electro transfer was carried out by 10V (about 400 mA) for 1h. Thereafter, the membrane was incubated in blocking buffer for at least 2h at RT (or overnight at 4°C) with gentle shaking. The membrane was washed 5 times for 5 min with gentle shaking in TBS buffer then incubated with the first antibody diluted in TBS buffer for 1h at RT (or overnight at 4°C). The membrane was washed as it has already described above, then incubated with the second antibody diluted in TBS for 1h and washed again using TBS buffer. Finally, the developing solution was added and the reaction was stopped with PBS.

2.2.1.4. Dot blot analysis

The membrane was direct impregnated with 100 ng of TbAQP1-3 peptides and the detection methods used was the same than those for western blotting analysis.

2.2.1.5. Northen blot analysis

The Northern blot analysis was performed according to Jungwirth *et al*., (2001). Samples of total RNA from procyclic form and bloodstream form (growing in exponential and stationary phase) were prepared as described in the Qiagen RNeasy hand-book. RNA sample (15 µg) were denatured and separated on a 1.2% agarose gel containing 1.2 M

formaldehyde. Amount of rRNA was used as control to monitor RNA loading. The gels were transferred to a Hybond-N filter and hybridized with a probe containing about 500bp from coding sequence of the *TbAQP* genes and of the *ß-tubulin* as control. Northern blots were visualized by autoradiography

2.2.2. Standard protocols in molecular biology

2.2.2.1. DNA precipitation

The sample was mixed with 1 volume isopropanol and 1/10 volume 3 M sodium acetate (pH: 5.2), incubated at RT for 10 min and then centrifuged at 17,000 rpm for 15 min at 4°C. The supernatant was removed and the pellet was washed twice using 70% ethanol (-20°C) by centrifugation, 17,000 rpm for 15 min at 4°C. The supernatant was discarded and the pellet was store at RT until the last trace of fluid had been evaporated. Immediately, DNA was dissolved in the desired water volume (or in TE buffer).

2.2.2.2. DNA digestion

DNA was digested with endonucleases (1µg/U) usually in 20-50 µl end volume, for 2 h (sometimes overnight) incubation at 37°C (only by Sma I at 25°C) using producer's buffer according to the manufacturer's instruction. Digestion products were checked by gel electrophoresis.

2.2.2.3. DNA purification

Plasmids, DNA and PCR products were purified by mini -midi- preps and gel extraction using Qiagen kit (see materials). The procedures were performed as described in the Qiagen RNeasy handbook.

2.2.2.4. Agarose gel electrophoresis for DNA

The samples were mixed with loading solution and were electrophoresed along with size markers on horizontal agarose gels (1% in TAE buffer) with 0.5 µg/ml ethidium bromide. The electrophoresis was carried out in TAE buffer at 90 kV for 45 min and DNA was visualized under UV light.

2.2.2.5. PCR

PCR reactions were performed using Taq-polymerase (Hot Star Taq®) according to manufacture's instruction. The reaction was cycled through the following temperature profile, preceded by an unique 5 min denaturation step at 94°C:

Denaturation	45 sec, 94°C
Annealing	30 sec, (temperature according to Primers)
DNA synthesis	2 min, 68°C
N° of cycles	33
Final DNA synthesis	3 min, 68°C

Annealing temperatures for each pair of primer were calculated using DNAMAN software. Negatives controls were made performing the reaction without templates.

2.2.2.6. Phosphorylation of 5`-end.

The DNA fragment was incubated with T4 polynucleotide kinase (New England Biolabs) (10-20 U), T4 polynucleotide kinase buffer and 1 mM ATP. The sample was incubated 1-1.5 h at 37°C.

2.2.2.7. Dephosphorylation of 5`-end.

The DNA fragment was incubated with buffer and 10 U of calf intestine alkaline phosphatase (CIP) (New England Biolabs) 3-4 h at 37°C.

2.2.2.8. Production of blunt-end fragments

The DNA with protruding termini was incubated with T4 DNA polymerase buffer, T4 DNA polymerase(3-6 U) and additional required product (New England Biolabs) at 14°C for 1 h.

2.2.2.9. Ligation

50 ng of Vector were used in the ratio of 1 to 2-5 with the insert DNA. The T4 DNA ligase and ligase buffer (New England Biolabs) were used according to manufacture's instruction.

2.2.2.10. Agarose gel electrophoresis for RNA

The samples were mixed with loading buffer and were electrophoresed on horizontal agarose gels (1.2% in FA buffer) with 0.5 μg/ml ethidium bromide. The electrophoresis was carried out in FA running buffer at 90 kV for 45 min and RNA was visualized under UV light

2.2.3. Handling and cultivation of organisms

2.2.3.1. *Escherichia coli*

Bacteria were grown on plates incubated at 37°C or in liquid medium on a shaker, 180 rpm at 37°C. When it was required ampicillin (50 $\mu g.ml^{-1}$) was used as marker.

Preparation of competent cells (Chung *et al*., 1989)

A single bacterial colony was picked from a plate that has been incubated for 16-20 h at 37°C. The colony was transferred into LB medium incubated overnight at 37°C with shaking (225 rpm) and then diluted 1:100 into prewarmed LB medium in the same conditions to up an OD_{600} of 0.4. The cells were pelleted by centrifugation at 5,000g during 5 min at 4°C and careful resuspended in 10 ml cold TSS medium. Aliquots of 0.2 ml were frozen in liquid nitrogen and stored at -70°C.

Transformation procedure

An aliquot of competent cells was slowly thawed on ice. 0.1 ml of cells volume was pipetted into an eppendorf tube containing the DNA sample, incubated on ice 30 min, 2 min at 37°C and then, 0.7 mL of LB mediumin was added and ,thereafter, the cells were incubated 1h at 37°C. The transformed competent cells were plated on LB-agar plates containing ampicillin (50 μg/ml). The plates were incubated over night at 37°C.

2.2.3.2. *Saccharomyces cerevisiae*

Cells were grown on a shaker (180 rpm) at 30°C in rich liquid medium, YPD or on synthetic medium, CM (-S) for selection of transformants (Ausubel *et al*., 2000). The solid media were prepared using 2% of agar.

Transformation procedure in *Saccharomyces cerevisiae*

The Lithium-acetate procedure was performed according to Gietz *et al*., (1992) with few modifications. Cells were grown over night in 20 ml of YPD medium on a rotatory shaker at 30°C. When cells obtained 1-3 OD at 600nm an aliquot was taken so that it corresponds to $1x10^8$ cells (0.1 OD 0 $3x10^6$ cells/ml). This culture volume was centrifuged in falcon tube at 3,000 g for 3 min. The medium was discarded and cells were resuspended in 1 ml Litium-acetate washing solution and then transfer to a 1.5 ml microcentrifuge tube. The cells suspension was centrifuged at 10,000 rpm for 30 sec and then the supernatant was removed with a pipette. When necessary, the pellet was washed again. The pellet was resuspended in 310 µl of fresh prepared Mix-transformation solution and plasmid DNA was added. The tubes were vigorously vortexed, thereafter the resuspended cells were incubated on a rotatory shaker at 30°C for 1 h, during the incubation the tubes were vortexed three or four times, and then incubated at 42 °C for 10 min. The cells were centrifuged at 5,000 rpm for 60 sec and the supernatant was removed. The pellet was resuspended in 50 µl of sterile water pipetting up and down (without vortex). This aliquot was plated onto the selective CM plates.

2.2.3.3. *Trypanosoma brucei*

Isolation from blood and stabilate production of bloodstream form trypanosomes

Trypanosomes kept as frozen stabilates ("rat-stabilates") in liquid nitrogen were routinely used as a resource for the propagation of the parasite in Sprague-Dawley rats. The infection was performed by intraperitonal injection of 5×10^7 (rats) total parasites number. Animals were sacrificed at an infection rate between 5×10^8 and 1×10^9 parasite ml^{-1}. The animal thorax was open and the *vena cava inferior* cut. The blood was sterile collected in falcon tubes containing CGS cold solutions and centrifuged (1,300 g, 10 min, 4°C). The parasites were removed from the buffy coat and transferred to a 2ml CGS cold solution. Thereafter, this sample was loaded onto a DEAE-Cellulose Column equilibrated with separation buffer. The first eluted contains the parasite. The different stabilates from bloodstream form were briefly produced as following: For "rat- stabilates", the blood from the animal was mixed with freezing medium and for "bloodstream form- stabilates", bloodstream medium was added to the isolated buffy coat and finally, mixed with freezing medium. In both cases, the end cell density was adjusted to 1×10^8 parasite ml^{-1} incubated 2h at -20°C, 1 day at -70°C and then stored in liquid nitrogen until they were used.

Cultivation of bloodstream form trypanosomes *in vitro*.

"Bloodstream form-stabilates" were used for axenic cultures of parasites. Stabilates were quickly thawed under warm water, the parasite suspension was transferred to a falcon tube containing 10 ml cold bloodstream medium and then centrifuged (1,500g, 5min, 4°C). The supernatant was eliminated and cellular pellet was resuspended in 500 µl bloodstream medium to determine cell density. Suspension cellular was adjusted to 2 x 10^5 parasite ml^{-1} with pre-warmed (37°C) bloodstream medium. Cells were incubated to 37°C in a water saturated atmosphere containing 5 % CO_2.

Cultivation of procyclic form trypanosomes *in vitro*

For the axenic cultivation of procyclic form trypanosomes, as for bloodstream form, stabiates ("procyclic, Stabilates") were used. This stabilate is prepared by mixing cultures of procyclic form with freezing medium to obtain 1 x 10^8 parasite ml^{-1} as final density. Thereafter, they were treated as bloodstream form stabilates. Cultivation of procyclic form from stabilates follows the same procedure than that of bloodstream form, but the cells were cultivated at 27°C with procyclic medium in an incubator without CO_2.

Preparation of conditioned medium for procyclic transformation

Cultures of Trypanosoma procyclic form were grown to reach the late log-phase (7 to 9 x 10^6/ml). Cells were harvested and the medium supernatant filtered. The filtered "conditioned medium" was used immediately or stored at 4°C (not longer than 1 week) until its use. Appropriate combinations of inhibitors and/or inducers (hygromycin, G418, phleomycin +/-Tc) were added to the conditioned medium before use. Undiluted culture (1 ml) was placed into the first row of wells and then diluted 1:1 with conditioned medium (0.5 ml original culture plus 0.5 ml conditioned medium) in the 2nd row. The 3rd and 4th rows contained serial dilutions of the second row (1:1 or 1:2), in conditioned medium.

2.2.4. Cloning of aquaglyceroporin genes from *Trypanosoma brucei*

The complete cDNAs of *TbAQP1–3* were cloned by reverse transcriptase-PCR using RNA obtained from bloodstream form and primers against the spliced leader sequence or against the poly-A tail (see materials) along with primers derived from

aquaporin-like sequences published by the TIGR data base (www.tigr.org). The open reading frames (ORF) were cloned into pBSKS and sequenced.

2.2.5. Heterologous expression of aquaglyceroporins from *T. brucei* in *Saccharomyces cerevisiae*

PCR-products were also cloned into *Sma*I-cut pRS416 (Sikorski and Hieter, 1989) to give rise to yeast expression vectors (*MET17* inducible). EGFP-fusions of *TbAQP1-3* were constructed by cloning *Hind*III-cut PCR products obtained with primers carrying *Hind*III-sites immediately adjacent to sequences flanking the respective ORFs into *Hind*III of pRS416 with an EGFP-gene of which the stop codon was replaced by a *Hind*III-site.

2.2.6. Phenotypic analysis

Cells were grown on CM (or CM-S) at room temperature and 160 rpm overnight and then transferred to CM (or CM-S) plates, control conditions, or plate with any determined compound, experimental conditions. In the hypo-osmotic experiments, the control was cultivated in both liquid media and the agar plate contained 1M glycerol, for the experimental conditions (hypo-osmotic shock) the CM (or CM-S) agar plates were prepared without glycerol. Drop tests in agar plate were done from $1/10^1$ to$1/10^5$ dilution of overnight-grown cultures in exponential phase adjusted to the same cell density.

2.2.7. Glycerol efflux experiments of TbAQP1, TbAQP2, TbAQP3 in *S. cerevisiae* under iso-osmotic and hyperosmotic conditions

Cells were grown at iso-osmotic conditions overnight in synthetic media until an optical density of 1 OD at λ = 600 nm was obtained. Part of this culture was harvested by centrifugation (4°C, 3,500 g, 10 min), resuspended in the same medium containing 5% NaCl (hyperosmotic stress) and further incubated for 2 h at room temperature and 160 rpm. Determination of intracellular glycerol was performed by filtration according to Albertyn *et al.* (1994). Briefly, cells were collected under vacuum using Whatman filter paper type GF/C, washed twice with an isotonic (or hypertonic, in case of osmotic stress experiments) solution at 4^{o}C and placed in 2 ml of 0.5 M Tris buffer pH 7.0. Cells were boiled for 10 min and centrifuged at 15,000 g for 10 min. The pellet was discarded and the supernatant

was deproteinated by addition of 50 µl perchloric acid (70%) per ml solution. The sample was stored for up to one week at 4°C until glycerol was determined as described. For the determination of extracellular glycerol, an aliquot of the cell-free supernatant was used. To determine dry weight of yeast, aliquots of cells were collected onto Whatman GF/C filters and dried at 37ºC for one week.

2.2.8. Transfection of the stream 29–13 procyclic-form with GFP-TbAQPs

Procyclic form *T. brucei* cells (strain 29:13; a gift from G.A.M. Cross),were grown in procyclic medium in the presence of 50 µg/ml hygromycin and 15 µg/ml G418 to maintain selection for the constitutively expressed *T7RNAP* and *TETR* genes, respectively.

29-23 Procyclic form of *T. brucei* was harvested from a log phase culture by centrifugation at 1,000 g at 4°C. Cells were washed once in ice-cold ZPFM, resuspended at 2 x 10^7 in 0.5 ml ZPFM aliquots and transfected with 10-20 µg of *Not* I-linearized GFP-TbAQP-pLew100 DNA per cuvette, using two pulse from a Bio-Rad electroporator set for peak discharge at 1.0 kV. After electroporation, cells were transferred to procyclic medium and incubated overnight. Next day, transformants were cloned by serial dilution starting with 1:1 using conditioned procyclic medium containing the antibiotic concentrations necessary to obtain final concentrations of 15 µg/ml, 50 µg/ml and 2.5-5 µg/ml for G418, hygromycin and phleomycin, respectively. Antibiotic-resistant clones were induced to express the GFP-TbAQPs quimeric proteins by adding tetracycline (0.1-1 µM) into the culture. Pictures were made and analyzed using an Olympus BH2 fluorescent microscope and Biosis imaging software.

2.2.9. The *Xenopus laevis* oocyte expression system

Oocytes of *Xenopus laevis*, the South African clawed frog, were chosen as a system for the transient expression of heterologous proteins.

2.2.9.1. Surgery

Frog was anesthetized with a 0.1% 3-aminobenzoic acid ethyl ester solution. The animal was placed in a small cage containing the mentioned solution plus a part of ice, 1 litter total volume. After 10-15 min the extent of anesthesia was examined.

When the frog was fully anesthetized, it was placed on its back on ice under semi-sterile conditions. First, the animal's abdomen skin was cleaned with an iodine solution. Thereafter, a small horizontal incision about 1 cm long was made in the abdomen, trough both the skin and the underlying fascia, exposing ovaries. The required oocytes were removed by pulling out the lobes of ovary with a pair of forceps and using scissors to cut them. The oocytes were transferred to a tissue culture dish containing calcium-free ND96. The remnant ovary was replaced into the abdomen with forceps and the incision was sutured with one stich using 5/0 silk. Following anesthesia and surgery, the frog was allowed to recover in small container of water for 30-60 min, before it was taken back to the animal facility.

2.2.9.2. Oocytes preparation

The oocyte sacks were opened and all lobules cut into small pieces for better separation. Oocytes were washed several times with calcium-free ND96. In order to defolliculate large numbers of oocytes in a single step, oocytes were undergone to treatment with collagenase (2 mg/ml) for 1-2 h. During the treatment oocytes were subjected to rotation for 45 to 60 min in calcium-free ND96 containing 2 mg/ml collagenase and then the collagenase solution was replaced with a fresh one and the treatment was extended up to the most oocytes were defolliculated and before causing damage to a important part of these cells, usually not longer than 60 min. Afterwards, the oocytes were rinsed several times in calcium-free ND96 and were then washed repeated times in calcium-containing ND96 solution (about 1 L). Finally, cells were selected for size, stage and damage. Healthy oocytes of the last stage (V and VI) were used in this study; these cells were stored in ND96 storage solution at 16°C until next day, when they were injected with RNA.

2.2.9.3. Expression of TbAQP1, TbAQP2, TbAQP3 in *Xenopus laevis* oocytes

For expression in *Xenopus* oocytes, *TbAQP1*, *TbAQP2*, *TbAQP3* genes were subcloned into the EcoR V site of the pT7T5 expression vector which contains 5´ and 3´ untranslated regions of the *Xenopus* β-globin gene. After linearization with Sma I, 1 µg of cDNAs were transcribed in vitro with 20 U T7 RNA polymerase at 37^{o}C in the presence of 25 nM rNTPs, 40 U RNase inhibitor, and 300 µM cap analogue m^{7}G(5`)ppp(5´)G. Template plasmids were removed by digestion with 10 U RNase-free Dnase I for 15 min at 37^{o}C and before purification of complementary cRNAs by phenol/chloroform extraction

followed by precipitation with ammonium acetate/ethanol. Defolliculated oocytes of stages V-VI were injected with 10 ng of each cRNA. After injection, oocytes were kept at 16°C in ND96 storage solution containing 96 mM NaCl, 2 mM KCl, 1.8 mM $CaCl_2$, 1 mM $MgCl_2$ and 5 mM HEPES complemented with 5 mM pyruvate, 50 µg/ml gentamycin and 0.5 mM theophylline, pH 7.4 (Wagner *et al*., 2000).

2.2.9.4. Kinetic glycerol uptake of TbAQPs in oocytes.

For transport assays, 8-10 oocytes were washed and placed in 0.5 ml of fresh ND96 buffer. Glycerol uptake was started by replacement of the ND96 solution by ND96 containing 1 mM unlabelled glycerol and 1 µCi/ml of (U-^{14}C)-glycerol. Uptake of radiolabelled glycerol was stopped at defined time points by washing the cells three times in ND96 solution (at about -3°C) containing 100 mM unlabelled glycerol (Ma *et al*., 1994; Walsh *et al*., 1994). Individual oocytes were dissolved in 1 ml of 10% SDS and subject to scintillation counting.

2.2.9.5. Standard oocytes swelling assay

Xenopus laevis oocytes were injected either with 50 nl water (control); or 50 nl water containing 10 ng of cRNA (TbAQP1, TbAQP2 or TbAQP3); or 50 nl water containing a combination of 10 ng (TbAQP1, TbAQP2, and TbAQP3) and 2.5 ng of rAQP1 as described previously (Hansen *et al*., 2002).

To measure water permeability, oocytes were transferred into 1:3 diluted ND96 media. Solute permeability was assayed in iso-osmotic ND96 where 65 mM NaCl were replaced by 130 mM of a non-ionic test solute or 96 mM NaCl were replaced by the salt of an ionic test solute. Swelling assays were carried out at room temperature and were video monitored using a 2.5x objective. The relative oocyte volume was calculated from the covered area. Osmotic water permeability (Pf, µm/s) was calculated from the oocyte surface area (S = 0.045 cm^2), the initial slope of the relative volume increase [d(V/Vo)/dt in s^{-1}], the molecular water volume (V_w= 18 cm^3/mol) and the osmotic gradient (osm_{in}-osm_{out}) by the following equation:

$$\mathbf{Pf = Vo \times \mathit{d}(V/Vo)/\mathit{dt}[S \times V_w \times (osm_{in}-osm_{out})]}$$

The initial swelling rates [d(V/Vo)/dt in s^{-1}] were used, to compare solute permeability.

2.2.10. Immunofluorescence microscopy

Procedure 1: 1-3 x 10^6 trypanosomes were harvested and washed once with PBS (or HBS). The cells were carefully resuspended in 0.2 ml of PBS, mixed gentle with 0.3 ml of fix-solution and incubated for at least 2 h (or overnight) at 4°C. After fixation, the cells were pelleted by centrifugation (10,000 rpm for 30 sec) and washed with 1 ml of PBS. The pellet was resuspended in sodium-glycine buffer, incubated for 15 min at 4°C and then carefully mixed with 0.5 ml of 0.2% Triton X-100. After 5 min incubation, permeabilized cells were washed twice in PBS containing 1% BSA and resuspended in 100 µl of the first antibody dilution (in PBS/1% BSA). Follow 1 h incubation at 4°C cells were washed twice in PBS/1% BSA solution and resuspended in 100 µl of second antibody solution. After 1 h incubation at 4°C in the dark, DAPI was added (0.1 mg/ml final concentration) to the cells and they were incubated for additional 5 min before parasites were washed. The samples were resuspended in water, placed on the immune-slide and dried. Thereafter, they were embedded with mowiol® according to the manufacture's instruction. Pictures were made and analyzed using an Olympus BH2 fluororesent microscope and Biosis imaging software.

Procedure 2: 5 x 10^5 trypanosomes were harvested and washed once with PBS (or HBS). Cells were resuspended in a volume of PBS buffer to reach a cell density of 3 x 10^4 parasites/µl. 10 µl of this suspension were pipetted in each well of the immune-slide and fixed using methanol. Wells were washed 3 times with 30 µl of PBS buffer, incubated with PBS/1% BSA at 37 °C for 15 min and washed again. Cells were incubated with the first antibody diluted in PBS/1% BSA at 37°C for 1 h, washed as above described and then incubated with the second antibody at 37°C for 1 h in dark. DAPI staining, embedding and images analysis were performed as described in procedure 1.

2.2.11. Electron Microscopy: Transmission electron microscopy (TEM) and Scanning electron microscopy (SEM)

Fixation

For TEM, at least 10^8 trypanosomes treated or not treated (control) with dihydroxyacetone were taken after 24 hours of in vitro cultivation. Fixation was performed in 2% (vol/vol) glutaraldehyde in EM-buffer for 1 h at 4°C. After washing, four times (10 min each) and storage over night in sodium cacodylate buffer, cells were postfixed in osmium tetroxide (1.5%, wt/vol) and stained in 0.5% uranyl acetate at RT for 60 min and washed with distilled water (Hirsch and Fedorko, 1968). The fixed cells were dehydrated

using ethanol solutions of increasing concentrations (30%, 50%, 70%, 95%, 100%, 100%, 1 h each at RT) and washed twice 10 min each with propylenoxide. Alternative, for analysis in SEM samples were dehydrated up to 70% ethanol. The subsequent steps for the preparation of these samples as well as the SEM picture were carried out in the laboratory of Prof. Bardele.

Embedding

The sample was incubated with Epon:propylenoxide (1:1, 60 min, RT), infiltrated with pure Epon (60 min, RT) and transferred to Beem®-Cups. The polymerization was carried out for 12 h at 45°C and 24 h at 60°C.

Ultra sectioning

After polymerization the tip of the sample was trimmed to trapezoidal shape on Primetime 11800, sectioned using an Ultra tome and fished with copper grits.

Contrasting

The grit was contrasted on a 50 µl 5% uranyl acetate drop (60 min, RT, face down) (Lewis and Knight, 1977). The grit was washed with distilled water and incubated in Reynolds lead citrate solution (7 min, RT) and again washed and dried.

Microscopy

The sample was photographed on Zeiss EM 109 transmission electron microscope with TFP-camera using negative film Kodak Plus-X-Plan 120 (125 ASA, 60 x 70 mm).

2.2.12. FACS analysis

2.2.12.1. DNA content

For content of DNA within the nucleus, a propidium iodide staining method was used (Nicoletti *et al*., 1991). To this end, at least $5x10^5$ cells were centrifuged, washed once with PBS (pH 7.4) and lysed in 100 ml phosphate buffer (10 mM) pH 7.4, containing 6 mM digitonin. Samples were vortexed and incubated for 30 min at room temperature. Nuclei were stained with a propidium iodide solution (10 mg/ml final concentration in phosphate buffer) 1 h before measurement of the nuclei in a FACS Caliburs apparatus.

2.2.12.2. Cellular permeability

Plasma membrane integrity of trypanosomes was tested using propidium iodide (5 mg/ml) staining. Cells were analyzed by flow cytometry, using digitonin (6 mM) as a positive control of necrosis inductor.

2.2.12.3. Phosphatidylserine exposure

Exposed phosphatidylserine was detected using annexin-V-fluos® according to the manufacturer's protocol. Fluorescence was measured using FACS analysis.

2.2.12.4. Reactive oxygen species (ROS)

DCFH-DA was used to determinate intracellular reactive oxygen species. Control and treated cells were incubated with 10 µM DCFH-DA for 1 h at 37°C. The cellular fluorescence intensity was measured using a flow cytometer as described above.

2.2.13. Cytotoxicity assay

The IC_{50} values were determined according to Bodley *et al.* (1995). Exponentially growing parasites, bloodstream form, were diluted to 2 x 10^5 cells/ml, placed in a 96-well microtiter plate (199 µl) and grown with or without DHA (1 µl/well) at different concentrations. Plates were incubated for 24 h at 37°C and 5% CO_2. Cell growth was stopped by the addition of 20 µl cytotoxicity buffer. Finally, following 5h incubation at 37°C, the phosphatase activity was measured at 405 nm using an ELISA reader. For procyclic form of parasites, the culture was diluted to 4 x 10^5 cells/ml and plates were incubated for 48 h at 26°C.

2.2.14. Bioinformatics methods

The most of the sequence analysis; e.g alignment, phylogenetic tree analysis, primer design, etc, were performed using DNAMAN software (Lynnon Corp., Quebec, Canada). Bioinformatic support information was obtained from **N**ational **C**enter of **B**iotechnology **I**nformation (NCBI) (http://www.ncbi.nih.gov). Further information of sequences were obtained using bioinformatics tools in Expasy web site (http://www.expasy.org) e.g. transmembrane regions, phosphorylation sites, pI, compositions, etc. Representation of transmembrane domain was performed using $Latex2_E$ according to Beitz (2000).

3. Results

3.1. Cloning of TbAQPs and characteristic feature of protein sequences

The *T. brucei* genome contains three genes with similarities to the major intrinsic proteins (MIP). These genes are located on chromosome 6 (AQP1) and 10 (AQP2 and 3). We have cloned all three genes from the parasite using the bloodstream form stage and an RT-PCR approach. The sequences have been submitted to the EMBL database as TbAQP1 to 3 (accession numbers: AJ697889; AJ697890; AJ697891). The open reading frames encode proteins of 321 (TbAQP1), 312 (TbAQP2), and 304 (TbAQP3) amino acids very similar to each other (77% identity, Fig. 3.1). Analysis of the hydropathy plot predicts the usual six transmembrane regions separated by five connecting loops as described for MIPs.

TbAQP1 and 3 possess two canonical NPA motifs and are more related to AQP3 from *Rattus norvegicus* (45% and 44% identity, respectively), whereas TbAQP2 is more related to the human AQP9 (40% identity). TbAQP2 contains unusual NSA/NPS motifs as part of the pore region, and a leucine residue instead of the highly conserved arginine residue following the second NPA or –in this case– NPS motif (Fig. 3.1).

Sequence alignments and analysis of the phylogenetic tree suggest that these proteins are more closely related to aquaglyceroporins than to aquaporins (Fig. 3.2). In addition, these protein sequences are putative aquaglyceroporins according to the signature pattern proposed for this protein family (Froger *et al*., 1998). For example, the external C and E loops are shorter in AQPs than in GLPs, and have an average length of 18 amino acid compared with 28 amino acids in GLPs. All three TbAQPs present long external loops with same length, the first of them constitutes for 30 amino acids and the second one for 26 amino acids (Fig. 3.3, 3.4 and 3.5).

As judged by the calculated transmembrane regions (Fig. 3.3, 3.4 and 3.5), the three TbAQPs do not possess long free C-termini, but possess short C-terminal ends of maximal two amino acids on the cytosolic side immediately following the sixth transmembrane domain. In contrast, all TbAQPs contain characteristically elongated N-termini with 83, 73 and 65 amino acid for TbAQP1, 2 and 3, respectively. The sequences of TbAQP2-3 N-termini are closely related to each other, whereas the N-terminal sequence of TbAQP1 is the longest and is completely different from TbAQP2-3. This characteristic feature of TbAQP1 could indicate particular properties of this protein associated to its function, e.g. unique localization, a different regulation of its open-close status, etc.

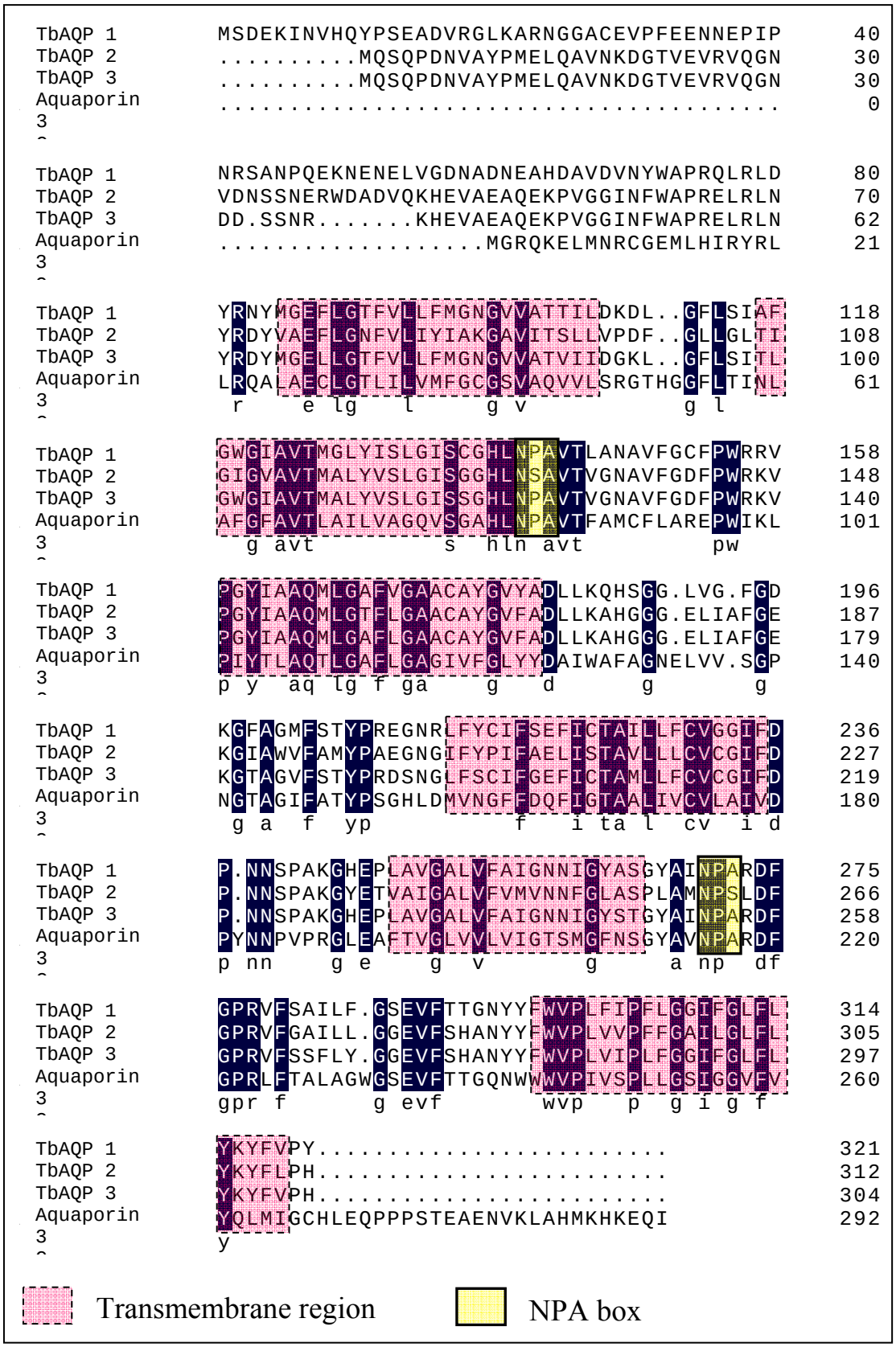

Figure 3.1. Amino acid sequence alignment of TbAQPs, including mammalian AQP3. Identical amino acids are in white on a black background.

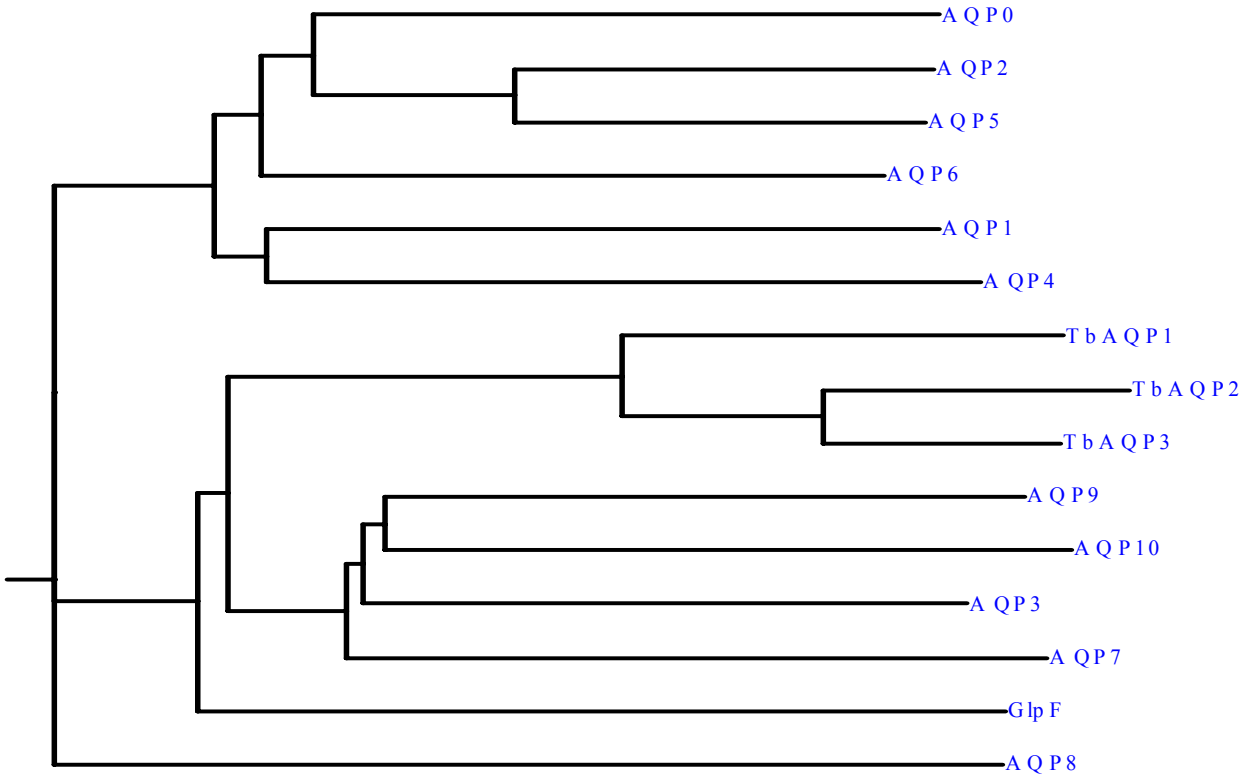

Figure3.2. Phylogenetic tree analysis of TbAQPs.

3.2. Functional expression of TbAQPs in *S. cerevisiae*

In order to characterize the channel activity of TbAQPs, the corresponding proteins were N-terminally fused with GFP and functionally expressed in a *S. cerevisiae* fps1Δ mutant strain, which lacks a functional glycerol channel. Heterologous expression of GFP alone served as a control. Expression of GFP-TbAQPs was induced using CM-S medium (see material and methods) and the cells were monitored by fluorescence microscopy. These cells clearly showed the presence of GFP-TbAQPs within the yeast's cellular membrane (Fig. 3.6). For a functional characterization, cells expressing TbAQPs without GFP were grown overnight in isotonic media. Subsequently, intra- and extracellular glycerol concentrations were determined. As shown in figure 3.7, control cells produced very low amounts of glycerol, which was equally distributed between the cells and the surrounding medium, while TbAQP1- and TbAQP3-transformed fps1Δ mutant cells showed a dramatic increase of glycerol production, which was almost exclusively secreted into the medium. Notably, yeast TbAQP2-transformants produced twice as much glycerol as compared to TbAQP 1 and 3, which was also mainly secreted, although in this case some glycerol was retained intracellularly (Fig. 3.7).

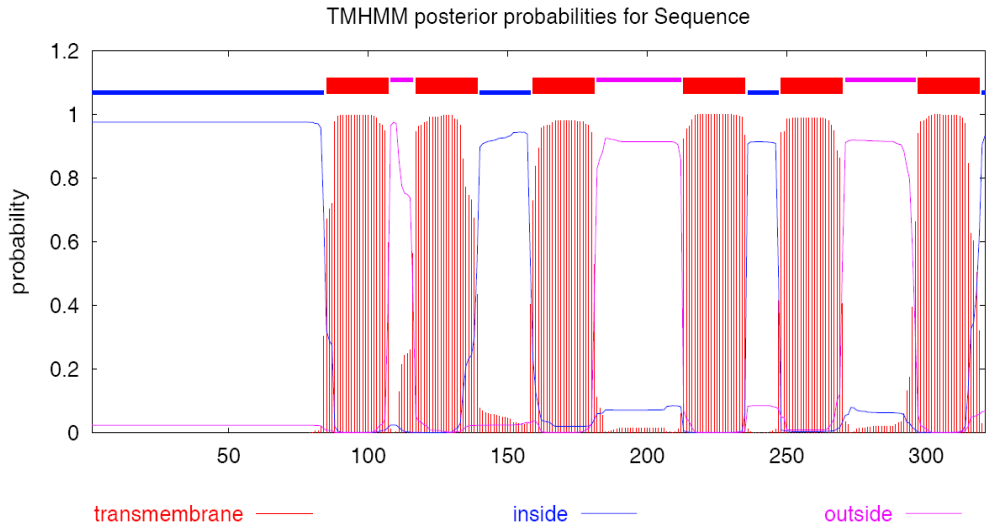

Sequence Length: 321

Sequence Number of predicted TMHs: 6 Probability of N-terminus-inside: 0.97647

Sequence	A	inside	1	84	Sequence	B	TMhelix	85	107
Sequence	C	outside	108	116	Sequence	D	TMhelix	117	139
Sequence	E	inside	140	158	Sequence	F	TMhelix	159	181
Sequence	G	outside	182	212	Sequence	H	TMhelix	213	235
Sequence	I	inside	236	247	Sequence	J	TMhelix	248	270
Sequence	K	outside	271	296	Sequence	L	TMhelix	297	319
Sequence	M	inside	320	321					

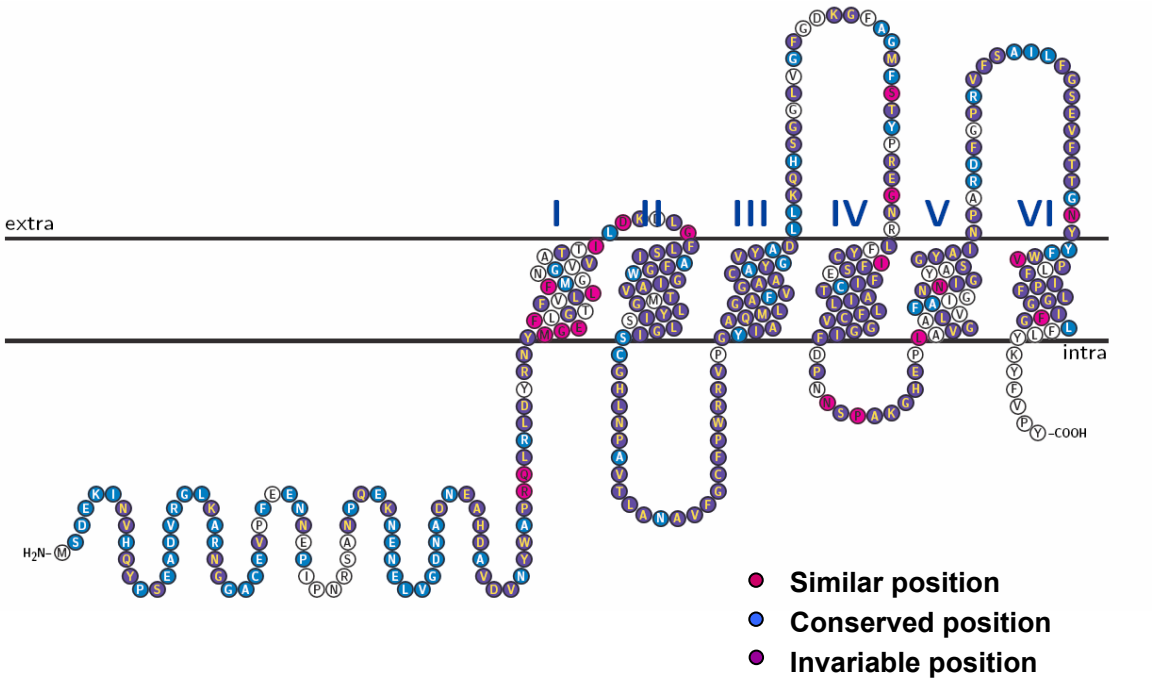

Figure 3.3 Predicting transmembrane helices and topology of TbAQP1

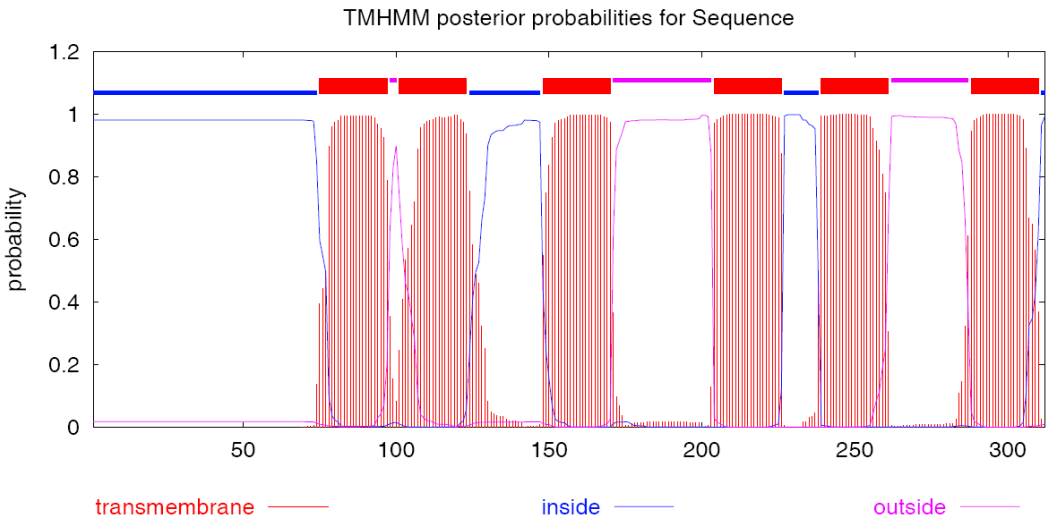

Sequence Length: 312

Sequence Number of predicted TMHs: 6 Probability of N-terminus-inside: 0.98252

Sequence	A	inside	1	74	Sequence	B	TMhelix	75	97
Sequence	C	outside	98	100	Sequence	D	TMhelix	101	123
Sequence	E	inside	124	147	Sequence	F	TMhelix	148	170
Sequence	G	outside	171	203	Sequence	H	TMhelix	204	226
Sequence	I	inside	227	238	Sequence	J	TMhelix	239	261
Sequence	K	outside	262	287	Sequence	L	TMhelix	288	310
Sequence	M	inside	311	312					

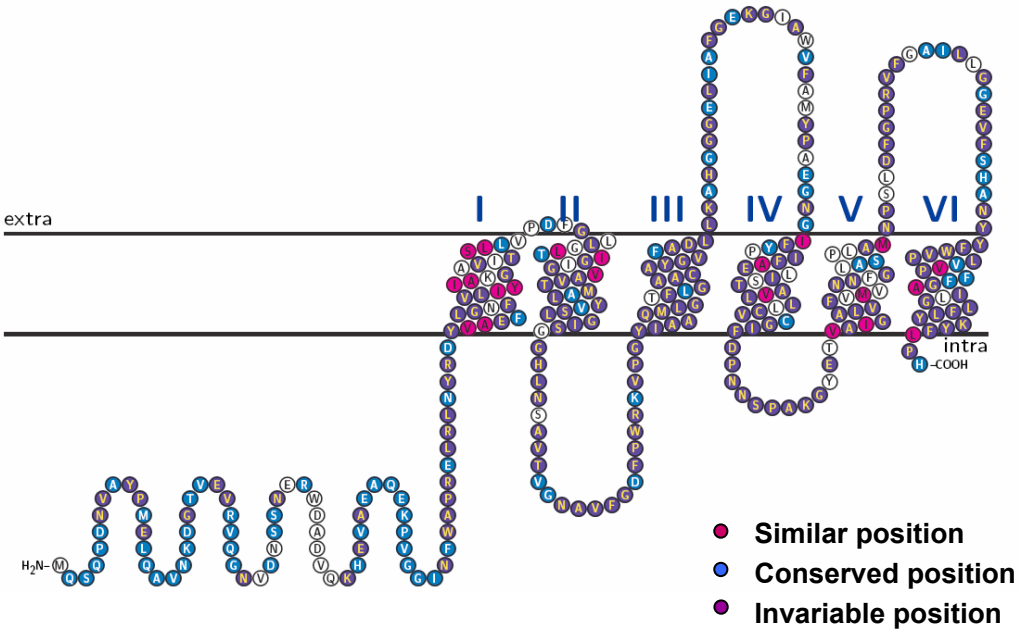

Figure 3.4 Predicting transmembrane helices and topology of TbAQP2

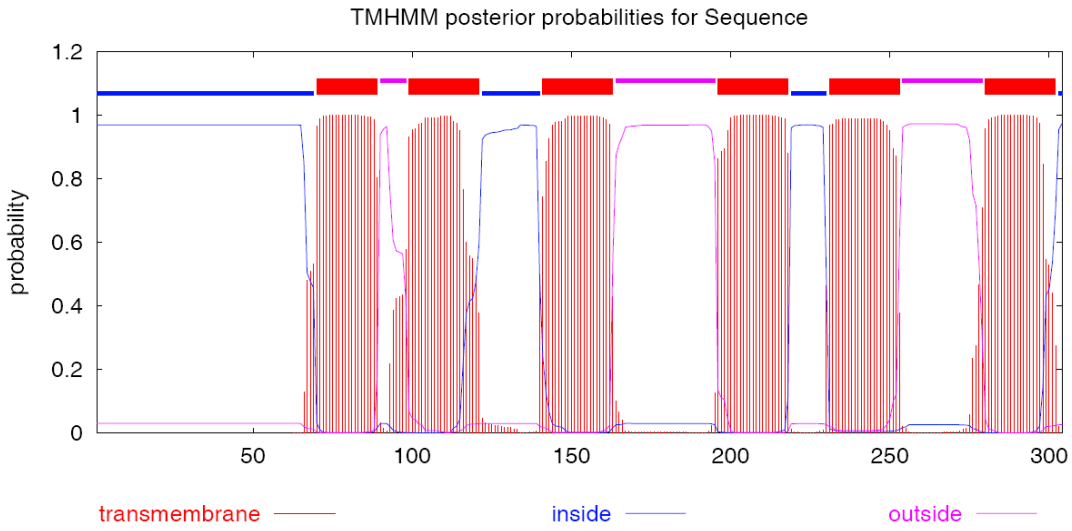

Sequence Length: 304

Sequence Number of predicted TMHs: 6# Probability of N-terminus-inside: 0.97008

Sequence	A	inside	1	69	Sequence	B	TMhelix	70	89
Sequence	C	outside	90	98	Sequence	D	TMhelix	99	121
Sequence	E	inside	122	140	Sequence	F	TMhelix	141	163
Sequence	G	outside	164	195	Sequence	H	TMhelix	196	218
Sequence	I	inside	219	230	Sequence	J	TMhelix	231	253
Sequence	K	outside	254	279	Sequence	L	TMhelix	280	302
Sequence	M	inside	303	304					

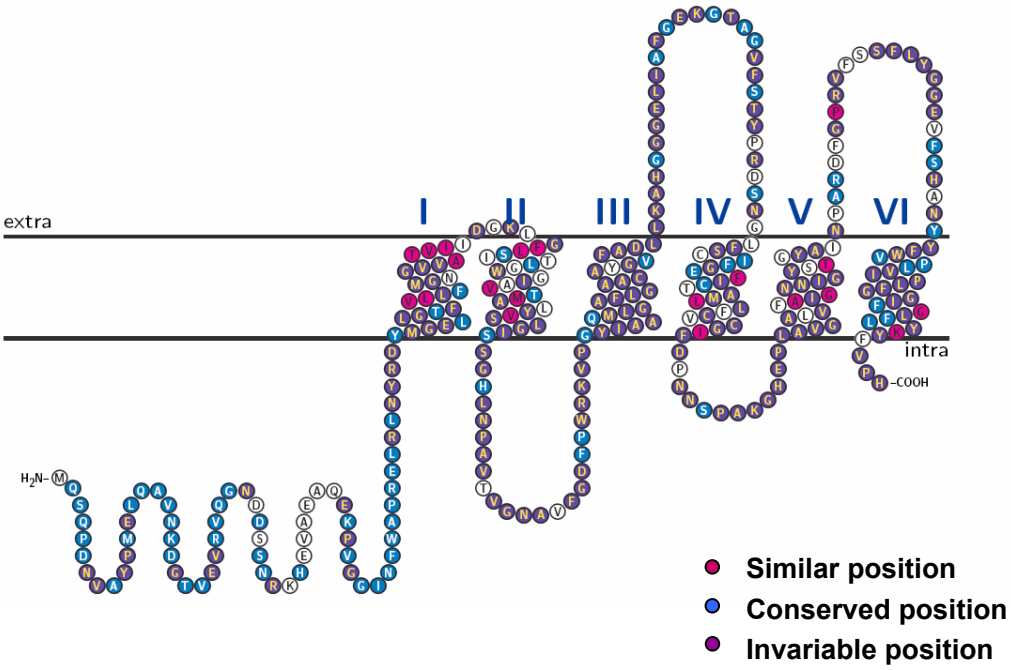

Figure 3.5. Predicting transmembrane helices and topology of TbAQP3

To further characterize this phenomenon, the experiment was repeated under hypertonic conditions (5% NaCl for 2 h), which was described to produce a very high accumulation of glycerol in *S. cerevisiae* (Albertyn *et al*., 1994). Due to the absence of a functional glycerol channel, control cells showed indeed a high retention of glycerol, although substantial amounts of glycerol appeared also in the medium, indicating significant free diffusion of glycerol across the membrane. TbAQP1- and TbAQP3-transformed fps1Δ mutant cells, however, showed similar results as those obtained under iso-osmotic conditions, i.e. these cells were unable to accumulate glycerol under iso-osmotic or hyper-osmotic conditions and constitutively released it into the medium (Fig. 3.7). This behaviour is similar as described for fps1Δ yeast cells expressing the glycerol facilitator from *E. coli* (GlpF) and indicates a non regulated high glycerol channel activity (Lyuten *et al*., 1995; Tamas *et al*., 1999; Hedfalk *et al*., 2004).

TbAQP2-transformed fps1Δ mutant cells showed a similar phenotype as fps1Δ mutant cells expressing TbAQP1 and TbAQP3, i.e. an increased glycerol production under isotonic as well as under hypertonic conditions, with most of this osmolyte released into the medium. On the other hand, TbAQP2 expressing cells retained a significant amount of glycerol within the cytosol, regardless of the ionic strength of the media (Fig. 3.7). In summary, the results are consistent with a role of TbAQPs in glycerol efflux. In addition, TbAQP2 appears to affect glycerol production and its intra/extra-cellular distribution in *S. cerevisiae* in a different way as compared to TbAQP1 and 3.

3.3. Phenotypes of TbAQPs

To analyse the phenotype of TbAQP1, 2 and 3 in yeast, TbAQP-transformed fps1 Δ mutant cells were grown and then spotted in 10 fold serial dilutions onto agar plates with different osmolytes (Fig. 3.8). In *S. cerevisiae*, Fps1 is involved in glycerol transport. This regulated glycerol channel is active under hypotonic conditions but inactive under hypertonic conditions (Tamas *et al*., 1999). Thus, growth of fps1Δ mutant cells was limited under hypoosmotic conditions, but did not show any phenotype under hyperosmotic conditions (Hedfalk *et al*., 2004). TbAQPs expressed in fps1Δ mutant cells suppressed the characteristics of hypo-osmosensitivity. In addition, these cells grew unaffected under hypertonic conditions, if the respective osmolyte was 1 M glycerol. Growth was drastically reduced, however, if 1 M sorbitol or 1% NaCl was applied instead of glycerol (Fig. 3.8).

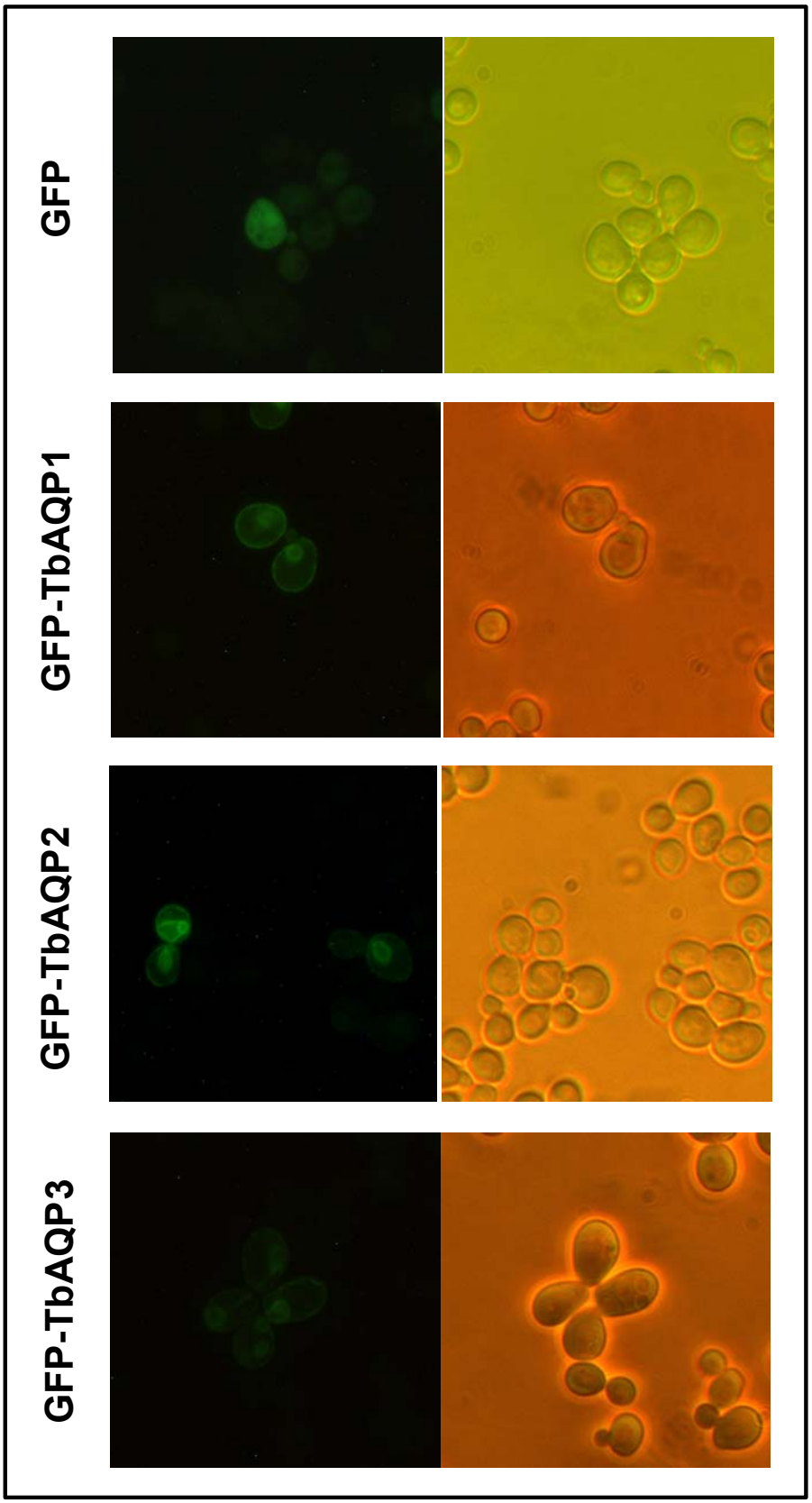

Figure 3.6 GFP-TbAQPs expression in *Saccharomyces cerevisiae*. First row, GFP transformants (control); second row GFP-TbAQP1 transformants; third row, GFP-TbAQP2 transformants; fourth row, GFP-TbAQP3 Transformants

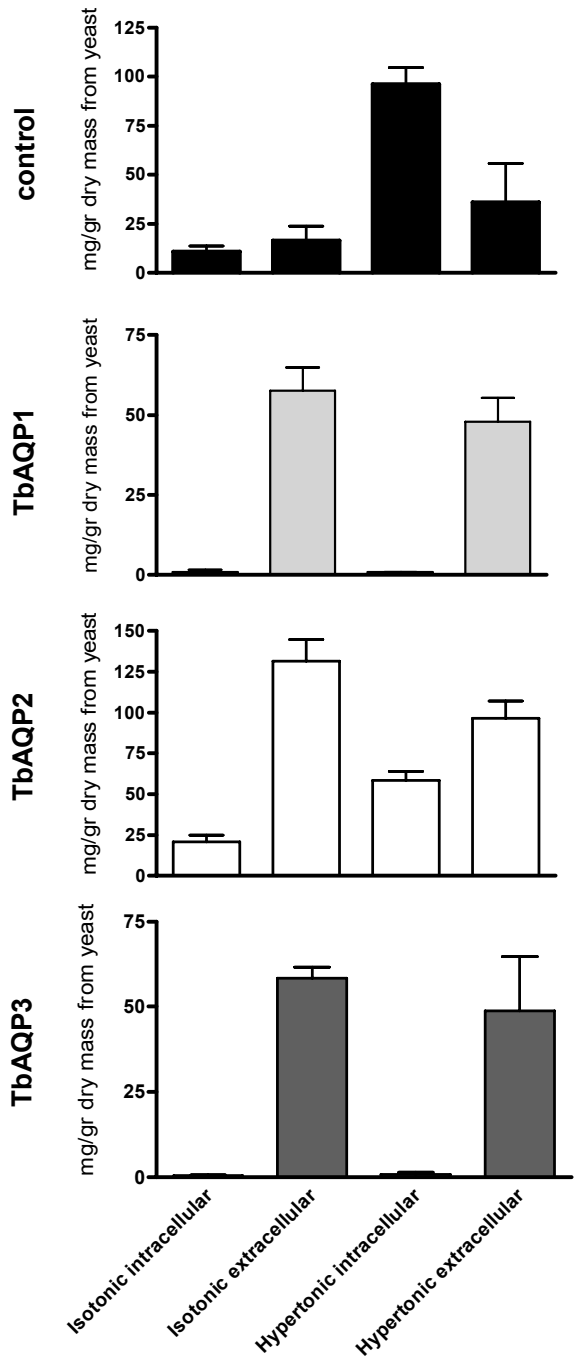

Figure 3.7. Glycerol efflux experiments of yeast fps1Δ mutant cells transformed with an empty vector (control), with TbAQP1, with TbAQP2, or with TbAQP3. Intra- and extracellular glycerol concentrations were determined under isoosmotic and hyperosmotic conditions. The values given are mean ± SD of three independents experiments.

This phenotype of hyper-osmosensitivity for other osmolytes than glycerol was also described for yeast mutants lacking either the N- or the C-terminal regulatory domains of Fps1, indicating that in yeast TbAQPs are non regulated glycerol channels (Lyuten *et al*., 1995; Tamas *et al*., 1999; Hedfalk *et al*., 2004).

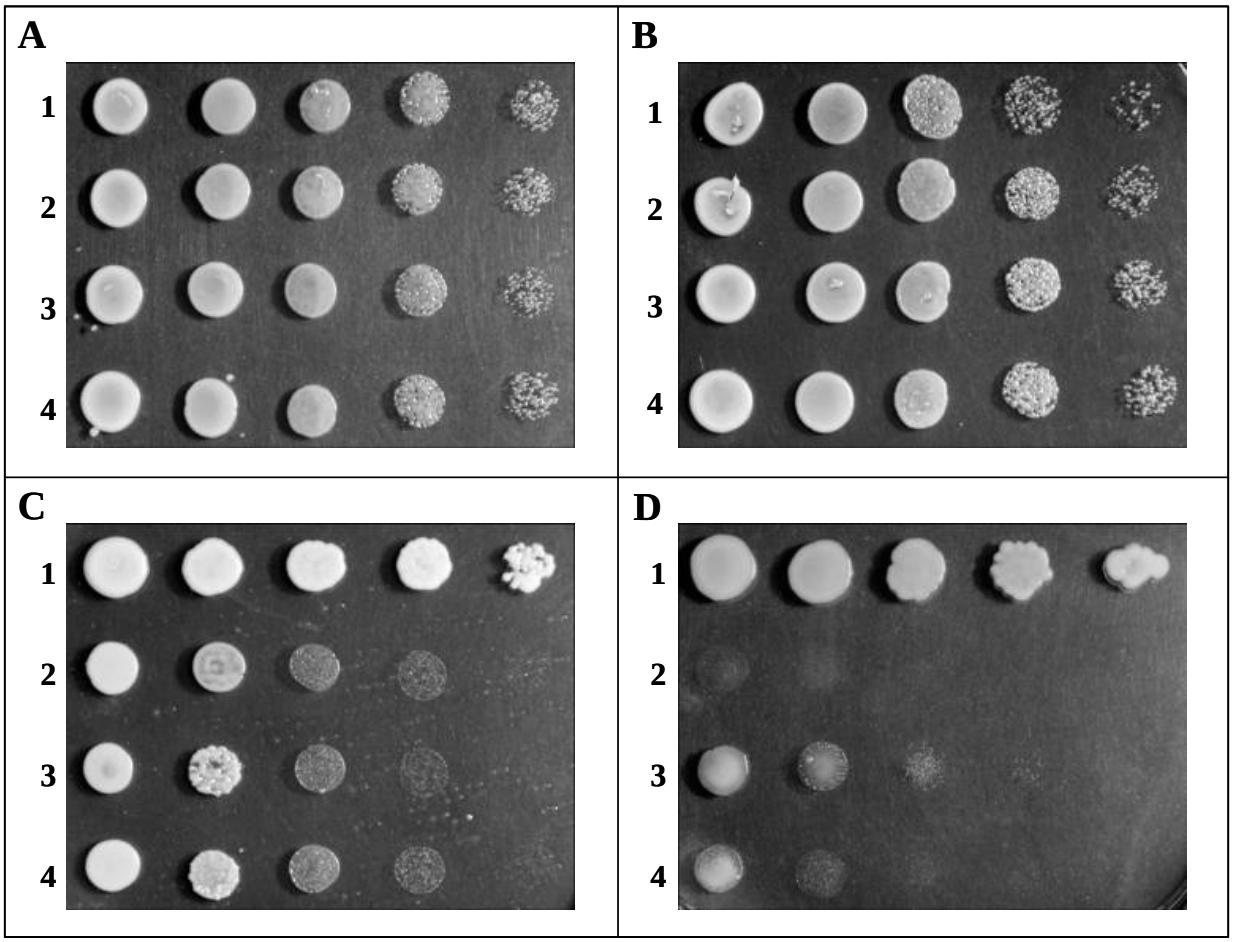

Figure 3.8. Phenotypes of fps1Δ mutant cells expressing TbAQPs. For treatment, yeast cells were pre-grown in selective liquid medium containing 1 M glycerol and transferred thereafter onto selective agar medium containing 1 M glycerol (control conditions) (*A*), medium without any additional osmolytes (hypoosmotic shock) (*B*), 1% NaCl (*C*), or 1 M sorbitol (*D*). In each panel: *first row*, control cells containing an empty vector; *second row*, TbAQP1; *third row*, TbAQP2; *fourth row*, TbAQP3.

3.4. Functional expression of TbAQPs in *Xenopus* oocytes

For a further functional characterization, TbAQPs were also heterologously expressed in *Xenopus* oocytes. Glycerol uptake was then measured for up to 40 min by incubation of oocytes expressing the different TbAQPs in the presence of 1 mM glycerol (1μCi/ml [^{14}C]-glycerol). As shown in figure 3.9, the highest expression for TbAQP1 and 3 after RNA injection was found on the second or the first day, respectively. On the other hand, TbAQP2 was expressed very well on the second day and expression increased thereafter slightly up to the fourth day (Fig. 3.9).

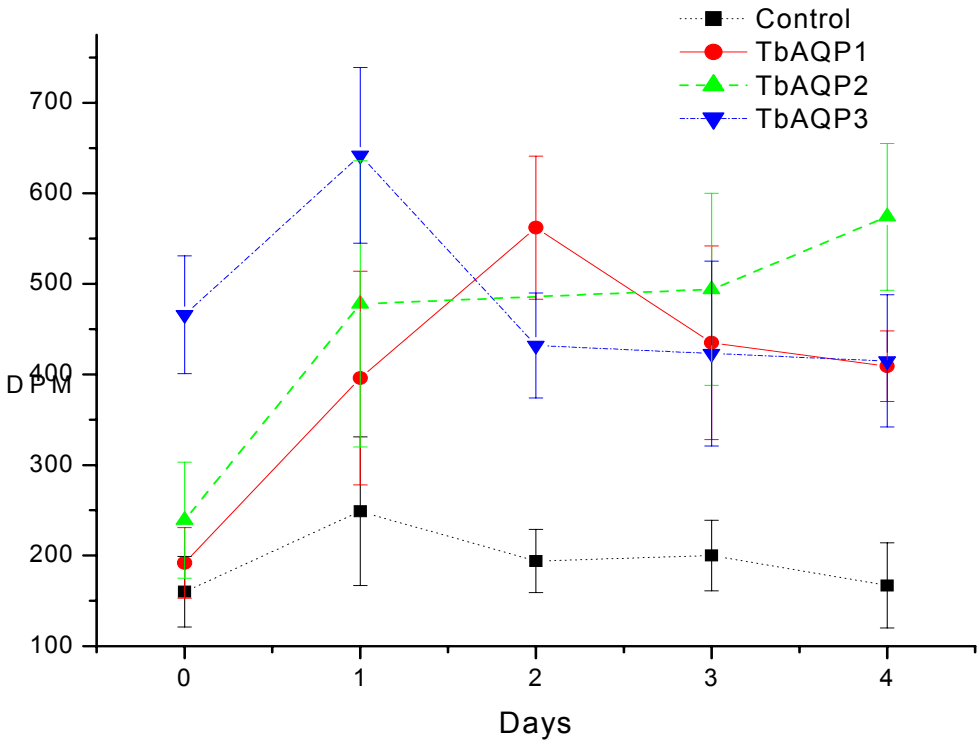

Figure 3.9. Efficiency of TbAQPs expression in *Xenopus* oocytes during the days.

3.4.1. Glycerol uptake

Control oocytes (injected with 50 nl distilled water) mediated only little glycerol uptake (57.9 pmol per oocyte within 40 min), consistent with simple membrane diffusion. In contrast, oocytes injected with 10 ng of any of the TbAQPs rapidly accumulated glycerol (about 240 pmol within 40 min), clearly indicating channel activity. In addition, transport kinetics of all TbAQPs was very similar (Fig. 3.10). In order to confirm these results and to compare with other aquaglyceroporins, glycerol permeability was tested using the oocyte swelling assay. The swelling rate in a 130 mM glycerol gradient was similar among all three TbAQPs and about 10 fold higher as compared to water-injected control oocytes (Fig. 3.11). This was consistent with the result of [^{14}C]-glycerol uptake during the same time interval of 1 min (Fig. 3.10). These results were comparable to those obtained by using aquaglyceroporins from other protozoa, e.g. *Plasmodium falciparum* and *Toxoplasma gondii*, which also possess very effective glycerol channels (Lyuten *et al*., 1995; Hansen *et al*., 2002).

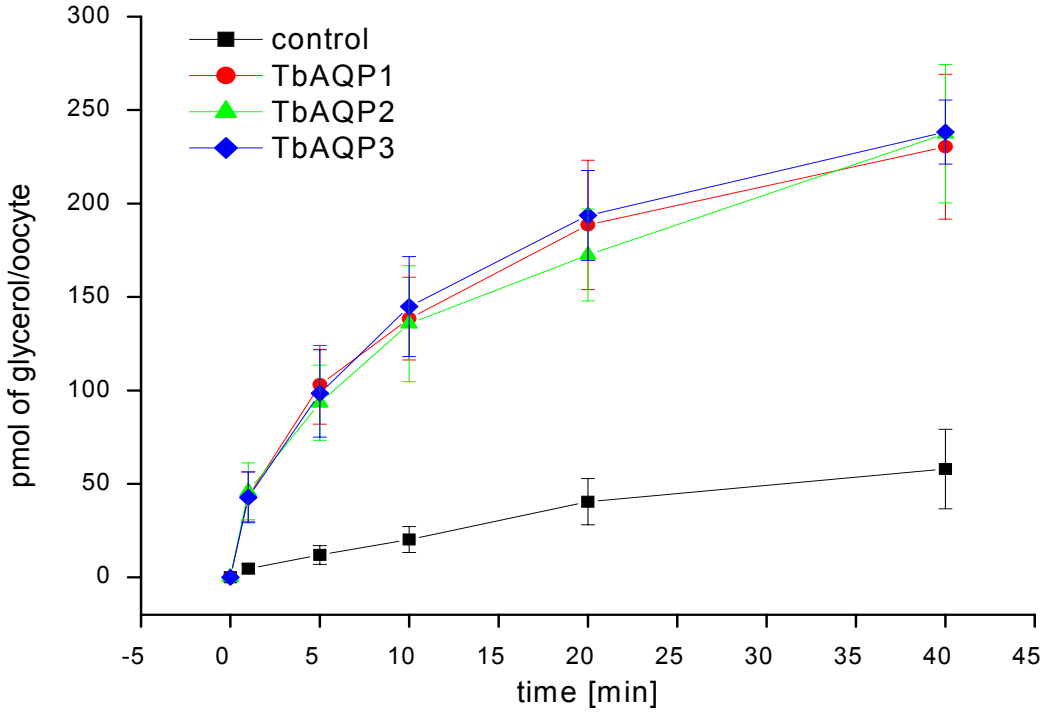

Figure 3.10. Glycerol uptake kinetics in *Xenopus* oocytes expressing TbAQPs. Water injected oocytes represent controls; Data are mean ± S.D. of at least three independent experiments.

3.4.2. Water permeability

In order to analyze water transport, oocytes expressing TbAQPs were exposed to hypotonic shock using a 1:3 diluted medium, which generates an osmotic gradient of 140 mosm per kg across the oocyte membrane (Hansen *et al*., 2002). Expression of any of the three TbAQPs in *Xenopus* oocytes led to a 6-7 fold increase of the swelling rate as compared to control oocytes (Fig. 3.12). From the calculated Pf values (150 – 180 µm per sec), TbAQPs can be characterized as channels expressing an intermediate water permeability between typical aquaglyceroporins, e.g. rAQP3 (Pf ≈ 70 µm per sec) and orthodox aquaporins, e.g. rAQP1 (Pf ≈ 290 µm per sec).

3.4.3. Permeability for polyols and other conventional solutes

Aquaglyceroporins usually facilitate permeation of other small uncharged solutes, such as polyols and urea, although at different rates. To address this question, swelling rates of TbAQP-expressing oocytes were measured in the presence of a variety of polyols in the range of 4 to 6 carbon atoms. Urea was also evaluated and alanine and pyruvate,

which should not pass through the pore, were used as negative controls. In general, the permeability for polyols was restricted. Only TbAQP3 expression yielded considerable oocyte swelling with erythritol and ribitol, which was about 50% of the swelling rate for glycerol (Fig. 3.11). Urea passed the pores of TbAQP2 and 3, with an efficiency similar to the erythritol and ribitol, but was hardly transported by TbAQP1 (Fig. 3.11).

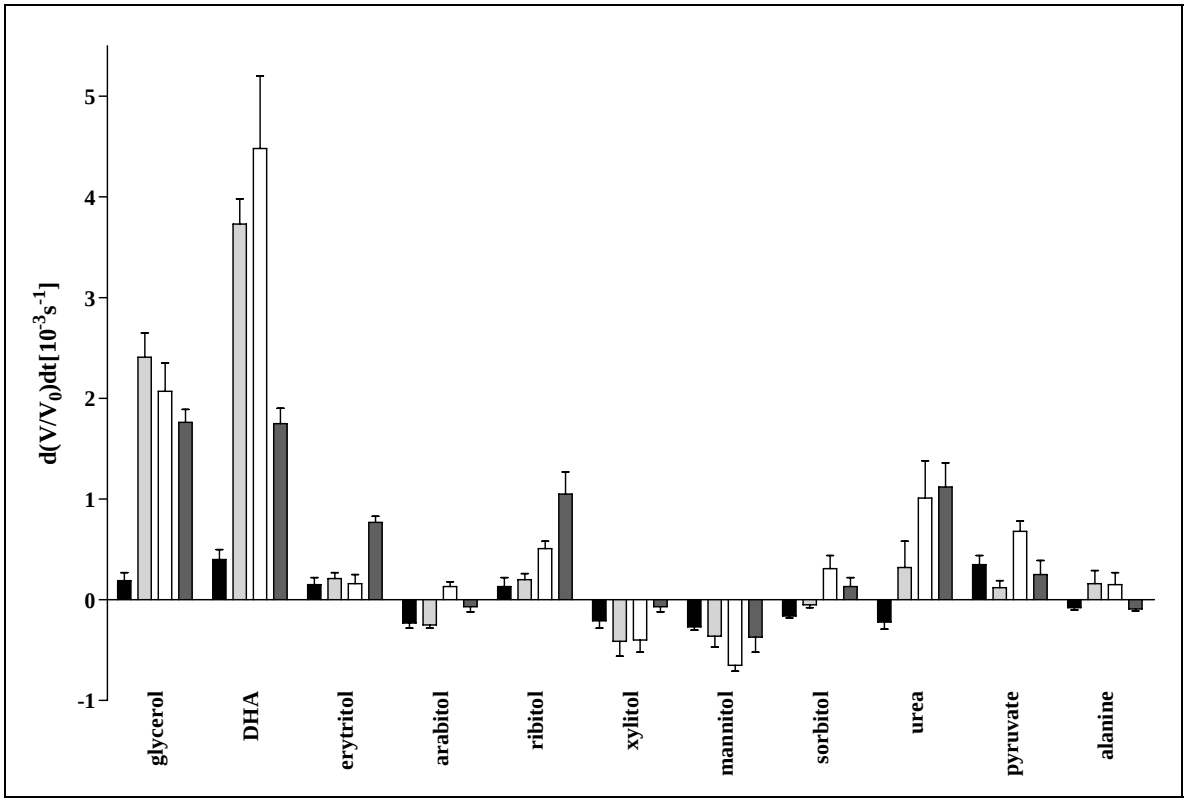

Figure 3.11. Substrate permeability in *Xenopus* oocytes expressing TbAQPs. Control cells without any TbAQP are shown as black columns, cells with TbAQP1 are shown as light gray shaded columns, cells with TbAQP2 are shown as white columns, and cells with TbAQP3 are shown as dark gray shaded columns.

3.5. Selectivity profile for non-conventional substrate: Looking for physiological function and pharmacological application

The relatively recent discovery of the aquaporin family, along with its wide diversity and distribution throughout nature, justifies the suggestion that these proteins could play a key role in different aspects of the biology of living organisms, possibly many of which are not discovered yet. Although the transport of the classical substrates of aqua-glyceroporins such as water, polyols and urea are very important for the existence of life, it is likely that these proteins are involved in other cellular functions as well. Indeed, it was

recently published that aquaglyceroporins transport ammonia (Jahn *et al.*, 2004), nitrate (Ikeda *et al.*, 2002) and even, although controversially discussed, CO_2 (Cooper *et al.*, 2002). On the other hand, aquaglyceroporins as an access pathway to the cell, represent a hope of exploiting as a target for chemotherapeutic intervention in parasitic protozoa like *Trypanosoma brucei*. For all these reasons, the permeability of TbAQPs for non conventional substrates was investigated.

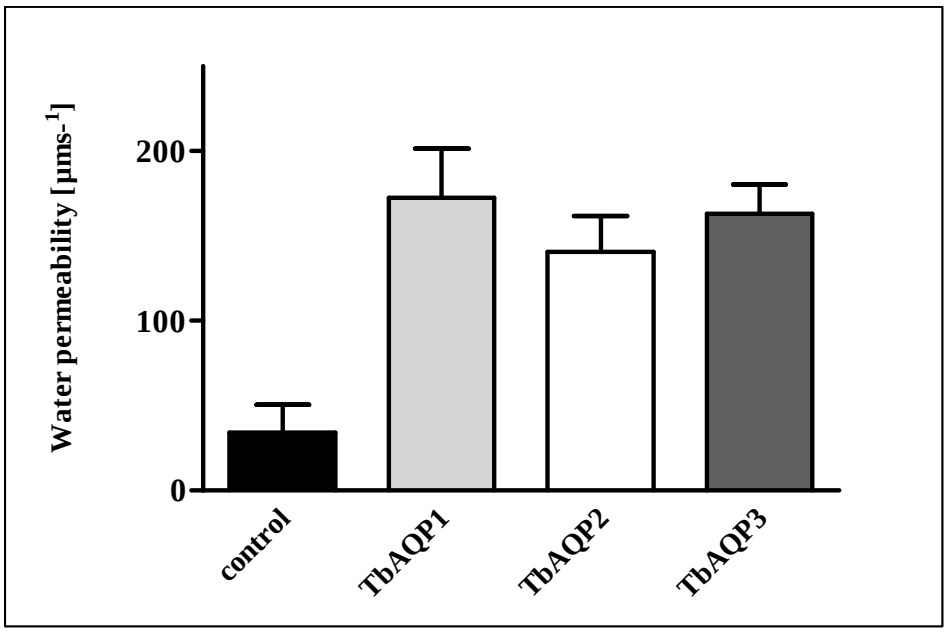

Figure 3.12
Water permeability in *Xenopus* oocytes expressing TbAQPs. Oocytes injected with water, Controls, are shown as black columns. Oocytes expressing TbAQP1, 2 and 3 are shown as light gray shaded columns, white columns and dark gray shaded column, respectively.

3.5.1. Dihydroxyacetone

3.5.1.1. TbAQPs permeability for dihydroxyacetone

Dihydroxyacetone (DHA) is one of the first reasonable candidates to be transported by aquaglyceroporins due to its similarity with the spatial structure of glycerol. TbAQPs permeability for dihydroxyacetone was evaluated by the standard oocytes swelling assay. Surprisingly, DHA was excellently transported by all TbAQPs: the transport rate was about 2 fold higher for TbAQP2, 1.5 fold higher for TbAQP1 and about equal for TbAQP3 when compared to glycerol (Fig. 3.11). Further confirmation of these results was obtained using *S. cerevisiae* as another heterologous expression system. It was recently shown that a relative high concentration of DHA is toxic for yeast cells (Molin *et al.*, 2003). TbAQPs-transformed fps1Δ mutant cells and control cells were grown in liquid

media in the presence of 0.2 M DHA. In glucose containing media, 0.2 M DHA led to a slightly decreased growth rate of the fps1Δ strain, which implicates a resistant phenotype for this drug. In contrast, TbAQP-transformed fps1Δ yeast cells showed a highly sensitive phenotype; their cellular growth, if any, was drastically reduced (Fig. 3.13). These results are consistent with a role of TbAQPs for DHA permeation.

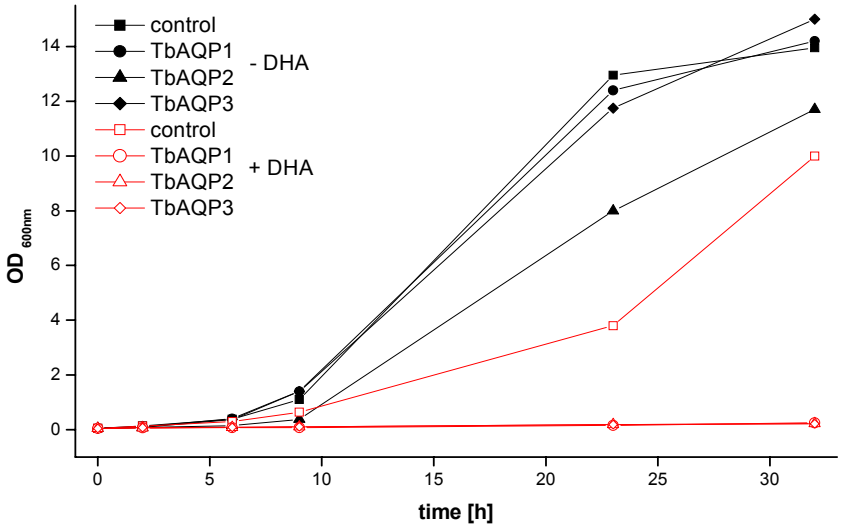

Figure 3.13. Growth of TbAQP-transformed fps1Δ mutant cells. Growth is characterized as increase in optical density at 600 nm in the absence(*filled symbols*) or presence (*open symbols*) of 200 mM DHA.

3.5.1.2. Evaluation of dihydroxyacetone as energy source on *T. brucei*

Dihydroxyacetone can be used as energy source for many cells. It is known that bacteria cultured in the presence of dihydroxyacetone proliferate as well as with glycerol as carbon source (Tang *et al.*, 1982). In erythrocytes, DHA and glyceraldehyde have been shown to be metabolized efficiently to L-lactate (Taguchi *et al.*, 2002) and, in animals, DHA is considered as a gluconeogenic precursor (Siebold *et al.*, 2003). Likewise, DHA has been involved in other functions such as, for example, osmoregulation in yeast and algae (Akhtar *et al.*, 1997; Garcia-Alles *et al.*, 2004). All of these DHA functions depend on the expression of dihydroxyacetone kinase (DHAK), which allows access to cellular metabolism. This enzyme converts free DHA into the glycolytic intermediate DHA phosphate (DAHP). However, in *Trypanosoma brucei* this seems not to be the case, since detailed searches DHAK gene (TIGR and Sanger) and other related enzymes to DHA consumption such as glycerol dehydrogenase showed only negative results.

In order to evaluate whether DHA can be used as an energy source, parasite cells were incubated at 37°C in buffer containing only this compound as carbon source. Under these conditions, cell death occurred quickly (within minutes) whereas control cells-incubated with buffer and glucose- survived for longer time period. These experiments were repeated under more favourable conditions, using basic medium for trypanosomes (see Material and Methods). Parasites incubated in basic medium containing DHA concentrations equal or less than 1 mM, survived slightly longer than the negative control (basic medium without carbon source), at least for the first hours; their cell density was about 60% than that observed for positive control (cells in basic medium with 1 mM glucose). However, they died rapidly thereafter. On the other hand, DHA concentrations higher than 1 mM caused immediate cell death. Taken together, these results indicate that low DHA concentrations can sustain parasite survival at least for a short period of time. Therefore, the absence of a gene with enough homology to DHAK in the parasite genome and the poor ability of DHA to serve as energy source, strongly argue for lack of DHAK enzyme in the Trypanosoma. Biochemical evidence confirming this fact has been obtained in our laboratory (Carmona-Gutierrez, 2005).

3.5.1.3. Dihydroxyacetone toxicity on *Trypanosoma brucei*

3.5.1.3.1. Anti-proliferative effects on trypanosomes

It has been published that DHAKs are involved in DHA detoxification in *S. cerevisiae*. The Dhak1Δ/Dhak2Δ yeast mutant showed a highly sensitive phenotype to DHA. In contrast, over-expression of either DHAK1 or DHAK2 made the Dhak1Δ/ Dhak2Δ yeast mutant highly resistant to DHA. In fact, this over-expression of either DHAK provided cells with the capacity to grow efficiently on DHA as the only energy source (Molin *et al.*, 2003). Therefore, the lack of this enzyme in *Trypanosoma brucei* could indicate susceptibility to DHA. We thus questioned if DHA may have an influence on the growth characteristics of trypanosomes. Indeed, addition of DHA to parasite cultures led to a dose-dependent decrease of cell growth (Fig. 3.14). After 20 h of DHA treatment, the parasites grew, or at least maintained their initial cell density , if the concentrations used were less than 3 mM. On the other hand, 4 mM and 5 mM of DHA averted cell proliferation.

In order to quantify the anti-proliferative effect of DHA on *Trypanosoma brucei*, the IC_{50}, *i.e.* the concentration necessary to inhibit cell growth by 50%, was determined.

The IC_{50} for DHA was 1.03 ± 0.14 mM (Fig. 3.15), a comparatively high concentration to other compounds tested as a potential drug against trypanosomes. However, the most important characteristic in relation of this issue is not the absolute drug concentration but the difference of toxicity between the parasite and the host. The DHA effect on mammalians is negligible as it can be used as an immediate energy source or converted to glucose by gluconeogenesis and then stored as glycogen. This advantage of DHA in comparison to other drugs along with its efficient passage by TbAQPs and the absence of DHAK in the parasite, gives a considerable leverage for parasite specific drug development.

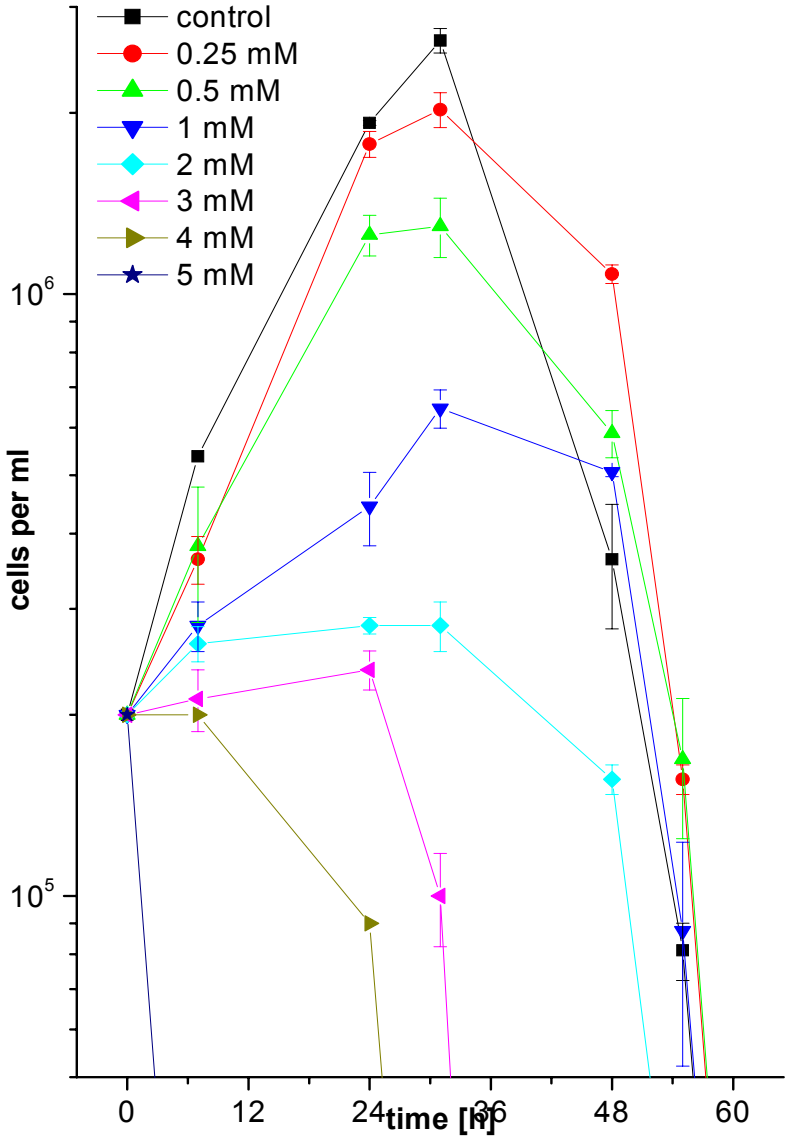

Figure 3.14. Growth of *Trypanosoma brucei* bloodstream form in presence of different concentrations of DHA

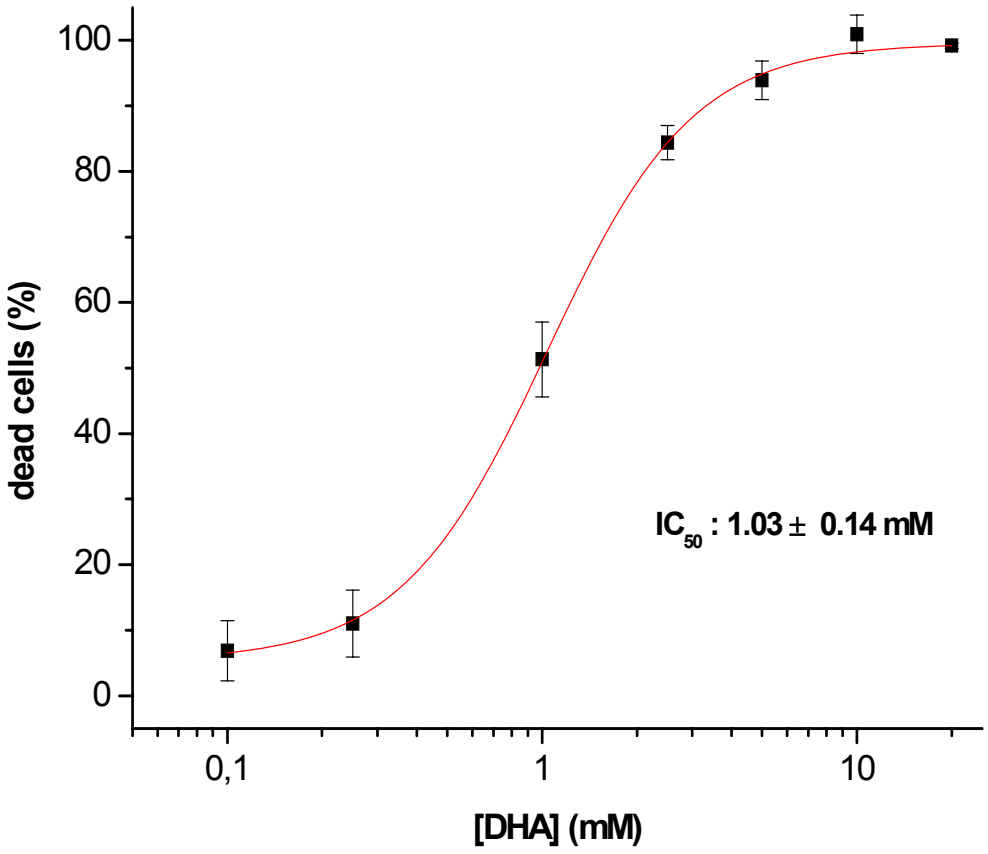

Figure 3.15. Toxicity of DHA for *Trypanosoma brucei* bloodstream form.

3.5.1.3.2. Morphological changes of trypanosomes induced by DHA

In order to detect morphological changes due to DHA treatment, trypanosomes were grown for 24 h in the presence or absence of DHA and then prepared for scanning (SEM) and transmission (TEM) electron microscopy.

Using SEM, a significantly elevated amount of cells containing more than one flagellum was observed (Fig. 3.16 a). These observations of unusual dividing forms indicate an abnormal cell division. In addition, some cells showed a significant increase in size as compared to untreated control cells. TEM images revealed that DHA caused alterations of the substructure of treated cell. The principal findings were two nuclei, condensation of chromatin in distinct areas of the nucleus, increase of the number of lysosomes, and alterations at the plasma membrane (Fig. 3.16 b).

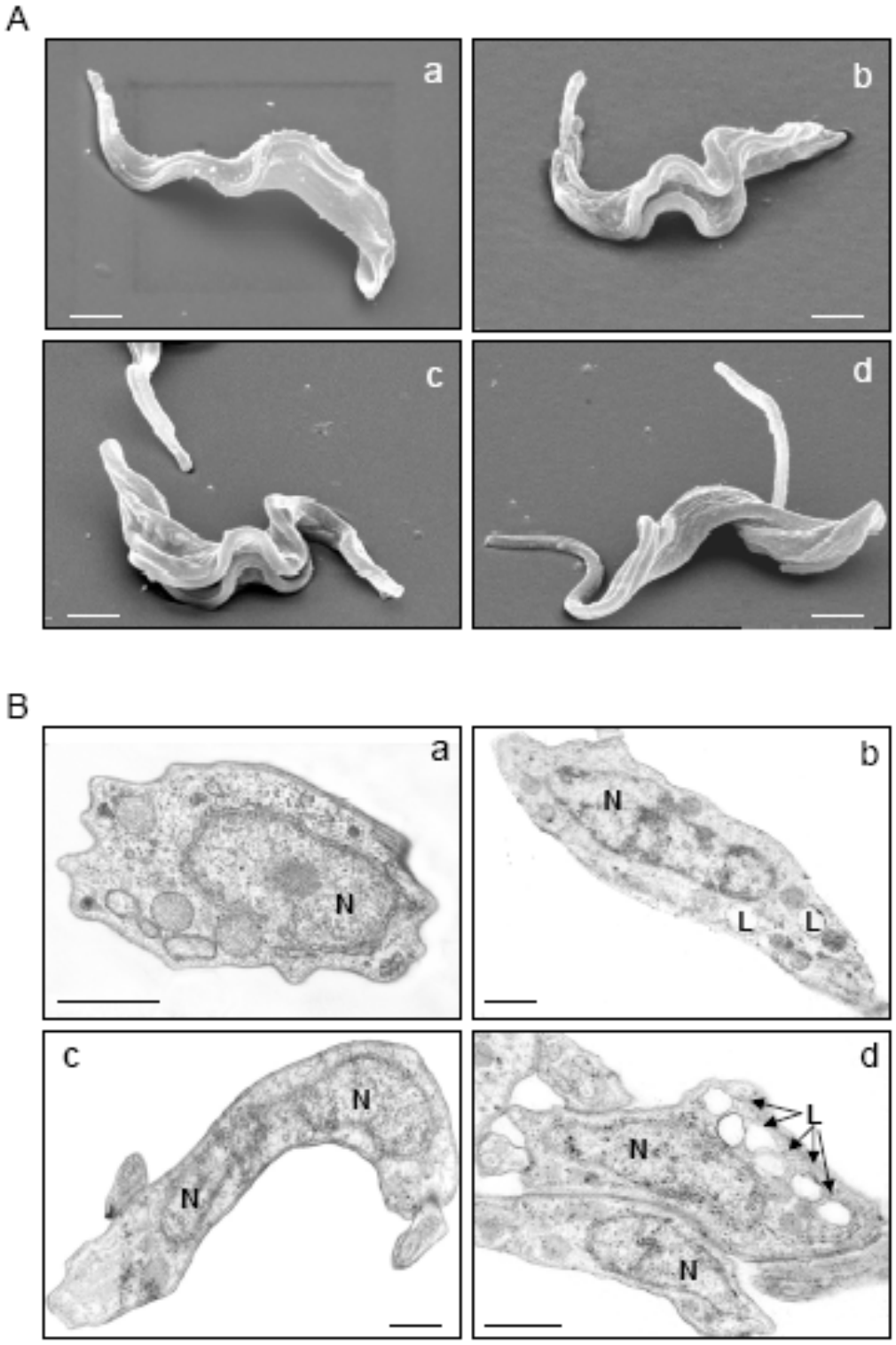

Figure 3.16. Electron microscopy of *Trypanosoma brucei* bloodstream form treated with DHA. A) Scanning electronic microscopy of untreated, control (a), and DHA treated parasite (b, c, d). B) Transmission electron microscopy of Epon-embedded cells. Abbreviations used in the control (a) and experimental (b, c, d) cells are: lysosome (L); nucleus (N).

3.5.1.3.3. Evaluation of cell cycle progression by FACS analysis in DHA treated trypanosomes

In order to determine the DNA content, DHA treated and untreated control cells were lysed hypotonically in 10 mM phosphate buffer containing 6 µM digitonin. DNA within the nuclei was stained using propidium iodide, before the nuclei were sorted according to size and fluorescence labelling using a FACScalibur® cell sorter. The respective distribution chart clearly discriminated between nuclei of the G1, S or G2 cell cycle stages and nuclei with a reduced DNA content due to DNA degradation processes. As shown in figure 3.17, cells treated with different DHA concentrations for 24 h showed cell cycle arrest in G2/M phase. This effect, even if not always dose-dependent, became markedly evident at concentration equal or above 2 mM DHA. This concentration was highly effective, since about 70% of the cells were arrested in the G2/M phase and about 10% of the cells were found in the G1 phase. In addition, 2 mM DHA caused an increase of poliploid cells up to 20%. Likewise, 3 and 4 mM DHA always showed a block in the G2/M phase; But in some cases less prominent than with 2 mM DHA (Fig. 3.17 a and b).

3.5.1.3.4. Search for cell death markers in DHA treated trypanosomes

An inhibition of cellular proliferation could indicate not only a cell cycle block but also cell death. In order to analyze if the most important DHA effect was indeed G2/M arrest, cell death in DHA-treated trypanosomes was investigated. So far, it is known that there are two possibilities of cell death: necrosis and programmed cell death, with the latter divided in different types, like autophagy and apoptosis.

Necrosis was evaluated using propidium iodide, a compound that only stains necrotic cells due to their lack of plasma membrane integrity. Untreated control trypanosomes showed only 2.8% of necrosis after 24 h of incubation. Compared with this, DHA treated cells showed a minor increase of necrosis which intensified in parallel with the DHA concentration, reaching a maximum of about 13% necrosis at 4 mM DHA (Fig. 3.18, first column). This level of necrosis is almost negligible if compared to the inhibition of the parasite's proliferation caused by the used DHA concentration (Fig. 3.14).

A further analysis of cell death was performed by evaluation of three known programmed cell death (PCD) markers: DNA degradation, loss of mitochondrial membrane potential (Ψm), and phosphatidylserine exposure. As judged from figure 3.18, columns 2, 3, and 4, these markers were detected after treatment of cells with 2 mM DHA and the respective signals increased in a dose-dependent manner up to 10% for DNA

degradation, 27% for the loss of Ψm, and 20% for phosphatidylserine exposure. Although the last two parameters (Ψm and phosphatidylserine exposure) were slightly higher than those observed for necrosis, the data are not indicative for PCD, because they are low and in the same range as for necrosis.

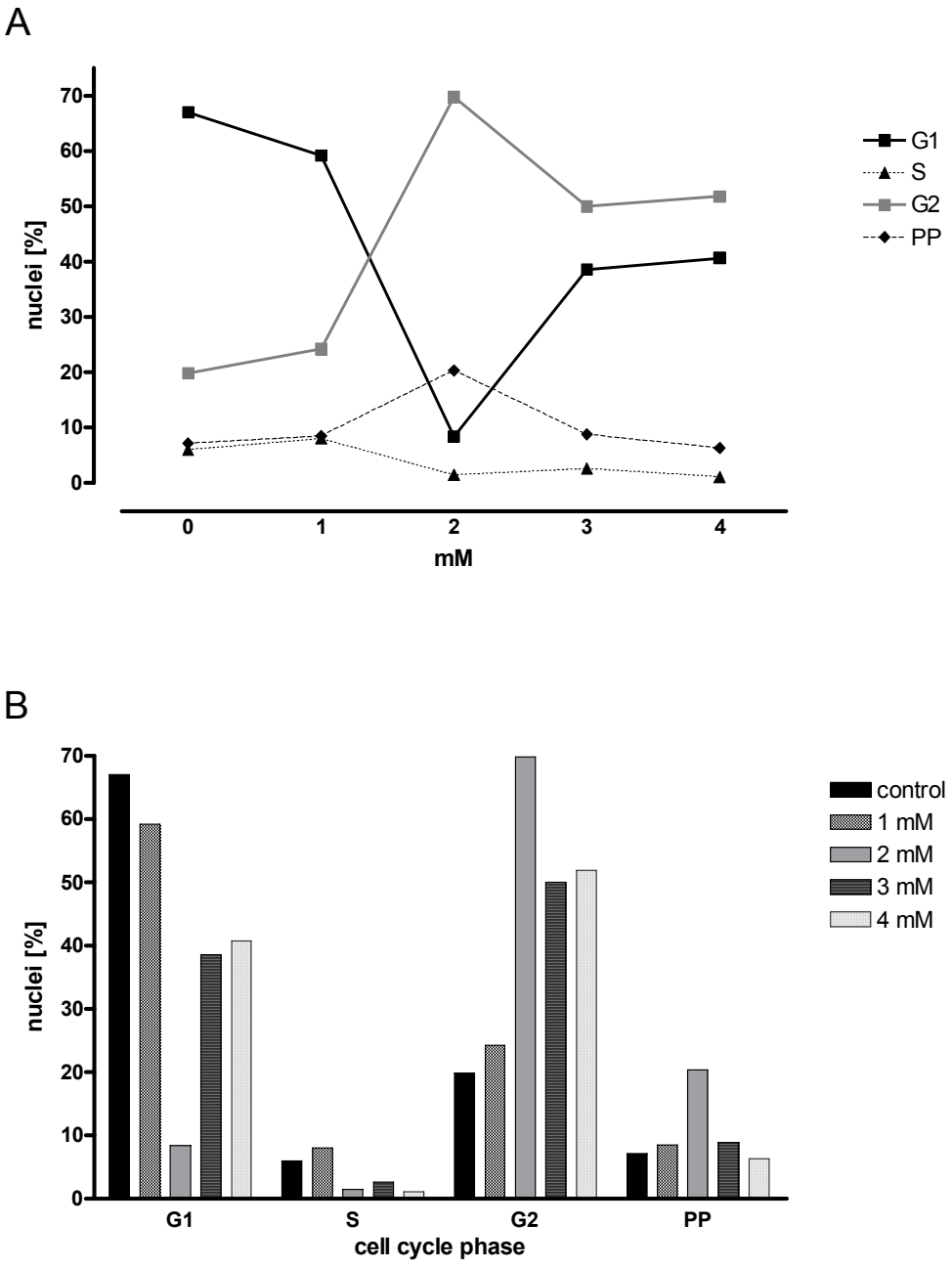

Figure 3.17. Two different representations of the DHA effect on the cell cycle of *Trypanosoma brucei* bloodstream form. Cells were treated with different concentrations of DHA. After 24h they were stained with propidium iodide and analysed FACS. The percentages were determined using the CellQuests software

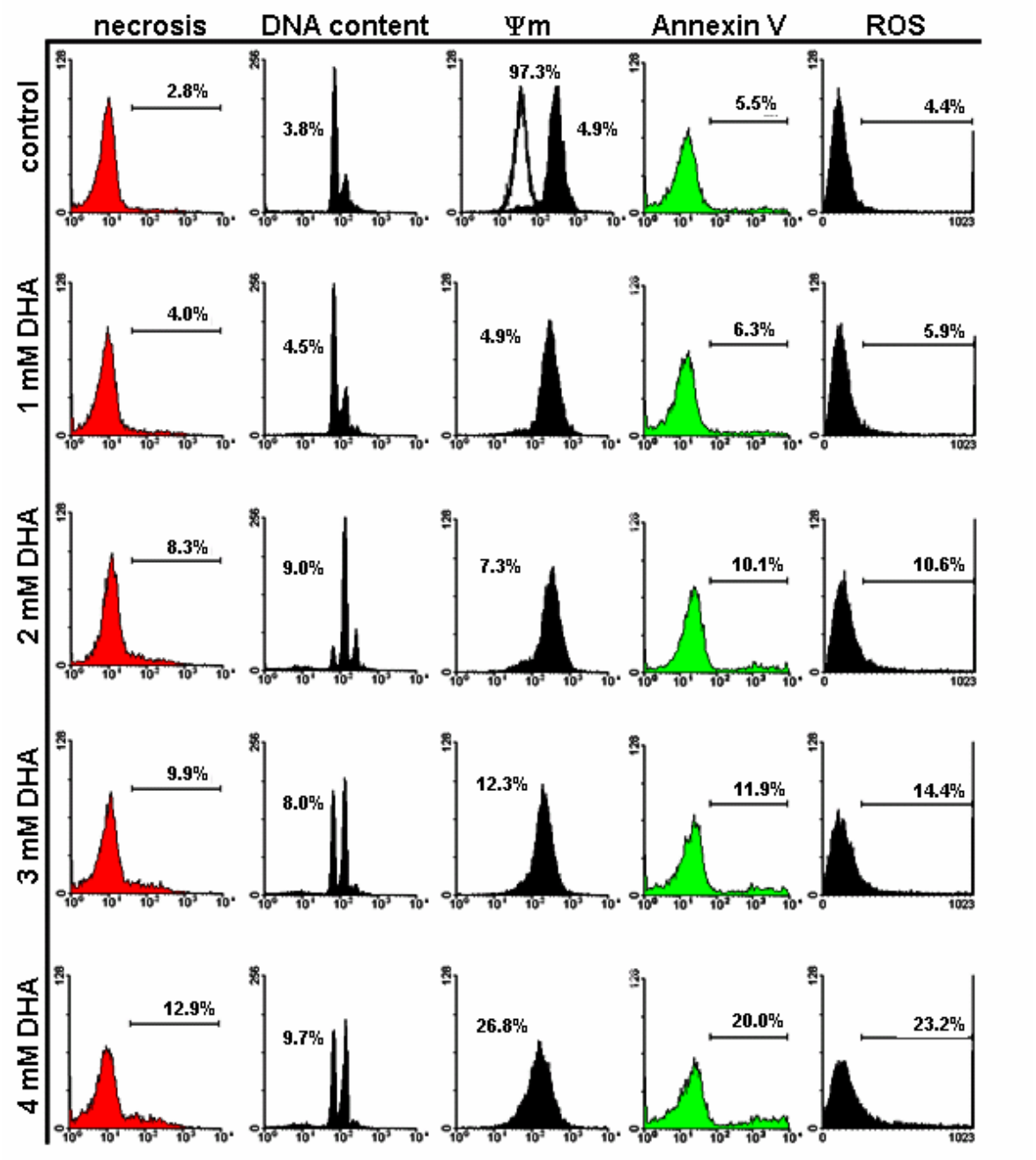

Figure 3.18. Evaluation of Cell death markers. Propidium iodide, TMRE, anexin V or DCFH-DA staining of *Trypanosoma brucei* bloodstream forms in FACS analysis. Cells were treated for 24 h with different concentrations of DHA.

In addition, it is known that reactive oxygen species (ROS) are involved in trypanosome PCD (Figarella *et al.*, 2006). For this reason, ROS production was evaluated in DHA-treated trypanosomes. As with the other PCD markers, the increase of the ROS signal was similar to PCD markers (Fig. 3.18, column 5). According to our results, PCD in treated cells is present only in high concentration of DHA but it is negligible when compared with the indication of cell cycle arrest in the G2/M phase.

3.5.2. Arsenic (As III) and antimony (Sb III)

Arsenic and antimony are toxic compounds which have been used as chemotherapeutic agents for a century. At the beginning of the twentieth century it was shown that trypanosomiasis could be successfully treated with organic derivatives of arsenic (Xu *et al.*, 1998). Nowadays, melarsoprol, an organic arsenical, is still in use for the treatment of sleeping sickness, being the compound most effective against chronic stage. Likewise, all forms of leishmaniasis are treated with drugs containing antimony (Borst and Ouellette, 1995). On the other hand, arsenic trioxide has been shown to be a highly effective drug in treating patients with acute promyelocytic leukaemia (Shen *et al.*, 1997; Soignet *et al.*, 1998). Interestingly, the uptake systems for these compounds were recently discovered. GlpFp, an aquaglyceroporin, was able to transport SbIII and AsIII (Sanders *et al.*, 1997, Meng *et al.*, 2004). Later, aquaglyceroporins were also found to be metalloid transporters in *S. cerevisiae* (Wysocki *et al.*, 2001), *Leishmania* (Gourbal *et al.*, 2004) and mammalian cells (Bhattacharjee *et al.*, 2004). Due to the historical and present importance of AsIII and SbIII compounds as effective drugs for the treatment of several diseases (especially for sleeping sickness), and considering the ability of some aquaglyceroporins to be permeated by AsIII and SbIII, the TbAQPs capacity to transport these metalloids was analyzed.

3.5.2.1. TbAQPs permeability for AsIII and SbIII

In order to evaluate the transport properties of TbAQPs for AsIII and SbIII, we used yeast as a channel expression system. TbAQPs-transformed fps1Δ mutant cells and control cells were grown and then spotted in a 10 fold serial dilution onto agar plates containing different concentrations of AsIII, AsV and SbIII. These compounds exert toxic effects inside yeast cells and by adjusting their concentration in the agar plate it is possible to show whether they are transported by TbAQPs by comparing growth rates of yeast expressing any of the 3 TbAQPs with control cells. As shown in figure 3.19, TbAQPs-transformed fps1Δ mutant cells were hypersensitive to AsIII and SbIII,. The only difference between the TbAQPs-transformants (sensitive to trivalent metalloids) and control cells (resistant to trivalent metalloids) was the heterologous expression of TbAQPs. Therefore, the enhanced sensitivity of these cells is, obviously, a consequence of the metalloids transport by TbAQPs.

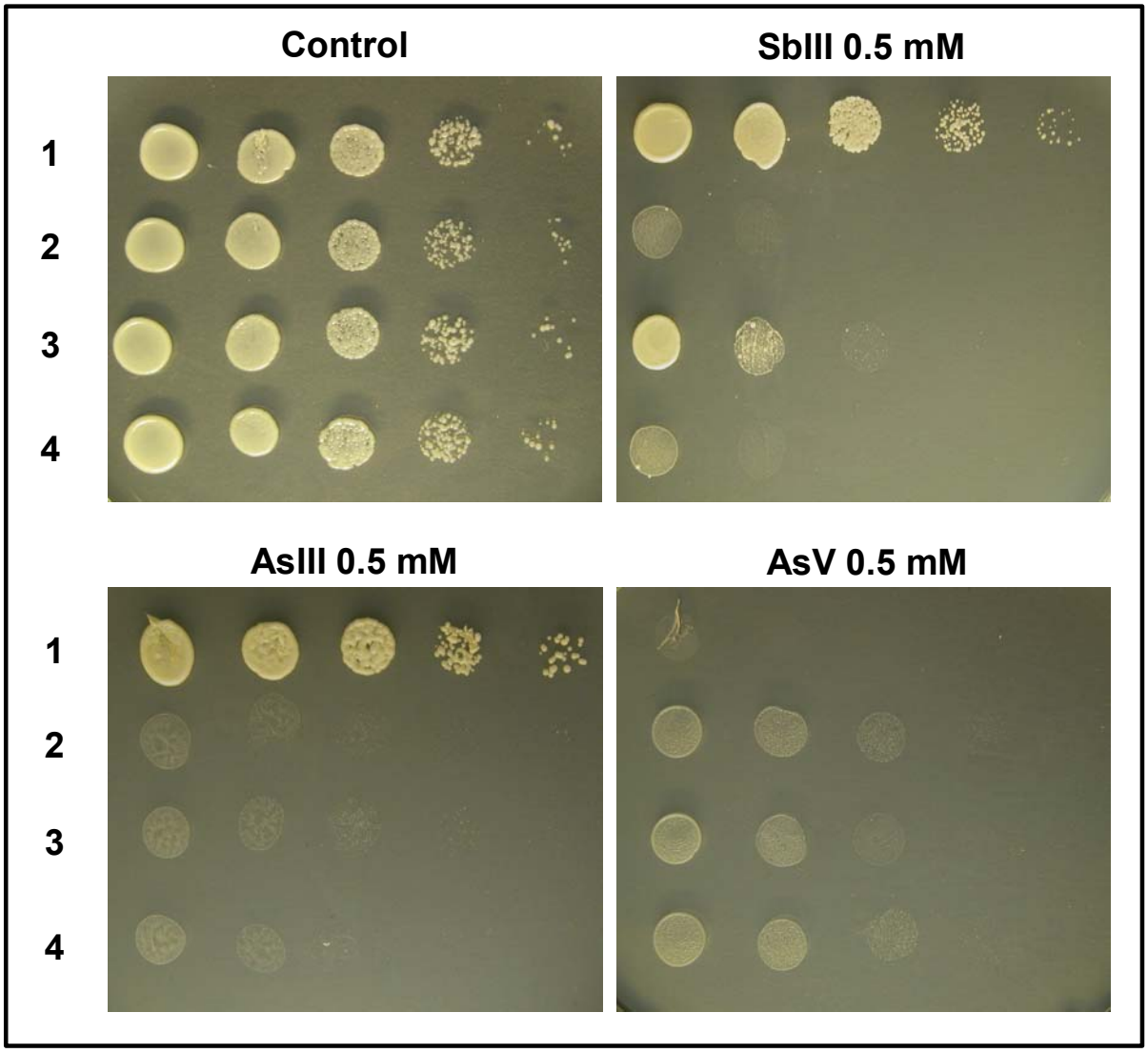

Figure 3.19. Phenotypes of fps1Δ mutant cells expressing TbAQPs in presence of As III, As V and Sb III. Transformed yeast cells expressing TbAQPs were grown over night in selective liquid media. Thereafter, they were spotted in 1:10 dilution series onto agar media containing the indicated compounds. Control cells were transformed with empty-plasmid. Control (1), TbAQP1 (2), TbAQP2 (3), TbAQP 3 (4).

It has been suggested for AsIII (and also for SbIII) that not the ionic As atom itself, but $As(OH)_3$, the most stable structure at neutral pH, is the permeable form which is taken up by the cells (Ramirez-Solis *et al*., 2004). In order to obtain further evidence for the role of aquaglyceroporins in AsIII and SbIII uptake, the yeast transformants were exposed to these metalloids on agar plate at different pH values. As shown in figure 3.20 for SbIII, the sensitivity of yeast TbAQPs-transformants for metalloids increased in parallel with the gradual increase in pH. The same results were obtained for AsIII at lower concentrations

(data not shown). These results indicate that the change of the spatial structure of these compounds from $As(OH)_3$ and $Sb(OH)_3$ to any other, decreased the permeability of TbAQPs for them.

On the other hand, yeast TbAQPs-transformants showed a resistant phenotype for AsV, indicating that this compound was not able to pass through the channels. In contrast, control cells were hypersensitive to this metalloid form. The most probable explanation is that AsV (due to its structural resemblance to inorganic phosphate) enters yeast cells via the phosphate transporter. Inside the cell AsV is converted to AsIII by an arsenate reductase, and is then eliminated from the cytosol via aquaglyceroporins. Since control cells lack a functional glycerol channel, AsIII is trapped inside the yeast and leads to cell death.

3.5.2.2. Anti-proliferative effects of AsIII, AsV and SbIII on *T. brucei*

The evaluation of the metalloid's cytotoxicities on trypanosomes was performed using the IC_{50} assay. These drugs killed the parasite in the nM to μM range. The order of potency was SbIII > AsIII > AsV, as indicated by IC_{50} values; 103 ± 6 nM, 308 ± 56 nM and 7.0 ± 0.3 μM, respectively (Table 3.1). Albeit the compounds tested have pronounced side effects on human beings, they are used for medical treatment of different diseases. In the case of AsIII, which is the basis of several drugs used against sleeping sickness, serum concentrations are well under concentrations observed in patients with acute promyelocytic leukaemia treated with Trisenox® (arsenic trioxide) (List *et al.*, 2003). In the case of Trisenox®, plasma concentration between 300- 2900 nM have been determined in treated patients, leading to concentrations between 450-2400 nM in red blood cells. The observed IC_{50} for AsIII in *T. brucei* bloodstream forms was equal or tenfold less, which would make Trisenox® a possible alternative drug to be used against trypanosomiasis.

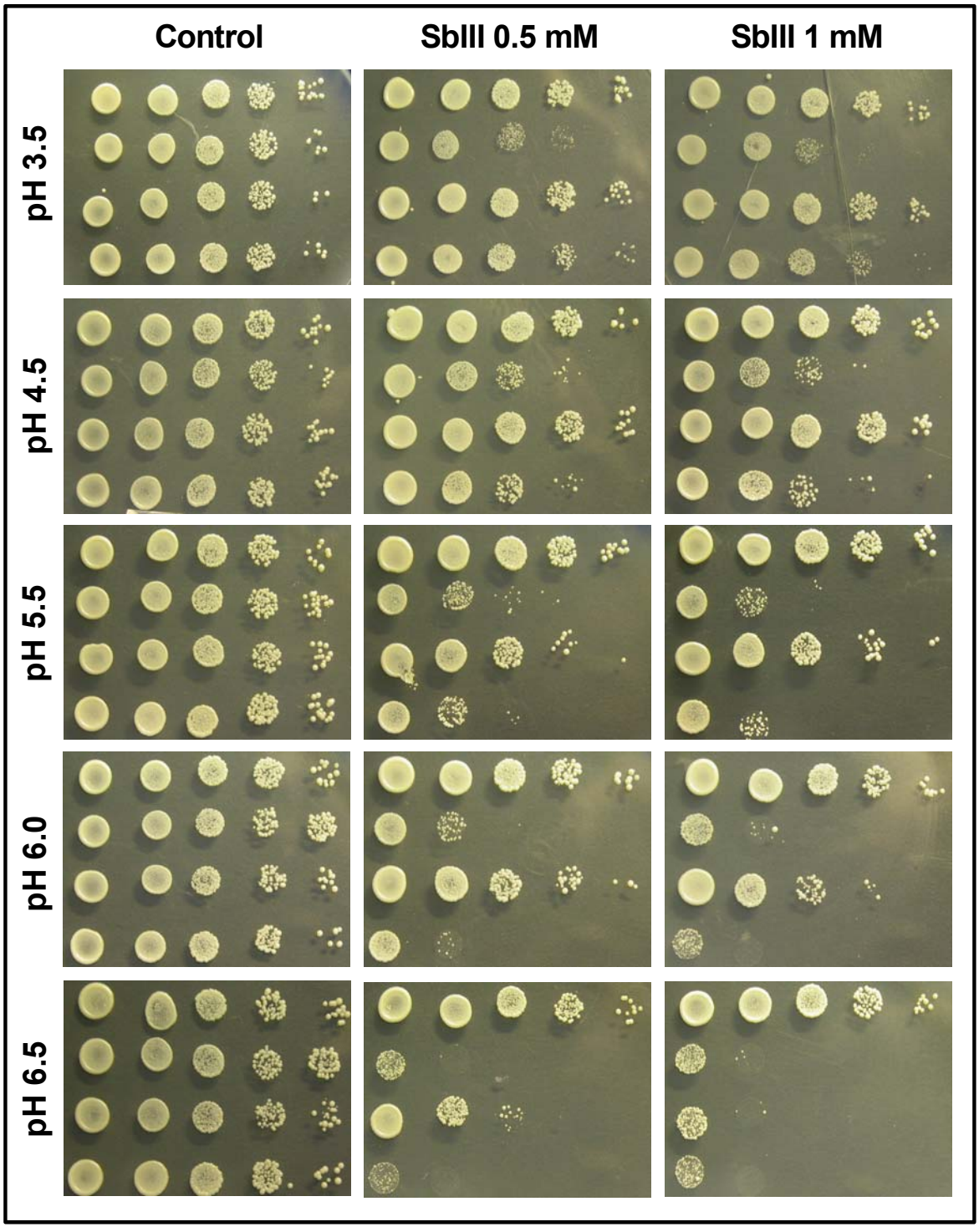

Figure 3.20. Effect of pH on Sb III Phenotypes of fps1Δ mutant cells expressing TbAQPs. Yeast cells were grown in selective liquid medium over night followed by spotting onto selective agar medium containing Sb III at the pH indicated. In each panel: first row, control cells containing an empty vector; second row, TbAQP1; third row, TbAQP2; fourth row, TbAQP3.

Table 1. Toxicity of different compounds on *Trypanosoma brucei*

Compound / parasite form	IC_{50} (µM)
Arsenic V / bloodstream	7.0 ± 0.3
Arsenic III / bloodstream	0.308 ± 0.056
Antimony III / bloodstream	0.103 ± 0.006
Methylglyoxal / bloodstream	21.1 ± 3.9
Ammonia / bloodstream	22,300 ± 1000
Ammonia / procyclic	25,300 ± 1400

3.5.3. Ammonia

Trypanosoma brucei, as well as other members of the order Kinetoplastida, possesses a particular energy metabolism. For bloodstream forms, glucose is the only energy source as the unique ATP production machinery is the glycolysis. Amino acid metabolism for ATP production, one of the most important sources of ammonia, is not active during this life cycle stage, and thus the major reactions involved in ammonia consumption-production should not be in place at an appreciable rate. It is thus expected that an excess of ammonia added externally should be toxic for the parasite. In contrast, in procyclic forms, the energy production from amino acids is essential for parasite survival. Indeed, media used for *in vitro* culture of this parasite stage possess proline as energy source and do not contain any glucose. Therefore, elimination of ammonia from the procyclic form parasite to avoid the ammonia accumulation due to active amino acid catabolism should require a specific transport pathway. On the other hand, it has recently been demonstrated that ammonia is transported by some aquaglyceroporins (Jahn *et al.*, 2004). These facts, together with the lack of any homologous genes of classical ammonia transporters in the gene databank of *Trypanosoma brucei*, led us to study the ammonia permeability of TbAQPs in more detail.

3.5.3.1. TbAQPs permeability for ammonia

Yeast cells expressing either one of the TbAQP proteins in the mutant strain fps1Δ were plotted in a 10-fold dilution on selection medium as indicated in material and methods: YNB containing glucose, 0.1% proline as sole nitrogen source and 100 mM

methyl-ammonium as a toxic analogue of ammonium. Transformed-empty-plasmid mutant yeast cells were used as a negative control and the isogenetic parental strain containing the functional chromosomal FPS1 gene served as a positive control. As shown in figure 3.21, the growth of experimental cells was similar to the positive control at low pH, whereas the growth of negative control cells was completely inhibited. When the pH was gradually shifted towards a neutral pH, the proliferation of both experimental and positive control cells was decreased to the same level as the negative control. This result can be interpreted by considering the physico-chemical properties of methyl-ammonium and its toxic effect on cells. When methyl-ammonium was dissolved in a solution of low pH, it possesses a positive charge and was therefore unable to pass the pore of the channels. However it reached the intracellular space because there are three specific transporters for ammonium (MEP1-3) in yeast (Marini *et al*., 1997). Once methyl-ammonium its way inside the cell it can exert its toxic effects. However, due to the neutral pH within the cell, this compound lost its charge and therefore recovered its ability to pass through the aquaglyceroporins and was thus efficiently eliminated from the cell. The toxic effects were only observed in negative control cells, which were depleted of aquaglyceroporins. However, methyl-ammonium became very toxic also for experimental and positive control cells when the pH of the medium was adjusted towards neutrality, as a consequence of the formation of an important amount of methyl-ammonia. In this chemical form this compound can rapidly enter cells via aquaglyceroporins and even, at an appreciable rate, across the membrane if the cells were exposed for a sufficient time to the drug. Therefore, the characterizations of this phenotype in yeast expressing TbAQPs demonstrate that these channels are also permeable to ammonia.

3.5.3.2. Ammonia production in culture by both bloodstream and procyclic form of *T. brucei*

Information about the ammonia production in protozoa is hardly found in the literature (Kleydman *et al.*, 2004), especially with regard to *T. brucei*. On the other hand, the different stages of *T. brucei*, bloodstream and procyclic forms have a dissimilar amino acid and carbohydrate metabolism. The increase in ammonium concentration has been used in *Leishmania* experiments as an indicator of amino acid catabolism (Cazzulo *et al.*, 1985; Louassini *et al.*, 1999). In order to obtain data about the importance of ammonia in the parasite and then, possibly, information about the difference of amino acid catabolism between *T. brucei* forms, the ammonia production was determined during growth of these

parasites. Both stages of the parasite were grown in culture media. Aliquots were taken at regular time intervals from the media to measure ammonia concentrations. Media incubated alone were used to determine the spontaneous ammonia production.

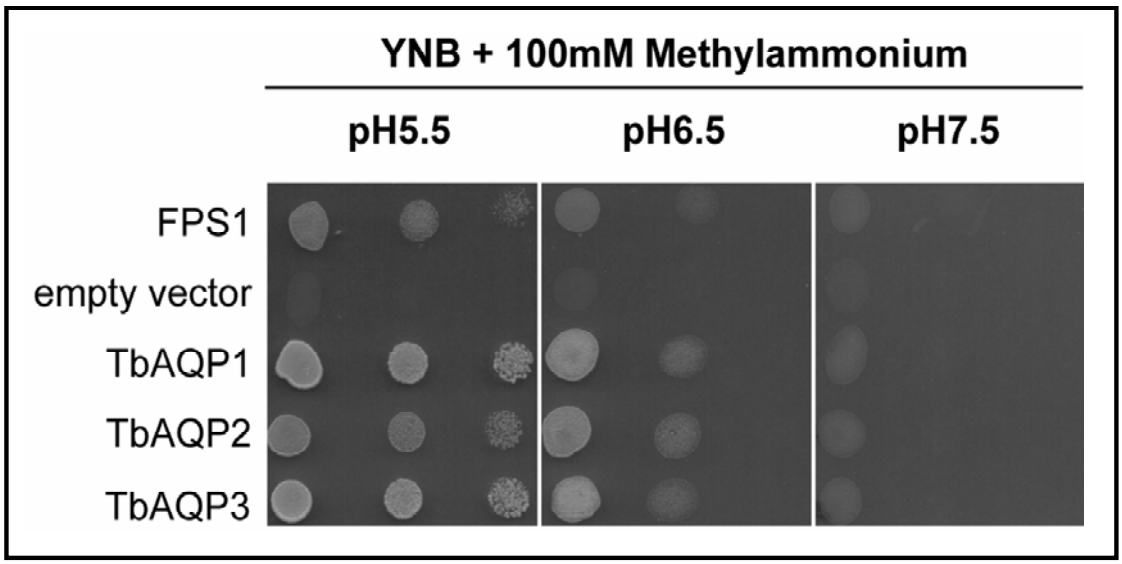

Figure 3.21. Phenotypes of fps1Δ mutant cells expressing TbAQPs in presence of Methylammonium at dofferent pH. Yeast cells expressing the TbAQP proteins in the fps1Δ strain, after pre-grow in liquid media, were plotted in a 10-fold dilution on YNB+glucose selection medium containing 0.1% proline as the sole nitrogen source and 100 mM methylammonium as the toxic analogue of ammonium. The isogenetic parent strain containing the functional chromosomal FPS1 gene was used as a positive control.

The ammonia production for the bloodstream form paralleled parasite's proliferation until 42 h, and then it started to decay, during the later stationary phase when parasites went into a clear declining phase (Fig. 3.22 a). In contrast, the ammonia production behaviour was different in procyclic forms: in the lag and at the beginning of the stationary phase, there was virtually no ammonia production. However, during the whole exponential phase, proliferation and generation of ammonia went on in parallel (Fig. 3.22 b). Although procyclic forms produced about 10 fold more ammonia than bloodstream forms, 3 mM versus 0.2 mM, the production rate per parasite, was in the same order of magnitude, since 300 nM per procyclic parasite and 100-200 nM per bloodstream form were obtained if the ammonia concentration was divided by the maximum parasite number. It is interesting to note that these values are in the same order of magnitude, because it should be expected that the ammonia production of bloodstream forms could not be compared to that of the procyclic forms. *Plasmodium falciparum* blood-form also produces ammonia in the same

range (Beitz, personal communication); this parasite, like *Trypanosoma brucei* bloodstream form, relays on glycolysis to obtain energy.

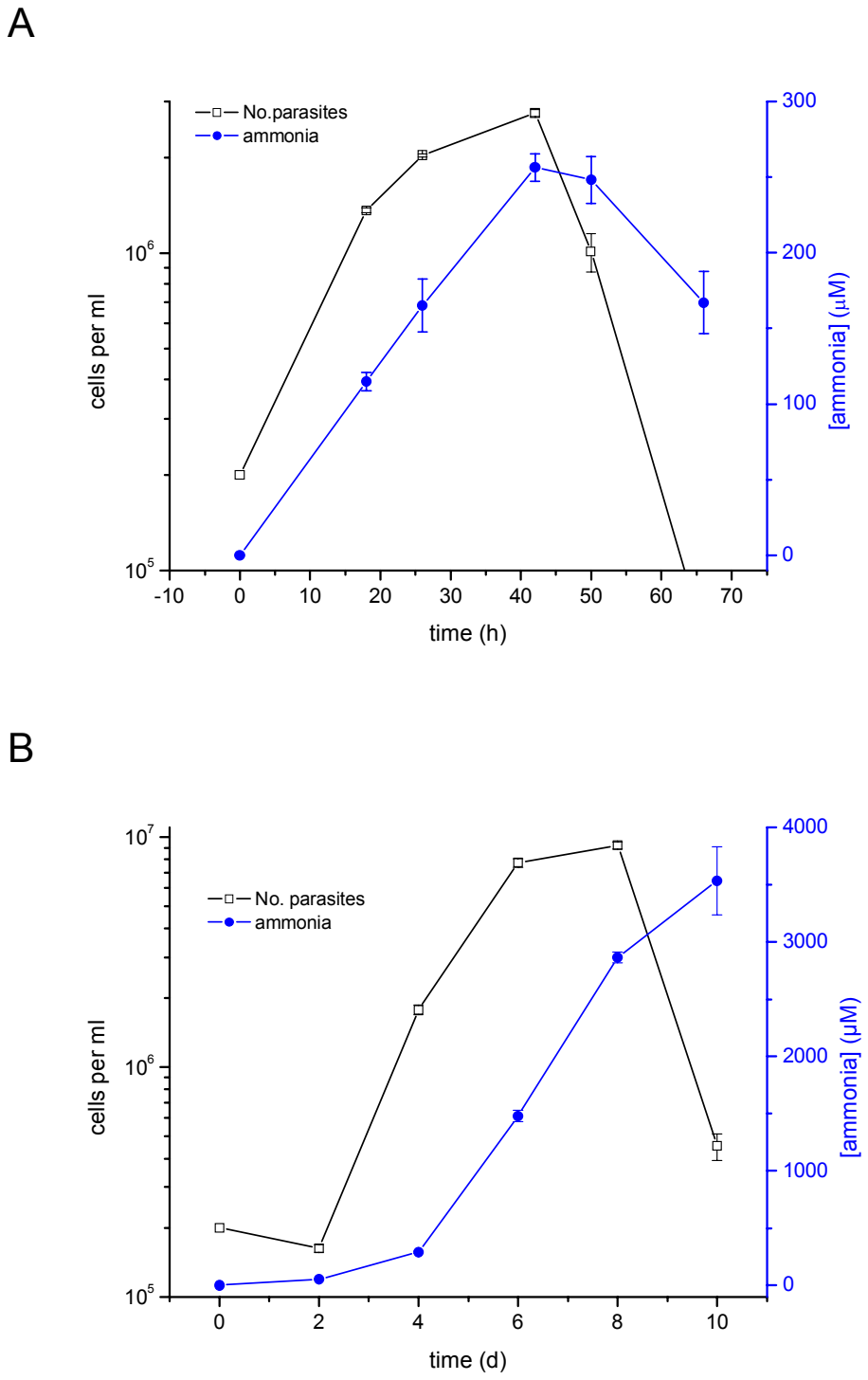

Figure 3.22. Cell growth and ammonium production by *Trypanosoma brucei* (A) bloodstream form B) procyclic form.

Altogether, theses results indicate two important aspects of the parasite biology: A) although the bloodstream form does not depend on amino acids as energy source, its ammonia production implicates that the metabolism of this biological compound may play an important role in this parasite stage. B) Procyclic forms of *T. brucei* showed a resistance against the toxic effects of ammonia as these parasite forms were able to proliferate in ammonia concentrations which are 10 fold higher than those in the normal range for human being.

3.5.3.3. Effects of ammonia on *Trypanosoma brucei* proliferation

Preliminary results concerning the ammonia production of procyclic forms of *T. brucei* suggest that this protozoon can cope with a relatively high concentration of ammonia, which is several times higher than those believed to be toxic to mammals (Huizenga *et al*., 2002). In order to quantify how important is this natural ammonia resistance phenotype of trypanosomes, the IC_{50} assay was performed.

In fact, both parasitic stages are highly ammonia resistant. The IC_{50} was 22.3 ± 1 mM and 25.3 ± 1.4 mM for bloodstream and procyclic forms, respectively (Table 3.1). These concentrations are 600-1200 fold higher than the normal values found in human blood. Therefore, therapeutic approaches based on this compound are probably irrelevant.

On the other hand, the fact that the different stages of the parasite, in spite of having a dissimilar amino acid metabolism, can cope with the high ammonia concentration in a similar manner, indicate that amino acid related enzymes, as the glutamate dehydrogenase, may have an important role in survival of the parasites and not merely a function in the amino acid catabolism.

3.5.4. Methylglyoxal

The main source of methylglyoxal is the enzymatic and nonenzymatic fragmentation of triose phosphates, mainly of dihydroxyacetone phosphate and glyceraldehyde-3-phosphate, both intermediates of glycolysis. In addition, it is produced by threonine catabolism and acetone oxidation (Vickers *et al.*, 2004). Methylglyoxal can react with various biological compounds within cells, such as proteins, DNA and RNA, and thus it shows cytotoxicity (Inoue *et al.*, 1998). Methylglyoxal is inevitably formed by the triosephosphate isomerase reaction. Therefore, an increased flux of glucose to the glycolytic pathway causes the enhancement of the intracellular methylglyoxal content

(Inoue *et al.*, 1998). As we already know, trypanosomes have one of the highest known glycolysis fluxes, this fact becomes methylglyoxal metabolism in an important parasite drug target. However, trypanosomes possess defence mechanisms against this compound with glyoxalase as a major enzyme detoxifying methylglyoxal, already described in the trypanosoma family (Vickers *et al.*, 2004).

In order to investigate the cytotoxic effect of methylglyoxal on *T. brucei* and to comprehend the importance of TbAQPs in this phenomenon, we performed IC_{50} assays and evaluated the methylglyoxal capacity to pass trough the pore of TbAQPs.

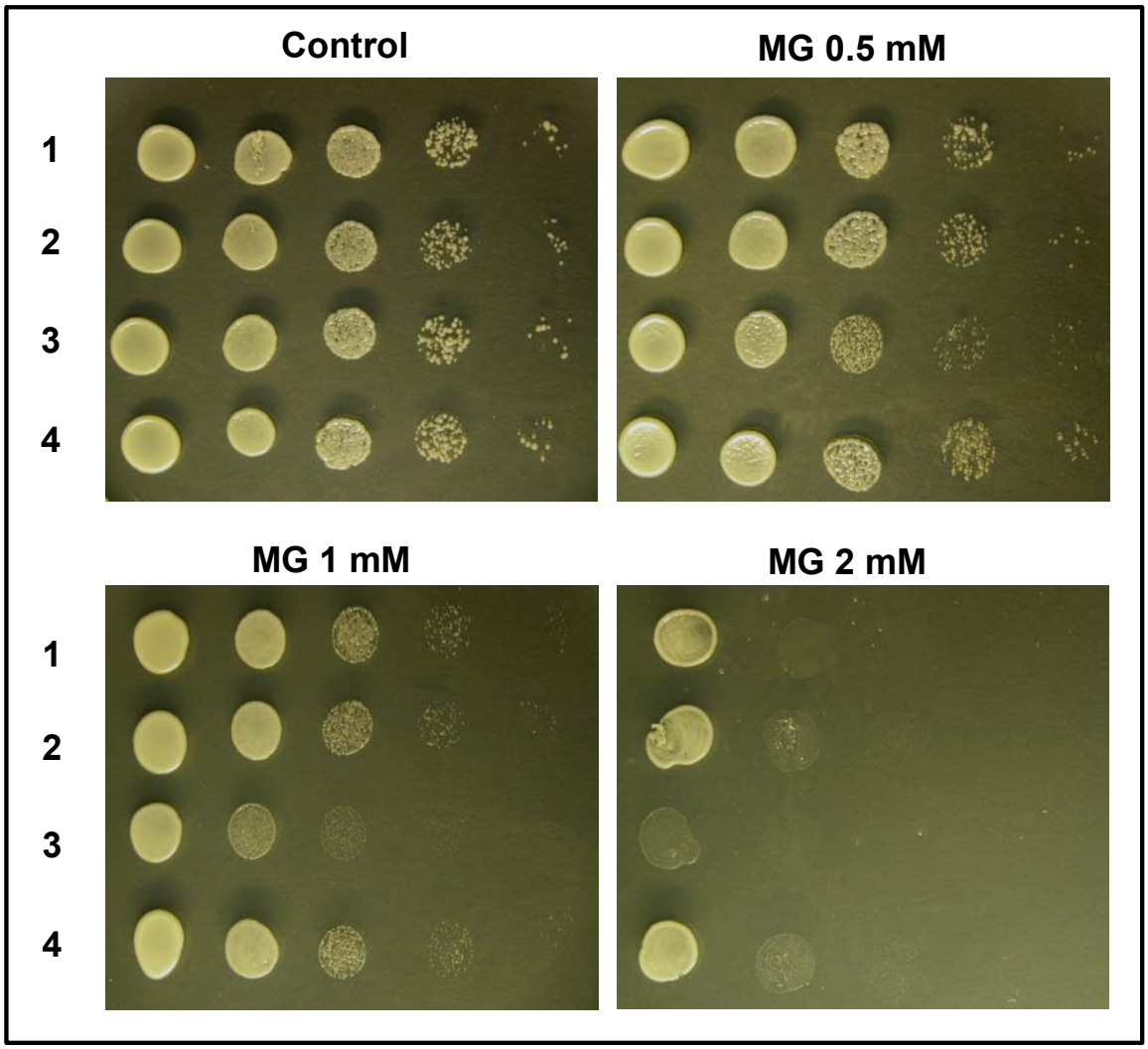

Figure 3.23. Phenotypes of fps1Δ mutant cells expressing TbAQPs in presence of Methylglyoxal (MG). TbAQP-transformed yeast cells were grown over night in selective liquid medium and then, were spotted in 1:10 dilution series onto agar medium containing Mg to the indicated concentrations. Empty-plasmid-transformed yeast cells were used as control. In each panel: Control (1), TbAQP1 (2), TbAQP2 (3), TbAQP 3 (4).

3.5.4.1. Methylglyoxal as both cytotoxic compound for Trypanosoma and solute for TbAQPs

The IC_{50} for methylglyoxal on *T. brucei* bloodstream form was 21.1 ± 3.9 µM (Table 3.1). As expected, this compound is toxic for the parasite, but its effect is more prominent if compared to other mammalian cells. Methylglyoxal killed trypanosomes in concentrations not toxic for human cells, e.g. for neuroblastoma cells the IC_{50} of methylglyoxal is 1.25 mM (Webster *et al*., 2005).

Interestingly, using yeast cells in cytotoxicity experiments, 0.5 mM methylglyoxal only affected cells expressing TbAQP2 (Fig. 3.23). When the methylglyoxal concentration was increased from 0.5 mM up to 2 mM, all cells showed a growth inhibition. The behaviour of TbAQP 1 and 3-transformed mutants was the same as that of the control, whereas TbAQP2 transformed mutants showed a drastic reduction of their proliferation if compared with control cells. These results indicate that TbAQP2 is a mediator of methylglyoxal entrance into yeast cells and stress the importance of the amino acids located in both canonical NPA motifs. TbAQP1 and 3 present two classical NPA motifs in the pore regions whereas TbAQP2 possesses NSA/NPS boxes. Additionally, the highly conserved arginine close to this region is replaced by a leucine.

3.6. Expression level and localization of TbAQPs in *Trypanosoma brucei*: First approaches

3.6.1. Transcription of the *TbAQP* genes from *T. brucei*

In order to know whether the expression of *TbAQP* genes from *T. brucei* differs in the respective stages and growth phases of the parasite, we performed Northern blot analysis. For this purpose, total RNA from different life cycle stages and growth phases was isolated and a part of each *TbAQP* gene sequence (see material and methods) was used as probe. *TbAQP* genes showed a stage-specific regulation of their transcripts (Fig. 3.24). *TbAQP1* was slightly expressed during the log phase of bloodstream forms, highly expressed during stationary phase, and almost the only one expressed in procyclic trypanosomes. *TbAQP2* was slightly expressed throughout the life cycle, and transcripts of *TbAQP3* were mainly detectable in bloodstream form parasites. Their band intensity was minor, but comparable to that of TbAQP1 (Fig. 3.24). Therefore, TbAQPs are expressed

throughout the life cycle of the parasite. They are also regulated in a different fashion which depends on both, the life cycle stage of the parasite and the growth phase.

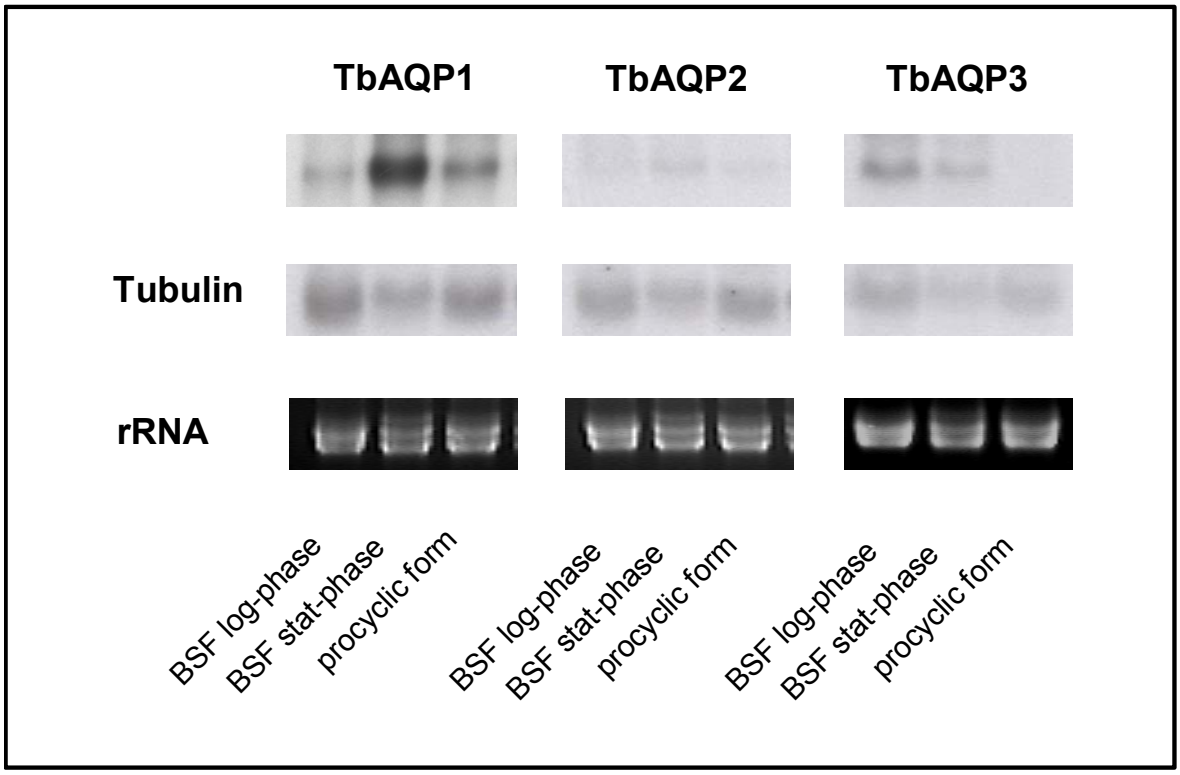

Figure 3.24. TbAQPs northern blot analysis of *Trypanosoma brucei*, bloodstream and procyclic form. Total RNA was isolated from the exponentially growing bloodstream form, the stationary phase bloodstream form, and exponentially growing procyclic forms and then separated on an agarose gel (15 μg/lane of each sample). After blotting, membranes were first hybridized with probes corresponding to the different *TbAQPs*, stripped thereafter, and reprobed with a α-tubulin sequence as a control for loading.

3.6.2. Localization of TbAQPs in *T. brucei*

3.6.2.1. Generation of chicken IgY antibodies against TbAQPs

Transcription analyses showed expression of TbAQPs throughout the whole life cycle of trypanosomes. The differential expression patterns gave us an idea concerning the protein level. However, the real amount of protein expression can not be estimated only by these results. Especially in Kinetoplastida, the most important regulatory mechanism of gene expression is post-transcriptionally regulated (Clayton, 2002). In order to obtain more information about TbAQPs expression on the protein level and to localize these proteins in the parasite, antibodies against TbAQPs were made.

In order to obtain antibodies against each protein, different short amino acid sequences of TbAQPs were chosen for peptide production (see material and methods). These sequences contain sufficient amino acid residues to confer an immunogenic characteristic. They are not located within the transmembrane domains of the proteins, and are thus expected to be exposed to the solvent. These sequences are not present in other proteins of the parasite and do not possess posttranscriptional modifications sites e.g. for glycosylation or phosphorylation which could interfere with the protein recognition by the antibodies.

Peptides were generated using a peptide synthesizer and applied to immunize chicken. Antibodies were prepared by the Biogenes Company using a standard immunization protocol; pre-immune antibodies from egg yolk were purified the same way and used to check for unspecific reactivity.

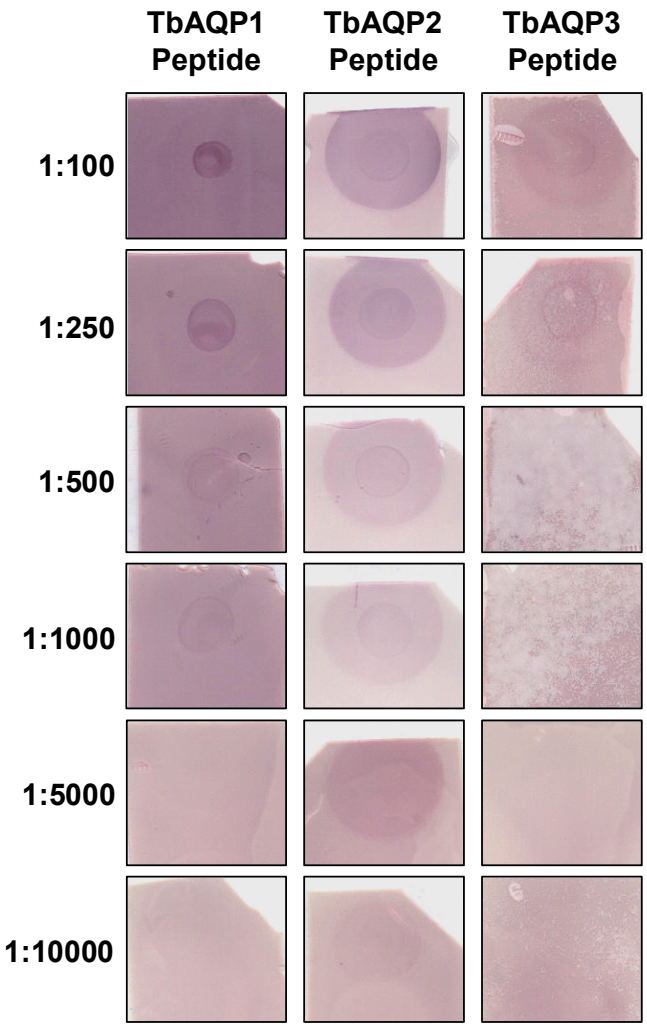

Figure 3.25. Dot-blot analysis of antibodies raised against the specific sequence of each TbAQPs. 100 ng of each TbAQP peptide was placed on the membrane and challenged with the corresponding anti-bodies at the indicated dilution.

3.6.2.2. Dot blot analysis

The obtained antibodies were tested using their peptides by Dot blot analysis. As shown in figure 3.25, all of these antibodies recognized their respective peptide. The highest dilution in which the antibodies were able to detect their peptides was 1:1,000; 1:10,000 and 1:250 for TbAQ1, 2 and 3, respectively. The development time of the Dot blot for anti-TbAQP1 and 3 were quite long, i.e. several hours, whereas

anti-TbAQP2 needed only 30 min. In addition, the antibodies did not show any cross reaction with the respective other two peptides (results not shown). These results indicate that the generated antibodies can recognize specifically their antigen, however with different affinities, anti-TbAQP2 being the most potent, followed by anti-TbAQP1 and anti-TbAQP3, as the weakest.

3.6.2.3. Western blot analysis

Next, we analyzed whether IgY antibodies were capable of recognizing native TbAQP proteins. To this end, total lysates prepared from TbAQP1-3 transformed yeast cells were subjected to Western blot analysis using the respective antibodies. Empty-plasmid-transformed yeast cells were used as control cells. No specific bands were detected by any antibody, even using different dilutions (results not shown). Therefore, enriched membrane fractions of these cells were prepared and challenged with anti-TbAQP1-3. Under these conditions, the antibodies TbQP1-2 were able to recognize a specific band of approximately 30-35 KDa, as expected considering the calculated molecular weight of these proteins. These bands were not present in the enriched membrane fraction of empty-plasmid-transformed yeast cells (Fig 3.26, lines a and b). Pre-immune antibodies were also not able to detect any specific band in a range of the molecular weight expected for TbAQPs within these membrane extracts (results not shown). Interestingly, only by using crude extracts prepared from both bloodstream and procyclic forms of *T. brucei*, it was possible to observe a defined band with these antibodies at the molecular weight expected (Fig 3.26, lines c and d). Regarding anti-TbAQP3, conditions used for yeast membrane preparations did not give satisfactory results (Fig 3.26, lines a and b). In contrast, cell lysates prepared from bloodstream and procyclic trypanosomes provided a band close to the predicted molecular weight when blotted with anti-TbAQP3. These results indicate that all the antibodies recognize their proteins specifically and that TbAQPs were expressed in both developmental stages of the parasite.

In order to obtain more insights into the specificity of anti-TbAQP3 signal, we generated fusion proteins containing GFP at the N-terminus of TbAQPs. GFP-TbAQP3-transfected *T. brucei* procyclic forms induced (experimental) and not induced (control) to express the chimeric protein were challenged with anti-TbAQP3. Crude extract of transfected parasites, expressing -or not- the chimerical protein, always presented a defined band at the range of the molecular weight expected for the TbAQP3 alone (Fig. 3.26, lines e and f, lower square). However, only total lysates from parasites expressing the chimeric

protein showed a band close to the molecular weight expected for this fusion protein (Fig. 3.26, lines e and f, upper square). Therefore, anti-TbAQP3 detected specifically TbAQP3.

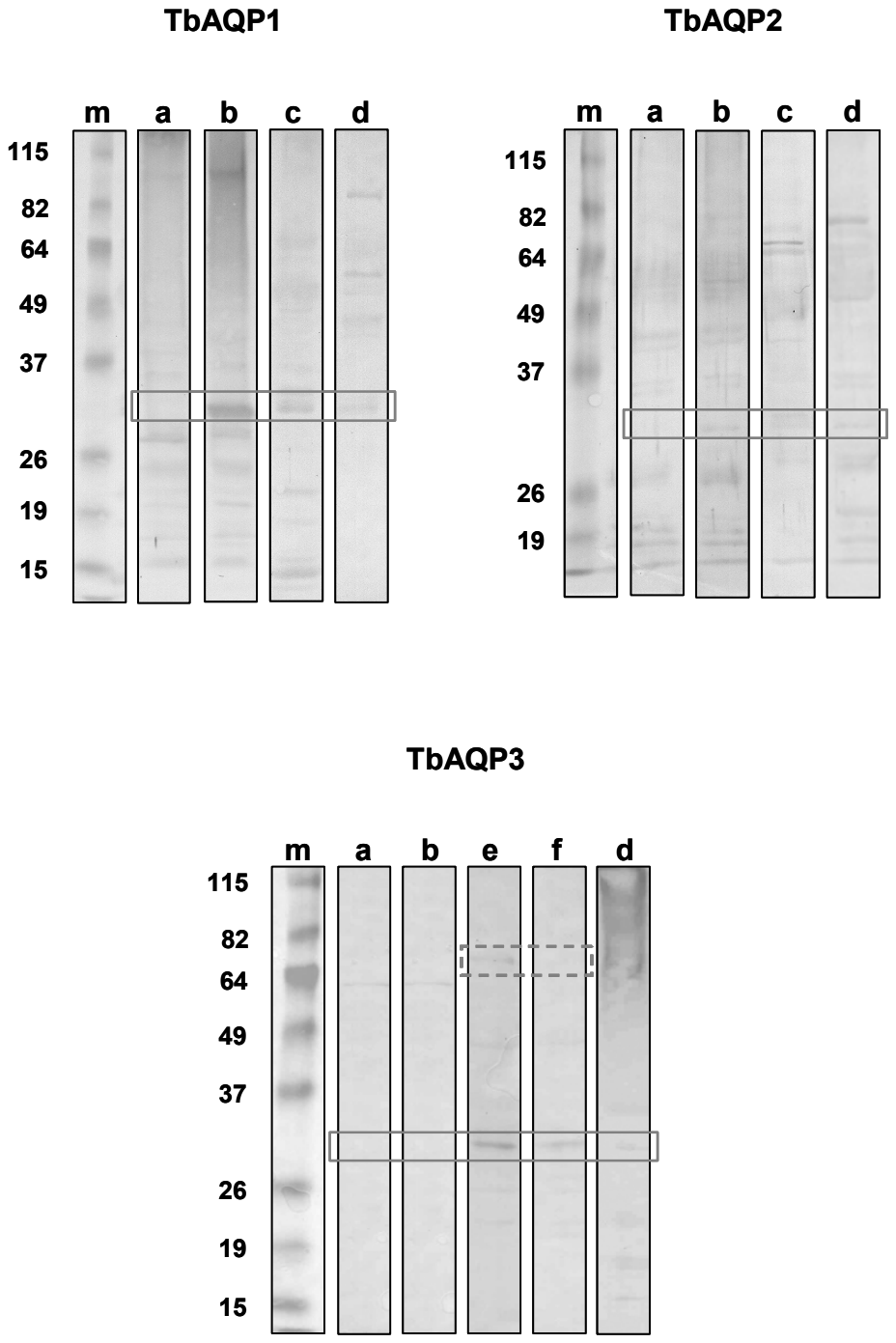

Figure 3.26. Western-blot analysis of TbAQPs in wild type of *T brucei*, as well as in homologous and heterologous expression system. Letters: (m), marker; (a) membrane fraction of empty-plasmid-transformed yeast cells, (b) membrane fraction of TbAQP-transformed yeast cells, (c) crude extract of *T brucei* bloodstream form, (d) crude extract of *T brucei* procyclic form, (e) crude extract of TbAQP3-transfected *T brucei* procyclic form, obtained from parasite induced to express the GFP-TbAQP3 fusion protein, (f) crude extract of TbAQP3-transfected *T brucei* procyclic form, obtained from parasite not induced to express the GFP-TbAQP3 fusion protein.

3.6.2.4. Immunofluorescence of TbAQPs

In order to localize of TbAQPs, immunofluorescence of TbAQPs using their respective specific antibody were performed. Immunofluorescence microscopy of *T. brucei* bloodstream forms using the pre-immune antibody preparation showed a minimal fluorescence without any recognizable localization pattern. On the other hand, when the specific antibody for TbAQP1 was used, a typically strong fluorescence in the flagellum was observed, indicating clear localization in this organelle (Fig. 3.27). When immunofluorescence microscopy of *T. brucei* procyclic forms was performed using pre-immune antibodies, there was again no specific recognition observed, although the background staining was stronger in this case. Specific targeting to the flagellar membrane in most of the procyclic forms was revealed when the anti-TbAQP1 was used for immunofluorescence (Fig. 3.28).

Control images of TbAQP2 using the pre-immune antibody preparation in bloodstream form parasites, again led to background staining only. In contrast, anti-TbAQP2 immunofluorescence images exhibited a strong fluorescence of the plasma membrane and in some cells especially of the flagellum (Fig. 3.27). In addition, it is notable that many cells with plasma membrane staining also showed staining of intracellular structures (result not shown), although the latter were not able to be well defined, probably due to the fixation method. We used methanol as fixing solution, which obviously was inefficient for conservation of internal structures. In summary, there is a clear localization in the plasma membrane of the parasite, an intracelullar localization of TbAQP2 in many cells (which, however, could just be related to trafficking), and a possible flagellar position. Regarding procyclic forms, there is a quite different fluorescence pattern of pre-immune and immune antibodies images. Control cells stained with pre-immune antibodies showed low background, while the anti-TbAQP2 pictures exposed a more prominent signal. Here TbAQP2 seems to be located in two places, at the plasma membrane and in intracellular organelles (Fig. 3.28). However, since there is not enough fluorescence staining with a clear difference between parasites stained with pre-immune and immune antibodies, it is difficult to exactly determine the localization of TbAQP2 in procyclic forms.

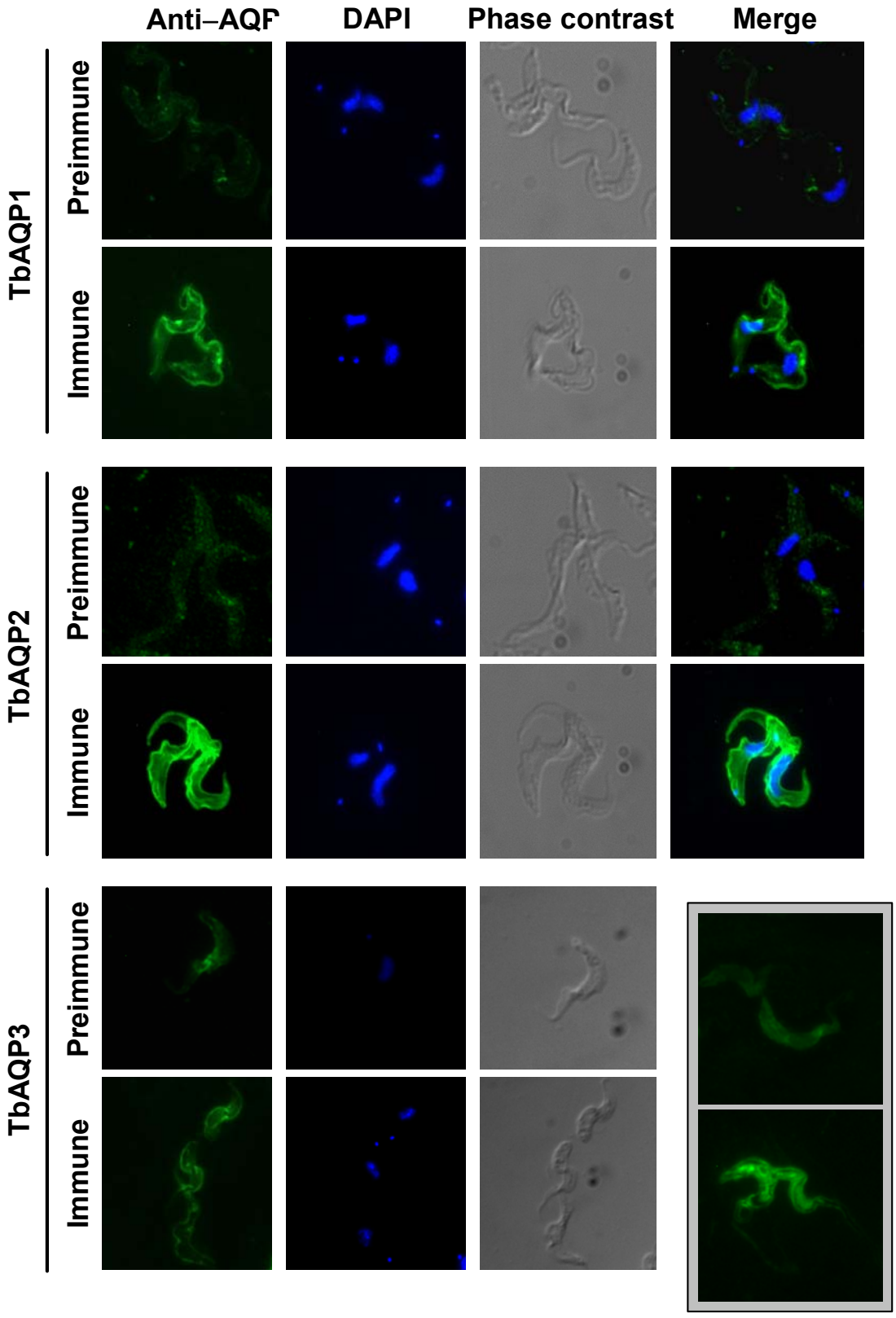

Figure 3.27. Localization of TbAQPs in *T. brucei* bloodstream form. Parasites were fixed and permeabilized as described in Materials and Methods. Cells were stained with Anti-TbAQPs. Staining was visualized with appropriate secondary anti-body and all samples were counterstained with DAPI . Lower right square: two more immunefluorescence images obtain by using of pre-inmune (up) and with Anti-TbAQP3 (down), in order to show the intracellular localization.

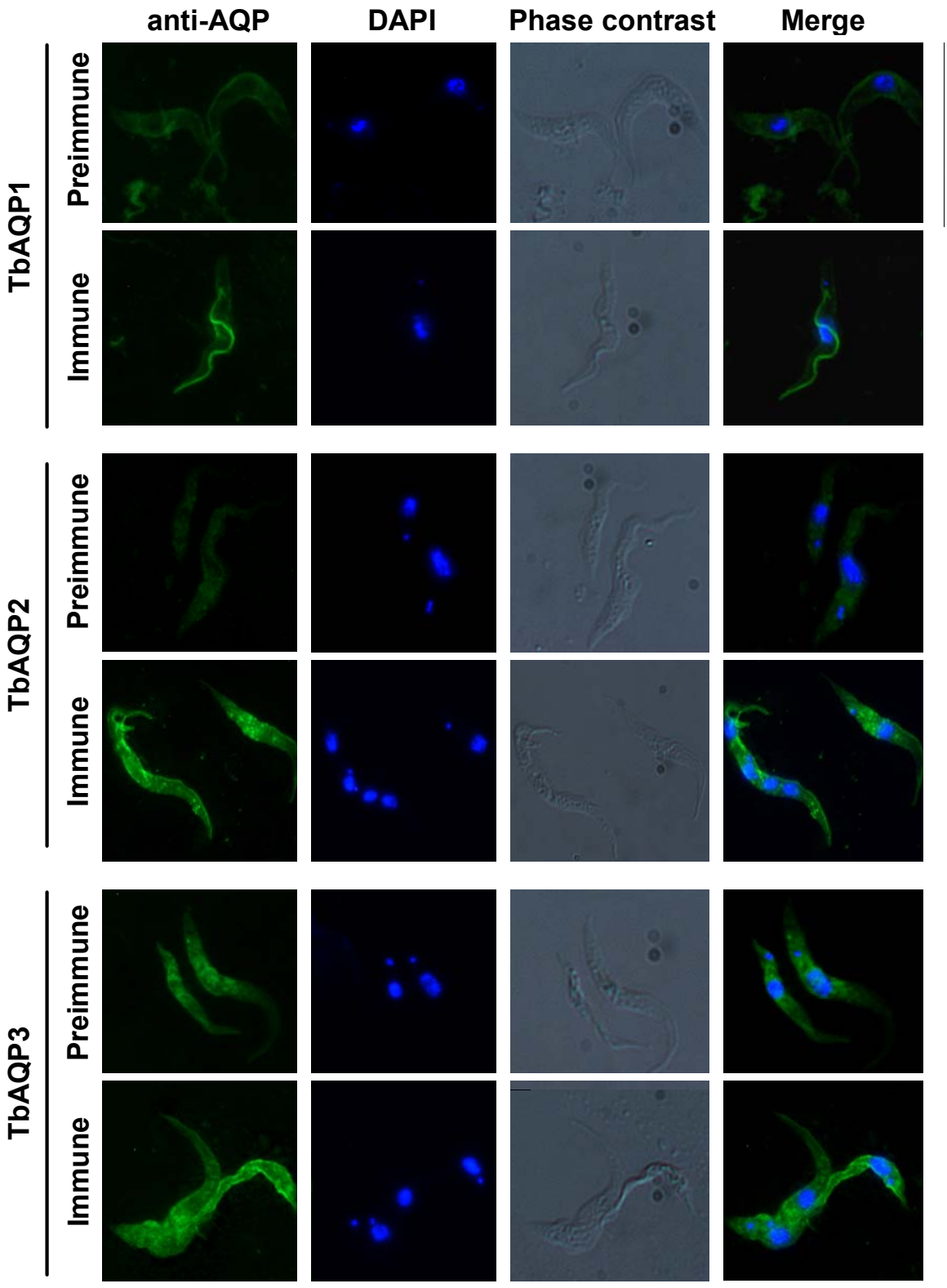

Figure 3.28. Localization of TbAQPs in *T. brucei* procyclic form. Parasites were fixed and permeabilized as indicated in Materials and Methods. Parasites were challenged with Anti-TbAQPs. Staining was visualized with appropriate secondary anti-body and all samples were counterstained with DAPI .

Images obtained from immunofluorescence microscopy of *T. brucei* bloodstream forms using anti-TbAQP3 showed a clear localization of this protein in the plasma membrane (Figs. 3.27 and 3.28). As in the case of TbAQP2 bloodstream forms, undefined intracellular positioning of TbAQP3 was also observed (Fig. 3.27, lower right square). Although it was easy to identify membrane localization of TbAQP3 and TbAQP2, it was difficult to define an intracellular localization in both cases, what could be either due to trafficking or just be an artefact as a result of the fixing methods.

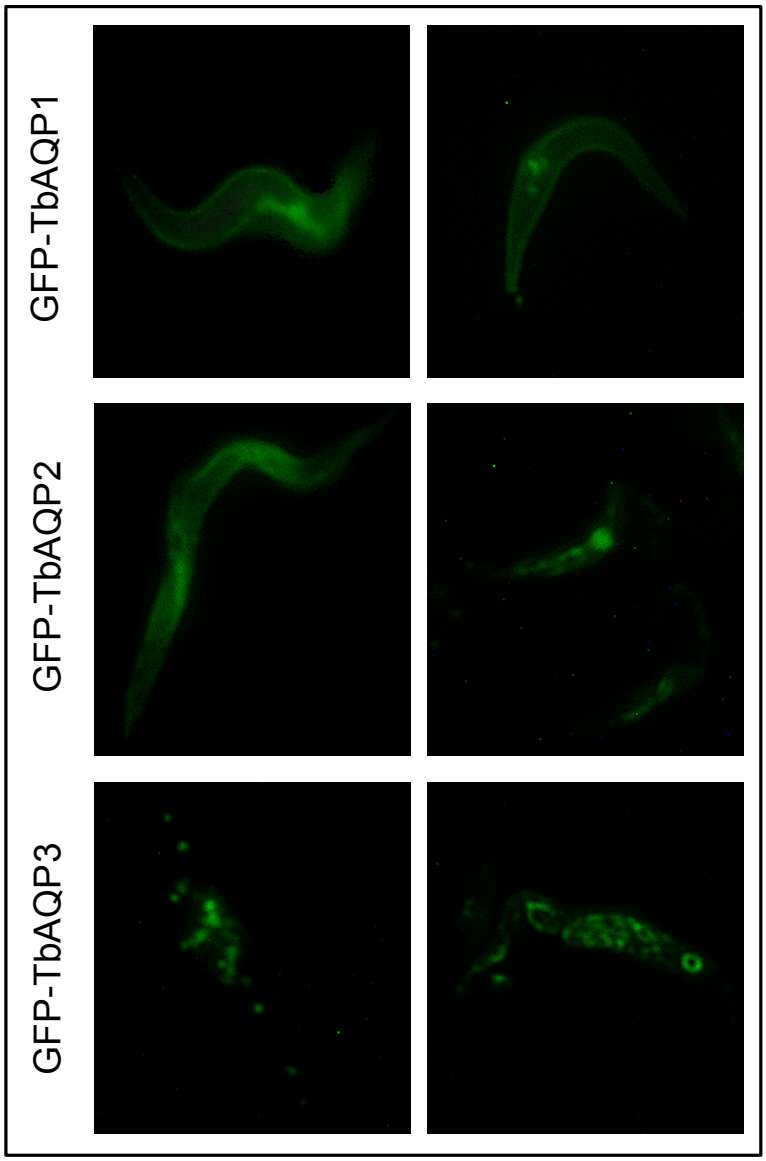

Figure 3.29. Localization of GFP-TbAQPs in tranfected *T. brucei* procyclic form. In each row two different immunefluorescence images of Transfected cell expressing GFP-TbAQPs.

3.6.2.5. Fluorescence microscopy

In order to obtain further information of the localization of TbAQPs by other approaches, GFP-TbAQPs-transfected trypanosomes were induced to express these chimeric proteins. Fluorescence images of *T. brucei* procyclics expressing GFP-TbAQP1 revealed that there was a significant targeting to the plasma membrane but not to the flagellum (Fig. 3.29). These results were not fully consistent with the inmunofluorescence results obtained with anti-TbAQP1 in procyclic forms. However, it is well known that GFP as a fusion partner may cause mistargeting of AQP (Ikeda *et al.*, 2002). The presence of GFP at the N-terminus (GFP-AQP6) led this fusion protein to the plasma membrane, while fusion of

GFP to the C-terminus (AQP6-GFP) led to an intracellular localization, similar to the untagged wild-type AQP6 (Beitz *et al.*, 2006). In our case it would have been inappropriate to test C-terminus fusion proteins, because TbAQPs do not have a free cytosolic C-terminus, as most of the AQPs. On the other hand, in transfectants expressing GFP-TbAQP1 there was also a small number of vacuoles observed which contained the fusion proteins. It is possible that this represents trafficking of this protein to the cell surface.

Fluorescence microscopy of *T. brucei* procyclic form expressing GFP-TbAQP2 showed a weak fluorescence and two different phenotypes (Fig. 3.29). Some cells exhibited strong and relative prominent stained vacuoles, while others showed a diffuse fluorescence throughout the whole cell. Fluorescence microscopy of GFP-TbAQP2 did not allow us to define any localization of this chimeric protein. Several hypotheses can explain this result. Again it is possible that the GFP tag or the over-expression of the chimeric protein cause mislocalization. We also tested several lower concentrations of tetracycline but it only resulted in a significantly decreased fluorescence. Induction of GFP-TbAQP2 to acceptable levels of fluorescence using tetracycline and elimination of the inductor by washing the parasites with medium without tetracycline afterwards, did not produce an important change of the staining pattern.

Images of GFP-TbAQP3-transfected procyclic cells showed different phenotypes. Most cells showed intracellular localization (Fig. 3.29), membrane localization (results not shown) and occasionally a diffuse fluorescence within the cytosol that could be interpreted as a stained dot at the posterior part of the parasite close to the kinetoplast. Since an occasional membrane localization was observed, hypo-osmotic shock was performed in order to cause alterations on the localization, e.g. in cells showing vacuole localization a targeting from this place to the plasma membrane. However, no conclusive change was observed. In summary, the GFP-TbAQP1 results strongly suggest that an N-terminus tag leads to a GFP-protein which localizes to the plasma membrane instead of the flagellum. GFP-TbAQP3 images support, but do not confirm, the inmunofluorescence findings obtained with the un-tagged protein, and GFP-TbAQP2 results were inconsistent with those obtained using anti-TbAQP2, so that other approaches must be used to clearly define TbAQP2 and 3 localization in procyclic forms of *T. brucei*, e.g. immunogold electron microscopy.

4. Discussion

The importance of aquaporins can be inferred from their wide distribution throughout nature from bacteria to man. In addition, single cell organisms may possess only one type, like *P. falciparum* (Hansen *et al*., 2002) or several of them, e.g. *S. cerevisiae* (Meyrial *et al*., 2001). Metazoa usually express numerous isoforms, e.g. 11 AQP isoforms in mammalia (Agre *et al*., 2002). The MIP family is especially abundant in plant cells: *Arabidopsis thaliana*, the model plant for genome sequencing, contains 38 aquaporin genes (Quigley *et al*., 2001). AQP are mainly involved in water and glycerol flux, but may also transport other non-ionic solutes. However, the transport capacity is quite different for the different solutes. All these characteristics show, at least in part, the variety of physiological functions which these membrane proteins may carry out.

Due to the presence of glycosomes in *Trypanosoma brucei*, the energy metabolism of this parasite is unique. Especially important is the sensitivity for glycerol under anaerobic conditions, which can be mimicked by SHAM. It has previously been demonstrated that glycerol transport in *T. brucei* occurs via specific membrane proteins (Wille *et al*., 1998). We have now cloned and characterized three proteins of the MIP family, TbAQP1, TbAQP2 and TbAQP3.

4.1. Functional characterization of TbAQPs through use of heterologous expression systems.

Heterologous expression systems for an efficient production of eukaryotic membrane proteins are available (Baldwin, 2000). Throughout the respective literature, the two systems mainly used for aquaporin expression are yeast and *Xenopus* oocytes (Agre *et al*., 2002; Agre *et al*., 1999). We have used both of them to characterize TbAQPs.

4.1.1. Functional expression and characterization of TbAQPs in *S. cerevisiae*

TbAQPs were functionally expressed in a *S. cerevisiae* Δfps1 mutant. We obtained experimental evidence for the function of TbAQPs as glycerol facilitators by complementation studies, expressing TbAQPs in a functionally form in this yeast mutant, which displayed sensitivity to hypo-osmotic shock because Fps1 modulates glycerol efflux

thereby maintaining an osmotic balance with the environment (Tamas *et al.*, 1999). *S. cerevisiae* Δfps1 sensitivity to hypo-osmotic shock was suppressed by TbAQPs expression. Similar phenomena has already been described in the literature for several aquaglyceroporins (Tamas *et al.*, 1999; Ciavatta *et al.*, 2001; Hedfalk *et al*., 2004) and are now routinely used as a phenotype assay to investigate aquaglyceroporin activity.

In addition, these transformants showed a new phenotype, hyper-osmotic sensitivity, which is not present in the control (empty-plasmid-transformed *S. cerevisiae* Δfps1 cells). This phenotype is a behaviour consistent with unregulated glycerol channel activity, as previously described for a yeast Δfps1 mutant expressing either GlpF or Fps1, with N- or C-terminal deletions (Tamas *et al.*, 1999; Hedfalk *et al*., 2004). TbAQPs transformants further showed incapacities to accumulate glycerol under isotonic and hypertonic conditions, indicating a glycerol efflux function of TbAQPs.

The existence of channels involved in glycerol efflux stresses the important role for glycerol release for *T. brucei*. Under anaerobic conditions or just when oxygen supply decreases it is fundamental for the parasite to eliminate the produced glycerol as consequence of reversed action of glycerol kinase. The action of this enzyme is pivotal in low oxygen pressure, because it participates in ATP production and re-oxidation of NADH, two essential functions for parasite survival (Steinborn *et al.*, 2000). However, the reverse reaction of this enzyme is not favourable thermodynamically so that it is necessary an efficient system to discard glycerol from the cell, which would otherwise become toxic for the parasite. According to our results, all of the three channels from *T. brucei* expressed in yeast release efficiently glycerol into the medium. Therefore, TbAQPs are involved in this important physiological function in the parasite.

4.1.2. Funtional expression and biochemical characterization of TbAQPs in *Xenopus leavis* oocytes.

Oocytes of *Xenopus laevis* represent a powerful system for the transient expression of heterologous proteins. TbAQPs were successfully expressed in *Xenopus* oocytes and their characterization was performed using uptake experiments and swelling assay.

As judged from both, uptake of radio-labelled glycerol and standard oocyte swelling assays, TbAQPs heterologously expressed in *Xenopus* oocytes transport glycerol efficiently, comparable to their closely related aquaglyceroporins; AQP3, AQP9 (Tsukaguchi *et al*., 1998) and transported glycerol even faster than AQP10 (Ishibashi *et al.*,

2002). On the other hand, transport of polyols containing more than 3 carbon atoms by TbAQPs was highly restricted. Urea was reasonably transported by all three TbAQP channels, and some polyols passed trough the pores of TbAQP2 and TbAQP3, but not TbAQP1.

TbAQPs can participate in glycerol catabolism; these may be inferred from glycerol influx experiments. Under aerobic conditions, glycerol serves as an alternative substrate to glucose in *T. brucei* (Eisenthal *et al*., 1998). It inhibits glucose uptake (50% at 0.8 mM glycerol; (Bakker *et al*., 1997), because increase of glycerol concentration lead to competition for ATP between glycerol kinase and hexokinase (Bakker, 1998). Therefore, a glycerol blood concentration of about 50 μM could be relevant as energy source for trypanosomes. It is also possible that this glycerol could be used for lipid construction by trypanosomes, as it has been reported for other parasite. It is known that malaria parasites are able to take up host serum glycerol by their single aquaglyceroporin (Hansen *et al*., 2002) and use it efficiently to make lipid backbone (Beitz, 2005). Hence, it could be speculated that TbAQPs could also be important for trypanosome growth, not only because glycerol is an alternate energy source but also, because this compound is required for lipid synthesis. It is remarkable important in bloodstream form of *T. brucei* since these parasites have an extremely abundant surface protein (10^7 copies/cell) known as variant surface glycoprotein (VSG). VSG, which functions in immune evasion, is linked to the plasma membrane by a glycosyl-phosphatidylinositol (GPI) anchor (Morita *et al.*, 2000), a structure which obviously requires glycerol for its synthesis. A similar situation occurs in the procyclic form, where procyclin is the counterpart of VSG (Vassella *et al.,* 2000). It has been reported that this glycoprotein is even regulated by glycerol concentration and oxygen supply (Vassella *et al.,* 2000).

TbAQPs are able to transport water, the Pf of oocytes expressing TbAQPs was between 150 and 180 μm s^{-1}. The Pf reported in literature for oocytes not expressing any AQP is below 20 μm s^{-1} (Hansen *et al*., 2002; Ishibashi *et al.*, 2002; Engel and Stahlberg, 2002). In contrast, Pf reported for aquaporin expressed in oocytes are up to 150 fold higher than that of oocytes not expressing these channels and one order of magnitude of difference among each other, being in the range 30-300 μm s^{-1}. *T. cruzi* possess an aquaporin located in acidocalcisomes, with shows a Pf of 30μm s^{-1} (Montalvetti *et al.*, 2004). On the other hand, the model of orthodox aquaporins from red blood cells, hAQP1, exhibit a Pf of about 200 μm s^{-1}, and a Pf of 300 μm s^{-1} has even been reported for oocytes expressing rat AQP1 (Hansen *et al.*, 2002). According to this scenario, aquaporins can be

arbitrarily classified in three groups taken into account the obtained oocytes Pf. AQP with a Pf between hAQP1 and rAQP (200-300 μm s^{-1}), which are the highest values of Pf reported in literature, are aquaporins with a high water permeability. AQPs possessing Pf values between 100 and 200 μm s^{-1} can be classify as AQP with an intermediate water permeability, and AQPs with a Pf value below 100 μm s^{-1} show a low water permeability. Considering this classification scheme, TbAQPs are aquaglyceroporins with intermediate water permeability. However, the transport rate of water for these aquaglyceroporins are still higher than those reported for aquaglyceroporins of several protozoa like *T. cruzi* and *Toxoplasma gondii* (Pf = 108 μm s^{-1}) (Pavlovic-Djuranovic et al., 2003). On the other hand, the AQP of *Plasmodium falciparum* (Pf = 276 μm s^{-1}) belongs to AQP with a high water permeability (Hansen *et al*., 2002). Notably, the water transport capacity of TbAQPs was close to those reported for rAQP9 (~150 μm/s) and, at least two-fold higher than Pf values for rAQP3 (~70 μm/s) (Tsukaguchi *et al.*, 1998; Hansen *et al*., 2002) and hAQP10 (~80 μm/s) (Ishibashi *et al.*, 2002). It is interesting to note that several Pf values more have been reported for rAQP3 in the literature, 200 μm/s (Ishibashi *et al*., 1994), 334 μm/s (Echevarria *et al*., 1994a).

TbAQPs, capable of transporting water efficiently, should be involved in osmo-regulation in the parasite. It is generally assumed that *T. brucei* live under constant conditions in blood and is thus not exposed to osmotic stress. However, it is well known that erythrocytes posses a high density of AQP1 in their plasma membrane, which demonstrates a high capacity for water transport. This aquaporin seems to be fundamental to respond to abrupt changes in extracellular osmolarity, e.g. when red blood cells travel through the renal medulla (Yang *et al*., 2001). This may also be important for trypanosomes within their mammalian host. But two other situations should be kept in mind, where osmoregulation may become pivotal for survival of trypanosomes, during the course of transmission, and during their life within the insect vector, i.e. within the mid-gut and the salivary gland of the tsetse fly. So far, the function of AQPs in protozoan parasites has been scarcely addressed. The only example of an aquaporin of these unicellular organisms that has been well characterized in terms of its biological function is TcAQP (Montalvetti *et al.*, 2004; Rohloff *et al.*, 2004). This aquaporin is located in the acidocalcisome membrane, in hypoosmotic shock conditions, swelling of these organelles occur due to the take-up of water. Acidocalcisomes fuses with the contractile vacuole complex, which is in charge of releasing water excess into the extracellular space (Rohloff

et al., 2004). So far it is unknown whether T. *brucei* uses a similar mechanism to perform osmoregulation, since a contractile vacuole has not been reported in this parasite.

The capacity of TbAQPs of carrying out water and glycerol transport efficiently, is consistent with the affirmation of Beitz (2005) that protozoan AQPs are typically bifunctional channels, which is an uncommon feature in nature. Even bacteria like *Escherichia coli* and yeasts possess, at least, one specialized protein for each function, water and glycerol passage (Luyten *et al.,* 1995; Meyrial *et al.,* 2001; Wang *et al.,* 2005).

4.2. Non-conventional solutes of aquaglyceroporins: validation of TbAQPs as entry pathway for potential drugs against *T. brucei*:

4.2.1. Dihydroxyacetone

Surprisingly, uptake of DHA in oocytes expressing TbAQPs was better, or at least similar to glycerol. This result was confirmed by experiments with TbAQPs transformed Δfps1 mutant yeast. So far the physiological relevance of the DHA transport in *Trypanosoma brucei* is unknown, but a simple explanation would be that DHA may be used as energy source, as it has already been published for different organisms (Tang *et al.*, 1982; Taguchi *et al.*, 2002). However, this seems not to be the case, since extensive searches of the completed trypanosome gene databank (TIGR and Sanger) for enzymes related to DHA consumption (i.e. glycerol dehydrogenase and dihydroxyacetone kinase) gave negative results. Moreover, trypanosomes incubated in basic medium containing DHA concentrations equal or lower than 1 mM as sole energy source, survived for a longer time than cells incubated in the same medium without any carbon source, but hardly longer than 1 h. In contrast, cells in the same condition with glycerol or glucose as energy source survived for several hours, without any decrease in cell numbers. The short survival of the parasite in presence of DHA could be explained by a minimal use of DHA as substrate due to a side reaction of glycerol kinase (Carmona-Gutierrez, 2005), as it has already been reported for other glycerol kinases (Jin *et al*., 1982).

However, since DHA is a toxic compound for yeast only in the absence of their DHAK (dhak1Δ/dhak2Δ) (because its detoxification depends on a functional dihydroxy-acetone kinase (Molin *et al*., 2003), it should be toxic also for trypanosomes. In fact, *T. brucei* showed the highest sensitivity to this compound reported so far (IC_{50} 1.03 ± 0.14 mM). This toxic effect was doses-dependent. Morphology changes included an increase of

the lysosome number, chromatin condensation and a highly increased number of cells showing two nuclei and more than one flagellum in a single cell. These changes are compatible with cell cycle alterations, and FACS analyses revealed indeed that there is a G2/M arrest, which is minor at 1 mM but becomes prominent at 2 mM, where about 70% of cells are blocked in G2/M. These results are fully consistent with those reported by Petersen and co-workers (2004), who found a G2/M arrest in HaCaT keratinocytes when cells were treated with DHA concentrations up to 50 fold higher than those used in our study. Interestingly, they also showed that DHA induce apoptosis in these cells via ROS production as a crucial intermediate. It is known that PGD_2 treatment lead to PCD via ROS production in *T. brucei* (Figarella *et al*., 2006). Necrosis was not detected up to 3 mM DHA and increased only by about 13% in the presence of 4 mM DHA. Likewise, no PCD markers (phosphatidylserine exposition, loss of mitochondrial membrane potential, DNA degradation) or a significant ROS production was observed up to 3 mM DHA. Although PCD markers were slightly increased at a concentration of 4 mM DHA (e.g. 27% loss of mitochondrial membrane potential), these obtained values are rather low and it seems unjustified to link the observed cell death to PCD. We can not completely rule out PCD in DHA treated cells, but it is rather negligible as compared to both growth inhibition and G2/M arrest.

In general, G2/M arrest is known to be due to DNA damage (Wang and Cho, 2004) which is induced by DHA (Petersen *et al*., 2004). The way, by which DHA cause G2/M arrest has not been clearly defined: it could either be directly involved in the primary toxic effect or, alternatively, DHA may generate another toxic compound. DHA can directly cause DNA damage through Maillard reaction, which is a non-enzymatic glycation of an amino group of any substance, usually proteins or nucleic acids (Petersen *et al*., 2004). DHA can also cause indirectly DNA damage through production of substances more toxic than DHA itself. For example, DHA induced ROS production has been suggested to be responsible for both DHA effects in keratinocytes, the G2/M arrest and apoptosis (Petersen *et al*., 2004). This may also be true for trypanosomes. DHA induced ROS production may be insufficient to produce a significant PCD, as compared with those produced by prostaglandins (Figarella *et al.,* 2006). However, the persistent presence of a low ROS concentration could be important, since the DHA effect was partially inhibit by using ROS scavenger such as glutathion (Carmona-Gutierrez, 2005).

Although aquaglyceroporins from *Trypanosoma brucei* were first identified in 2004 (in a publication associated to this work), the idea of TbAQPs as an anti-protozoan target is

quite old. It was demonstrated in the 1970ties that glycerol added exogenously can inhibit glycolysis sufficiently to result in cell death during anaerobic glycolysis *in vitro*, in the presence of SHAM (Brohn and Clarkson, 1978). As we know now, TbAQPs must play an important role in this effect and it can be assumed that glycolysis is inhibited since exogenously added glycerol reverses the gradient across the membrane and can not be eliminated by any of the TbAQPs. This chemotherapy approach has been used *in vivo*. Simultaneous administration of SHAM and glycerol rapidly clears the parasites from the blood of infected rats and mice. However, 5 to 6 days post treatment, a relapse occurs (Brohn and Clarkson, 1978). So far, unfortunately, a therapeutic exploitation of glycerol sensitivity to Trypanosomes has not been successful. The use of DHA would be another possibility based on the same principle, which is the inhibition of TbAQPs functions. DHA, as glycerol, is not toxic for humans. In contrast, it has been involved to enhance aerobic endurance capacity (Ivy, 1998), fatty acid oxidation and fat loss (Cortez *et al*. 1991; Stanko *et al.*, 1992); it has even been used as sunless tanning solution (Petersen *et al.*, 2004). The use of DHA in *in vivo* experiments may be promising, however, hitherto, it has not been explored systematically. Nevertheless, the DHA concentration that must be reached in blood to be effective against the parasite must be about 1mM and mammals possess the enzymatic machinery to convert DHA into their metabolisms. Therefore, successful experiments with animals could require several variations and not simply the use of DHA. At least two approaches seem applicable: 1) The treatment with DHA analogs in order to decrease the metabolic rate of this compound in mammals; 2) A combination of DHA with other active substances such as SHAM, glycerol, pyruvate etc., to look for synergistic effects. Combination of DHA with another substance, although in other context, has already been shown to be useful, e.g. DHA and thiosulfate exhibit a synergistic antidotal effect against cyanide poisoning (Niknahad and Ghelichkhani, 2002)

4.2.2. AsIII, SbIII and methylglyoxal.

The permeability of TbAQPs for compounds with similar spatial structures as glycerol was examined. Although all of them pass through the TbAQPs pore, important differences were observed. TbAQPs transport both SbIII and AsIII, but TbAQP2 was less efficient to transport SbIII than TbAQP1 and 3. In contrast, methylglyoxal did not pass the pore of TbAQP1 and 3, but was readily transported by TbAQP2. These observed permeability differences may be related to the unusual motif formed by the respective amino acids in the pore of TbAQPs. TbAQP1 and 3, which showed the same phenotype for

SbIII and methylglyoxal, possess two classical NPA motifs, whereas TbAQP2 possess NSA/NPS boxes, in addition to a leucine residue which replaces the highly conserved arginine close to this region. It is thus reasonable to speculate that the serine play an important role in the different capabilities to transport these substances. Especially interesting is the serine located in the second motif (NPS), because it has recently been shown that *P. falciparum* aquaporin allow the passage of methylglyoxal while rAQP3 does not (Pavlovic-Djuranovic *et al.*, 2006), and the canonical motif of these channels are NLA/NPS and NPA/NPA, respectively.

On the other hand, the cytotoxic effects of all these compounds on *T. brucei* were examined using the IC_{50} assay and compared with those published for mammalian cells of animal or human origin. In contrast to DHA these drugs have pronounced toxic or side effects. These compounds showed prominent effects on parasites, killing them in a low nM to μM range. IC_{50} values were in the range of therapeutic use or below the known concentrations to cause relevant cytotoxicity. Concentration of Trisenox® (arsenic trioxide) determined in plasma of Trisenox®-treated acute promyelocytic leukaemia patients were in the range of 300- 2900 nM (List *et al.*, 2003), equal or tenfold higher than the IC_{50} for this compound in *T. brucei*. Likewise, the IC_{50} of methylglyoxal for neuroblastoma cells is 1.25 mM (Webster *et al*., 2005), 60 fold higher than the IC_{50} in *T. brucei*. Some of these drugs could be used as alternative or potential drugs, because treatment of sleeping sickness still problematic as melarsoprol, the only drug used for late stage rhodesiense infections, has deadly side effects in about 5% of treated people. Arsenic trioxide (Trisenox®) is currently being used against acute promyelocytic leukaemia and, despite of its side effects, induces a complete remission in treated patients even if they experienced relapses after extensive prior therapy (Soignet *et al*., 1998).

4.2.3. Ammonium as permeant of *T. brucei* aquaglyceroporins

The interpretation of the phenotype observed in fps1Δ mutant yeast cells expressing TbAQPs lead to the conclusion that trypanosome aquaglyceroporins are permeable for ammonia (NH_3) but not to ammonium (NH_4^+). This pathway for uptake or release of ammonia maybe unique in trypanosomes as a classical ammonia permease (MEP1-3) seem not to be encoded in the genome of this parasite. However, exposition of the parasite to high ammonia concentrations did not have important effects on cell growth, showing an IC_{50} about 25 mM for both procyclic and bloodstream forms. Thus, the parasite exhibits a natural resistant against this substance as compared to mammals. Standard ammonia

concentrations in human blood are lower than 60 µM (Huizenga *et al.*, 2002), while arterial ammonia concentrations in patients suffering an acute liver failure and severe encephalopathy are in the 0.3–0.5 mM range. Experimental acute liver failure in laboratory animals results in blood ammonia concentrations between 0.5 and 1 mM and during coma stages of encephalopathy brain ammonia concentrations are 5 fold higher than the corresponding blood ammonia concentrations in these animals (Felipo and Butterworth, 2002). In culture media, the ammonia concentrations produced by the bloodstream form of *T. brucei* reached a 0.25 mM maximum when the parasite number was about 2 x 10^6 cells ml^{-1}. Therefore, it is reasonable to assume that ammonia production of the parasite could contribute in the pathology of sleeping sickness. Studies about the metabolism of ammonia in protozoa are scarce and difficult to find in the literature (Kleydman *et al.*, 2004), especially for *T. brucei*. Our findings stress the importance to investigate in detail how the parasite copes with the high ammonia concentration and whether the ammonia production by the parasite could somehow really influence the development of pathology.

4.3. Localization of TbAQPs in development stage of *T. brucei*

An approach to analyze the physiological function of TbAQPs requires information about the expression of these proteins and their distribution within the cell. Northern blot analysis indicated that gene transcripts were expressed and differentially regulated in each developmental stage of the parasite. All *TbAQP* RNAs were expressed in the bloodstream form and *TbAQP1, TbAQP2* in the procyclic form, where *TbAQP3* was not detected by Northern blot. In all cases, the *TbAQP2* expression was low. These results suggest a distinct importance of the respective proteins throughout the life cycle.

The expression of TbAQP proteins was confirmed by using antibodies directed against each channel. These antibodies were raised against different synthetic peptids specific for each of the three TbAQPs. Their reactivity was tested by using either the isolated peptides or membrane rich fractions prepared from yeast expressing one of the TbAQPs or an empty plasmid (control). The use of anti-TbAQPs confirmed that the channels where expressed throughout the whole life cycle.

Fluorescence images obtained using anti-TbAQP1 indicated clearly that in both parasite stages, the bloodstream and the procyclic form, TbAQP1 is located at the flagellum. These results resemble data published in the literature for glucose transporters. *Leishmania mexicana* possesses three glucose transporters; two are localized at the plasma

membrane, LmGT2 and 3, and one, LmGT1 is located at the flagellum (Burchmore *et al.*, 2003). A similar distribution was described for *Leishmania enriettii* (Nasser and Landfear, 2004). Its two glucose transporters, iso-1 and iso-2, are located in flagellum and plasma membrane, respectively. A defined signal peptide for flagellar localization is still missing. However, transporters located in the membrane around the flagellum possess a relatively long N-terminus which is different from their isoforms directed to different cellular locations. This characteristic N-terminus is also present in TbAQP1, indicating that the signal peptide is present in this unusual long N-Terminus. In fact, in *Leishmania*, experimental evaluation of the N-terminal sequence argue strongly against the existence of a simple linear target sequence (Nasser and Landfear, 2004), but it seems likely that the spatial structure of this N-terminus is required for localization. Likewise, in *Trypanosoma brucei* three out of seven adenylate kinases possess long N-terminal extensions and are also translocated to the flagellum (Ginger *et al.*, 2005).

It is reasonable to ask why a membrane protein like a glycerol channel or glucose transporters, localise in the flagellar membrane?. One hypothesis is that all these proteins may communicate with the surrounding, working as a sensor (McCarter *et al.*, 2001, Burchmore *et al.*, 2003, Thar and Kuhl, 2003). Therefore, a flagellum may not only be an organelle for motility, but also a sensor for the external environment. It was recently proposed in plants that aquaporins may work as osmosensors (Hill *et al.*, 2004). TbAQP1 within the flagellar membrane would be an ideal candidate to carry out this function in trypanosomes.

Localization of TbAQP2 and 3 was well defined in the bloodstream form, but not so clear in the procyclic form. Using fluorescent second antibodies and anti-TbAQP2 and 3, fluorescence microscopy revealed that in the bloodstream form these TbAQPs are primarily localized in the plasma membrane. An intracellular localization was also observed. Although this phenotype could indicate an organelle localization (e.g. the lysosme), we can not rule out yet that these proteins are on their way to their final destination. In the procyclic form, these channels seem to be located in both places, in the plasma membrane and in intracellular compartments, but the fluorescence signal was insufficient to make final allocations. These problems are possible a consequence of a low concentration or a low affinity of the used antibodies. The necessity of purifying plasma membrane to detect channels in Western blotting and the tardy development in dot blot analysis support this hypothesis. The clear localization of TbAQP1 can be explained by a much higher expression of this protein. Assuming that the Northern blot somehow showed

only a semi-quantitative relation among the channels, it is expected that TbAQP1 is highly expressed in the bloodstream as well as in the procyclic form. In addition, all transcript expressions are significantly lower in the procyclic form as compared to the bloodstream form.

Due to the low resolution, a second approach to localize the channels in the procyclic form was tested. For this end GFP-TbAQPs were expressed in the procyclic form. However, the obtained results were not fully consistent with those using TbAQP antibodies. A plausible explanation for this phenomenon is that overexpression of the protein and/or the GFP fusion caused mislocalization. Mislocalization due to overexpression of fusion proteins is a well known phenomenon (Lisenbee *et al.*, 2003), e.g .relocalization of aquaporin fused with GFP onto its N-terminus has been reported (Beitz *et al.*, 2006). Further investigations are necessary to clarify localization of TbAQP2 and 3 especially in the procyclic form.

4.4. Conclusion

We report the cloning and characterization of three aquaglyceroporins from *T. brucei*, TbAQP1-3. These proteins constitute channels with a high glycerol and dihydroxyacetone and an intermediate water permeability. These channels are probably mainly involved in glycerol uptake and release and in osmoregulation.

TbAQPs are differentially sorted toward their final destinations within the cell; TbAQP1 is localised almost exclusively at the parasite flagellum in both bloodstream and procyclic form, while TbAQP2 and 3 are targeted principally to the plasma membrane in bloodstream form parasites.

TbAQP1-3 may serve as targets to design new strategies to combat sleeping sickness, using them as importing system for toxic metabolites. DHA, which pass through the TbAQPs pore as fast as glycerol, shows to be toxic for the parasite. AsIII, SbIII and methylglyoxal also permeate the channels and killed the parasite in a nM to µM range, i.e. in concentrations reported to be used for treatment of certain diseases, or at least, to be below the toxicity for humans.

5. Summary

The protozoan parasite *Trypanosoma brucei* undergoes a complex life cycle including two dividing stages, *i.e.* the long slender form in blood, lymphatic fluid, and cerebrospinal fluid of its mammalian host and the procyclic form in the midgut of the tsetse fly. The bloodstream forms depend on glycolysis for ATP production, with glycerol as an alternative substrate (Bakker *et* al., 1997; Michels *et al*., 2000). Glycolysis in trypanosomes differs markedly from the corresponding pathway in higher eukaryotes. Most strikingly, the first seven glycolytic reactions occur in a peroxisome-like organelle called glycosome (Opperdoes and Borst, 1977). The Lactate dehydrogenase enzyme is absent and, therefore, the glycerol kinase reverse activity is fundamental for the survival of the parasite in low oxygen pressure. Under anaerobic conditions, glucose is converted to equimolar amounts of glycerol and pyruvate, which are both secreted from the parasite to ensure the essential continuity of glycolysis activity. On the other hand, the procyclic form possesses a functional Krebs cycle and oxidative phosphorylation capabilities, using amino acid as energy source. Procyclic form is subjected to considerable variations of osmolarity, as this parasite stage lives in the fly´s midgut where the conditions vary depending mainly on feed of the insect. In all these situations the ability of the parasite to cope with sudden gradients change of glycerol and water must be important for its survival and therefore, specialized systems as aquaglyceroporins must be present in this parasite. It was suggested previously that glycerol transport in *T. brucei* occurs via specific membrane proteins (Wille *et al*., 1998).

Here, we describe cloning and biochemical characterization of the three trypanosomal aquaglyceroporins (AQP; TbAQP1–3), which show a 40–45% identity to mammalian AQP3 and AQP9. AQPs belong to the major intrinsic protein family and represent channels for small non-ionic molecules. Both TbAQP1 and TbAQP3 contain two highly conserved NPA motifs within the pore-forming region, whereas TbAQP2 contains NSA and NPS motifs instead, which are only occasionally found in AQPs. For functional characterization, all three proteins were heterologously expressed in yeast and *Xenopus* oocytes. In the yeast fps1Δ mutant, TbAQPs suppressed hypoosmosensitivity and rendered cells to a hyper-osmosensitive phenotype, as expected for unregulated glycerol channels. Under iso- and hyperosmotic conditions, these cells constitutively released glycerol,

consistent with a glycerol efflux function of TbAQP proteins. TbAQP expression in *Xenopus* oocytes increased permeability for water, glycerol, dihydroxyacetone and urea, in a minor grade. TbAQPs were virtually impermeable for other polyols; only TbAQP3 transported appreciable erythritol and ribitol. Thus, TbAQPs represent mainly water/glycerol/dihydroxyacetone channels involved in osmoregulation and glycerol metabolism in *T. brucei*.

The expression of TbAQPs transcripts and their coded proteins throughout the live cycle of the parasite was confirmed by using Northern blot and respective antibodies directed specifically against each channels. On the other hand, the localization of these channels was dissimilar. TbAQP1 was localised almost exclusively at the parasite's flagellum in both bloodstream and procyclic form. This channel possesses a long N-terminus totally different and especially longer than that of their isoforms. This characteristic along with the information published in the literature (Nasser and Landfear, 2004), indicate that the N-terminus contains the signal peptide to target this protein to the flagellum. TbAQP2 and 3 targets principally to plasma membrane in bloodstream form parasites.

It was also demonstrated that TbAQPs are promising targets to design new strategies to control the parasite. TbAQPs can be used mainly as an importing system for toxic metabolites. DHA, which is highly transported by these channels, shows an important toxic effect on the parasite, represented by an IC_{50} of 1.03± 0.14 mM. As judged by FACS and electron microscopy experiments, the principal DHA effect was an arrest in G2/M in the cell cycle of the parasite. AsIII, SbIII and methylglyoxal also permeate the channels and killed the parasite in nM to µM range, with an IC_{50} of 0.308, 0.103, and 21 µM, respectively. Although these compounds are known to be toxic for human beings, the observed IC_{50} values were in the range of therapeutic use or below the known concentrations to cause relevant cytotoxic effects.

6. Zusammenfassung

Der Parasit *Trypanosoma brucei* unterliegt einem komplizierten Entwicklungszyklus. Er besitzt zwei vermehrungsfähige Formen: nämlich die *long slender* Blutform, die sich im Blut, im Lymphgefäßsystem und im *Liquor cerebrospinalis* des Säugetierwirts befindet, und die prozykliche Form, die im Mitteldarm des Insektenvektors vorkommt. Die Blutform hängt zur ATP-Herstellung vollständig von der Glycolyse ab und kann Glycerol als alternative Energiequelle nutzen. Die Glycolyse ist in Trypanosoma im Vergleich zu den höheren Eukaryonten unterschiedlich organisiert. Dabei ist die auffallenste Besonderheit, dass die sieben ersten Reaktionen in einem Organell, dem so genannten Glycosom (einem modifizierten Peroxysom) ablaufen (Opperdoes and Borst, 1977). Da Trypanosomen keine Lactat Dehydrogenase besitzen, ist die Aktivität der Glycerinkinase (insbesondere im Fall einer limitierten Sauerstoff-Versorgung) von besonderer Bedeutung für das Überleben des Parasiten. Während unter aeroben Bedingungen Glucose stöchiometrisch zu Pyruvat umgesetzt wird, entstehen unter anaeroben Bedingungen äquimolare Konzentrationen an Glycerin und Pyruvat, um die Energieversorgung durch die Glycolyse sicher zu stellen. Die prozyklische Form besitzt dagegen einen funktionellen Citratzyklus und die oxydative Phosphorylierung, wobei insbesondere Aminosäuren (Prolin) als Energiequelle benutzen werden können. Beim Transfer der Blutform durch die Niere, besonders aber auch für die procyclische Form im Mitteldarm, unterliegen die Parasiten beträchtlichen Schwankungen in der Osmolarität. In all diesen Fällen ist die Fähigkeit der Trypanosomen Glycerin und Wasser effizient zu transportieren von essentieller Bedeutung. Dabei sind die Aquaglyceroporine, die eine hoch-effiziente und selektive Wasser/Glycerin-Transportrate vermitteln, von zentraler Bedeutung.

In der vorliegenden Arbeit ging es um die Klonierung und Charakterisierung der drei Aquaglyceroporine (TbAQP1–3) von *Trypanosoma brucei*, wobei ihre Lokalisierung und die potenzielle Nutzung als Wirkstoff-Angriffspunkte im Vordergrund standen. TbAQP1-3 zeigen eine 40-45%ige Identität zu den menschlichen AQP3 and AQP9. TbAQP1 und 3 besitzen die beiden klassischen NPA-Motive, während TbAQP2 einige Abweichungen von der klassischen AQP-Sequenz enthält: die NPA-Motive sind durch ein NSA- und ein NPS-Motiv ersetzt, außerdem steht ein Leucin-Rest nach dem zweiten Motiv anstelle des hoch konservierten Arginin-Restes. Die funktionelle Charakterisierung wurde in zwei heterologen Expressionssystemen durchgeführt, in Hefe und Oocyten aus

Xenopus laevis. TbAQP1-3 haben sich dabei wie unregulierte Glycerin-Transporter verhalten, wenn sie in der Hefe-Mutante fps1Δ, die keine Glycerin-Kanäle besitzt, exprimiert wurden. Unter hypo-osmotische Bedingungen wurde die typische Empfindlichkeit dieser Hefe-Mutante durch TbAQP1-3 supprimiert, während die transformierten Zellen unter iso- und hyper-osmotischen Bedingungen Glycerin konstitutiv sezernierten. Durch die Expression von TbAQP1-3 in *Xenopus* Oocyten wurde bestätigt, dass diese Kanäle Glycerin, Wasser und Dihydroxyacetone mit hoher Leistung transportieren. Im Gegensatz dazu wurde eine eher geringe Fähigkeit zum Harnstoff-Transport gefunden. TbAQP1-3 zeigten praktisch keine Transportkapazität für andere Polyole, nur TbAQP3 ließ merkliche Mengen von Erythritol and Ribitol passieren. Deshalb stellen TbAQP1-3 hauptsächlich Wasser/Glycerin/Dihydroxyaceton-Kanäle dar, die für die Regulation der Osmolarität und des Glycerol-Stoffwechsel von *Trypanosoma brucei* von entscheidender Bedeutung sind.

Durch *Northern blot* Analyse, sowie durch Verwendung spezifischer Antikörper im *Western blot* wurde gezeigt, dass TbAQP1-3 unterschiedlich exprimiert und reguliert werden. Ebenso war die Lokalisierung den Kanälen unterschiedlich. TbAQP1 ist in der Blutform sowie in der prozyklichen Form fast ausschließlich im Flagellum lokalisiert. Dieser Kanal besitzt im Vergleich zu TbAQP2 und TbAQP3 einen längeren N-Terminus, der nach Vergleich mit Literaturdaten (Nasser and Landfear, 2004) als Signal-Peptid dienen könnte. TbAQP2 und 3 wurden dagegen hauptsächlich in der Plasmamembran der Blutform gefunden.

Schließlich wurden experimentelle Daten ermittelt, nach denen TbAQP1-3 vielversprechende *targets* für die Wirkstoffentwicklung sein könnten, wenn die TbAQP1-3 als Aufnahmesysteme für potenzielle Medikamente benutzt werden. DHA, das von TbAQP1-3 sehr gut transportiert wird, zeigte eine hohe Toxizität auf den Parasiten (IC_{50} = 1,03 ± 0,14 mM), wobei der hauptsächliche Effekt ein Zellzyklus-Arrest in der M/G2 Phase war. In der Ratte liegen die LD_{50}-Werte dagegen im molaren Bereich und in der Kosmetikindustrie wird DHA komplikationslos eingesetzt. AsIII, SbIII und Methylglyoxal passieren ebenfalls die Pore aller drei TbAQPs und induzierten den Zelltod im nano- bis mikromolaren Bereich, wobei IC_{50}-Werte von 31 nM, 10 nM bzw. 21 µM auftreten. Obwohl entsprechende chemischen Verbindungen eine erhebliche Toxizität für den Menschen besitzen, waren die beobachteten IC_{50}-Werte in einem tolerablen Bereich, da Antimon-Verbindungen z.B. bei Leukämie in ähnlicher Konzentration eingesetzt werden.

7. References

Agre, P., Mathai, J., Smith,B. and Preston, M. 1999. Funtional analysis of aquaporins water channles proteins. ***Methods in Enzimology***, 294: 551-572.

Agre, P. 2000. Homer W. Smith award lecture. Aquaporin water channels in kidney. ***Journal of the American Society of Nephrology***, 11: 764–777.

Agre, P., King, L., Yasui, M., Guggino, W.B., Ottersen, O.P., Fujiyoshi, Y., Engel, A. and Nielsen, S. 2002. Aquaporin water channels-from atomic structure to clinical medicine. ***Journal of Physiology***, 542: 3-16.

Akhtar, N., Blomberg, A. and Adler, L. 1997. Osmoregulation and protein expression in a pbs2delta mutant of Saccharomyces cerevisiae during adaptation to hypersaline stress. ***FEBS Letters***, 403(2): 173-180.

Albertyn, J., Hahmann, S. and Prior, B. 1994. Characterization of the osmotic-stress response in *Saccharomyces cerevisiae*: osmotic stress and glucose repression regulate glycerol-3-phosphate dehydrogenase independenly. ***Current genetics***, 25: 12-18.

Altschul, S.F., Madden, T.L., Schaffer, A.A., Zhang, J., Zhang, Z., Miller, W. and Lipman, D.J. 1997. Gapped BLAST and PSI-BLAST: a new generation of protein database search programs. ***Nucleic Acids Research***, 25(17): 3389-3402.

Ausubel, F., Brent, R., Kingston, R., Moore, D., Seidman, J. and Struhl, K. 2000. *Saccharomyces cerevisiae*. V (Ed.), ***Current Protocols in Molecular Biology***: John Wiley and Sons, Inc.

Bakker, B., Michels, P., Opperdoes, F. and Westerhoff, H. 1997. Glycolysis in Bloodstream form *Trypanosoma brucei* can be understood in terms of the kinetics of the glycolytic enzymes. ***The Journal of Biological Chemistry***, 272: 3207-3215.

Bakker, B. 1998. Control and regulation of glycolysis in *Trypanosoma brucei*. Amsterdam: University of Amsterdam.

Bakker, B.M., Westerhoff, H.V., Opperdoes, F.R. and Michels, P.A. 2000. Metabolic control analysis of glycolysis in trypanosomes as an approach to improve selectivity and effectiveness of drugs. ***Molecular & Biochemical Parasitology***, 106(1): 1-10.

Baldwin, S. 2000. ***Membrane transport*** (fisrt edition ed.): Oxfort University press.

Beitz, E. 2000. TEXshade: shading and labeling of multiple sequence alignments using LATEX2 epsilon. ***Bioinformatics***, 16(2): 135-139.

Beitz, E. 2005. Aquaporins from pathogenic protozoan parasites: structure, function and potential for chemotherapy. ***Biology of the Cell***, 97(6): 373-383.

Beitz, E., Liu, K., Ikeda, M., Guggino, W. B., Agre, P. and Yasui, M. 2006. Determinants of AQP6 trafficking to intracellular sites versus the plasma membrane in transfected mammalian cells. ***Biology of the Cell***, 98(2): 101-109.

Beitz, E., Pavlovic-Djuranovic, S., Yasui, M., Agre, P. and Schultz, J.E. 2004. Molecular dissection of water and glycerol permeability of the aquaglyceroporin from Plasmodium falciparum by mutational analysis. ***Proceedings of the National Academy of Sciences of the United States of America***, 101(5): 1153-1158.

Bergmeyer, H.U. 1984. ***Methods of Enzymatic Analysis. Metabolites 1: Carbohydrates*** (3 ed ed.). Weinheim Germany: Chemie GmbH.

Bergmeyer, H.U. and Beutler, H.O. 1990. ***Methods of Enzymatic Analysis: Ammonia*** (3rd Ed. ed.). Cambridge, UK: VCH Publishers.

Besteiro, S., Riviere, L., Biran, M., Biteau, N., Franconi, J.M., Boshart, M., Baltz, T. and Bringaud, F. 2005. Energy generation in insect stages of Trypanosoma brucei: metabolism in flux. ***Journal of Biological Chemistry***, 280(17): 16559-16570.

Bhattacharjee, H., Carbrey, J., Rosen, B.P. and Mukhopadhyay, R. 2004. Drug uptake and pharmacological modulation of drug sensitivity in leukemia by AQP9. ***Biochemical & Biophysical Research Communications***, 322(3): 836-841.

Bjerrum, O. J. and Schafer-Nielsen, C. 1986. Buffer systems and transfer parameters for semi-dry electroblotting with a horizontal apparatus. ***Electrphoresis***, 86: 315-327.

Bodley, A.L., McGarry, M.W. and Shapiro, T.A. 1995. Drug cytotoxicity assay for African trypanosomes and Leishmania species. ***J Infect Dis.***, 172((4)): 1157-1159.

Borgnia, M., Nielsen, S., Engel, A. and Agre, P. 1999. Cellular and molecular biology of the aquaporin water channels. ***Annual Review of Biochemistry***, 68: 425-458.

Borst, P. and Ouellette, M. 1995. New mechanisms of drug resistance in parasitic protozoa. ***Annual Review of Microbiology***, 49: 427-460.

Bouteille, B., Oukem, O., Bisser, S. and Dumas, M. 2003. Treatment perspectives for human African trypanosomiasis. ***Fundamental & Clinical Pharmacology***, 17(2): 171-181.

Bradford, M. 1976. A rapid and sensitive method for the quantification of microgram quantities of protein utilizing principle of protein-dye binding. ***Analitical Biochemistry***, 72: 246-254.

Braun, T., Philippsen, A., Wirtz, S., Borgnia, M.J., Agre, P., Kuhlbrandt, W., Engel, A. and Stahlberg, H. 2000. The 3.7 A projection map of the glycerol facilitator GlpF: a variant of the aquaporin tetramer. ***EMBO Reports***, 1(2): 183-189.

Brohn, F. J. and Clarkson, A.B. 1978. Quantitative effects of salycylhydroxamic acid and glycerol on trypanosoma brucei glycolysis *in vitro* and *in vivo*. ***Acta tropica***, 35: 23-33.

Burchmore, R.J., Rodriguez-Contreras, D., McBride, K., Merkel, P., Barrett, M.P., Modi, G., Sacks, D. and Landfear, S.M. 2003. Genetic characterization of glucose transporter function in Leishmania mexicana.[erratum appears in Proc Natl Acad Sci U S A. 2003 May 13;100(10):6287]. ***Proceedings of the National Academy of Sciences of the United States of America***, 100(7): 3901-3906.

Carmona-Gutierrez, D. 2005. ***Untersuchungen zur metabolischen Umwandlung und toxischen Wirkung von Dihydroxyaceton in Trypanosoma brucei***. Unpublished Diplomarbeit, Tuebingen University, Tuebingen.

Cazzulo, J.J., Franke de Cazzulo, B.M., Engel, J.C. and Cannata, J.J. 1985. End products and enzyme levels of aerobic glucose fermentation in trypanosomatids. ***Molecular & Biochemical Parasitology***, 16(3): 329-343.

Chaumont, F., Barrieu, F., Wojcik, E., Chrispeels, M.J. and Jung, R. 2001. Aquaporins constitute a large and highly divergent protein family in maize. ***Plant Physiology***, 125(3): 1206-1215.

Chung, C.T., Niemela, S.L. and Miller, R.H. 1989. One-step preparation of competent Escherichia coli: transformation and storage of bacterial cells in the same solution. ***Proceedings of the National Academy of Sciences of the United States of America***, 86(7): 2172-2175.

Ciavatta, V.T., Morillon, R., Pullman, G.S., Chrispeels, M.J. and Cairney, J. 2001. An aquaglyceroporin is abundantly expressed early in the development of the suspensor and the embryo proper of loblolly pine. ***Plant Physiology***, 127(4): 1556-1567.

Clayton, C.E. and Michels, P. 1996. Metabolic Compartmentation in African Trypanosomes. ***Parasitology Today***, 12: 465-471.

Clayton, C.E. 2002. Life without transcriptional control? From fly to man and back again.[erratum appears in EMBO J 2002 Jul 15;21(14):3917]. ***EMBO Journal***, 21(8): 1881-1888.

Cooper, G.J., Zhou, Y., Bouyer, P., Grichtchenko, II. and Boron, W.F. 2002. Transport of volatile solutes through AQP1. ***Journal of Physiology***, 542(1): 17-29.

Cortez, M.Y., Torgan, C.E., Brozinick, J.T., Miller, R.H. and Ivy, J.L. 1991. Effects of pyruvate and dihydroxyacetone consumption on the growth and metabolic state of obese Zucker rats. ***American Journal of Clinical Nutrition***, 53(4): 847-853.

Croft, S.L. 1997. The current status of antiparasite chemotherapy. ***Parasitology***, 114 Suppl: S3-15.

Cross, G.A.M. 1975. Identification, purification and properties of clone-specific glycoprotein antigens constituting the surface coat of *Trypanosoma brucei*. ***Parasitology***, 71: 393-417.

Dacks, J. and Doolittle, W. 2001. Reconstructing/Deconstructing the Earliest eukaryotes: How Comparative Genomics Can Help. ***Cell***, 107: 419–425.

de Groot, B.L. and Grubmuller, H. 2001. Water permeation across biological membranes: mechanism and dynamics of aquaporin-1 and GlpF.[see comment]. ***Science***, 294(5550): 2353-2357.

Despommier, D.D., Gwadz, R.W., Hotez, P.J. and Knirsch, C.A. 2000. ***Parasitic diseases***. New York: Apple Trees Productions.

Docampo, R. and Moreno, S.N. 1999. Acidocalcisome: A novel Ca2+ storage compartment in trypanosomatids and apicomplexan parasites. ***Parasitology Today***, 15(11): 443-448.

Duszenko, M., Ferguson, M.A., Lamont, G.S., Rifkin, M.R. and Cross, G.A. 1985. Cysteine eliminates the feeder cell requirement for cultivation of Trypanosoma brucei bloodstream forms in vitro. ***Journal of Experimental Medicine***, 162(4): 1256-1263.

Duszenko, M., Muhlstadt, K. and Broder, A. 1992. Cysteine is an essential growth factor for Trypanosoma brucei bloodstream forms. ***Molecular & Biochemical Parasitology***, 50(2): 269-273.

Eagle, H. 1959. Amino acid metabolism in mammalian cell cultures. ***Science***, 130(3373): 432-437.

Echevarria, M., Windhager, E.E., Tate, S.S. and Frindt, G. 1994a. Cloning and expression of AQP3, a water channel from the medullary collecting duct of rat kidney. ***Proceedings of the National Academy of Sciences of the United States of America***, 91(23): 10997-11001.

Echevarria, M., Gonzalez, E., Gutierrez, A. and Whittembury, G. 1994b. Water and urea diffusive permeabilities in isolated proximal tubule cells. ***American Journal of Physiology***, 267(5 Pt 2): F709-715.

Eisenthal, R. and Cornish-Bowden, A. 1998. Prospects for Antiparasitic Drugs. The case of *Trypanosoma brucei*, the causative agent of africans sleeping sickness. ***The Journal of Biological Chemistry***, 273: 5500-5505.

Elkjaer, M.L., Nejsum, L.N., Gresz, V., Kwon, T.H., Jensen, U.B., Frokiaer, J. and Nielsen, S. 2001. Immunolocalization of aquaporin-8 in rat kidney, gastrointestinal tract, testis, and airways. ***American Journal of Physiology - Renal Physiology***, 281(6): F1047-1057.

Engel, A. and Stahlberg, H. 2002. Aquaglyceroporins: channel proteins with a conserved core, multiple functions, and variable surfaces. ***International Review of Cytology***, 215: 75-104.

Felipo, V. and Butterworth, R.F. 2002. Neurobiology of ammonia. ***Neurochemistry International***, 40(6): 487-491.

Ferguson, M.A. and Cross, G.A. 1984. Myristylation of the membrane form of a Trypanosoma brucei variant surface glycoprotein. ***Journal of Biological Chemistry***, 259(5): 3011-3015.

Field, M.C., Allen, C.L., Dhir, V., Goulding, D., Hall, B.S., Morgan, G.W., Veazey, P. and Engstler, M. 2004. New approaches to the microscopic imaging of Trypanosoma brucei. ***Microscopy & Microanalysis***, 10(5): 621-636.

Figarella, K., Uzcategui, N.L., Beck, A., Schoenfeld, C., Kubata, B.K., Lang, F. and Duszenko, M. 2006. Prostaglandin-induced programmed cell death in Trypanosoma brucei involves oxidative stress. ***Cell Death and Differentiation***, Feb 3; [Epub ahead of print].

Flick, K.M., Shaulsky, G. and Loomis, W.F. 1997. The wacA gene of Dictyostelium discoideum is a developmentally regulated member of the MIP family. ***Gene***, 195(2): 127-130.

Froger, A., Tallur, B., Thomas, D. and Delamarche, C. 1998. Prediction of functional residues in water channels and related proteins. ***Protein Science***, 7(6): 1458-1468.

Fu, D., Libson, A., Miercke, L. J., Weitzman, C., Nollert, P., Krucinski, J., & Stroud, R. M. 2000. Structure of a glycerol-conducting channel and the basis for its selectivity. ***Science***, 290(5491): 481-486.

Garcia-Alles, L.F., Siebold, C., Nyffeler, T.L., Flukiger-Bruhwiler, K., Schneider, P., Burgi, H.B., Baumann, U. and Erni, B. 2004. Phosphoenolpyruvate- and ATP-dependent dihydroxyacetone kinases: covalent substrate-binding and kinetic mechanism. ***Biochemistry***, 43(41): 13037-13045.

Gelb, M.H. and Hol, W.G. 2002. Parasitology. Drugs to combat tropical protozoan parasites. ***Science***, 297(5580): 343-344.

Gietz, D., St Jean, A., Woods, R.A. and Schiestl, R.H. 1992. Improved method for high efficiency transformation of intact yeast cells. ***Nucleic Acids Research***, 20(6): 1425.

Ginger, M.L., Ngazoa, E.S., Pereira, C.A., Pullen, T.J., Kabiri, M., Becker, K., Gull, K. and Steverding, D. 2005. Intracellular positioning of isoforms explains an unusually large adenylate kinase gene family in the parasite Trypanosoma brucei. ***The Journal of Biological Chemistry***, 280(12): 11781-11789.

Glauert, A.M. 1975. ***Practical methods in electron microscopy: Fixation, dehydration and embedding of biological specimens***. Amsterdam: Biomedical Press.

Gourbal, B., Sonuc, N., Bhattacharjee, H., Legare, D., Sundar, S., Ouellette, M., Rosen, B. P. and Mukhopadhyay, R. 2004. Drug uptake and modulation of drug resistance in Leishmania by an aquaglyceroporin. ***Journal of Biological Chemistry***, 279(30): 31010-31017.

Hamm, B., Schindler, A., Mecke, D. and Duszenko, M. 1990. Differentiation of *Trypanosoma brucei* bloodstream trypomastigotes from long slender to short stumpy-like forms in axenic culture. ***Molecular Biochemical Parasitology***, 40: 13-22.

Hannaert, V., Albert, M.A., Rigden, D.J., da Silva Giotto, M.T., Thiemann, O., Garratt, R.C., Van Roy, J., Opperdoes, F.R. and Michels, P.A. 2003. Kinetic characterization, structure modelling studies and crystallization of Trypanosoma brucei enolase. ***European Journal of Biochemistry***, 270(15): 3205-3213.

Hansen, M., Kun ,J., Schultz, J., Beitz, E. 2002. A single, bi-functional aquaglyceroporin in Blood-stage *Plasmodium falciparum* Malaria Parasites. ***The Journal of Biological Chemistry***, 277: 4874-4882.

Hatakeyama, S., Yoshida, Y., Tani, T., Koyama, Y., Nihei, K., Ohshiro, K., Kamiie, J. I., Yaoita, E., Suda, T., Hatakeyama, K. and Yamamoto, T. 2001. Cloning of a new aquaporin (AQP10) abundantly expressed in duodenum and jejunum. ***Biochemical & Biophysical Research Communications***, 287(4): 814-819.

Hedfalk, K., Bill R., Mullins, J., Karlgren, S., Filipsson, C., Bergstrom, J., Tamas, M., Rydstrom, J. and Hohmann, S. 2004. A regulatory domain in the C-terminal extension of the yeast glycerol channel Fps1p. ***Journal of Biological Chemistry***, 279(15): 14954-14960.

Hesse, F., Selzer, P.M., Muhlstadt, K. and Duszenko, M. 1995. A novel cultivation technique for long-term maintenance of bloodstream form trypanosomes *in vitro*. ***Molecular Biochemical Parasitology***, 70: 157-166.

Heymann, J.B. and Engel, A. 2000. Structural clues in the sequences of the aquaporins. ***Journal of Molecular Biology***, 295(4): 1039-1053.

Hill, A.E., Shachar-Hill, B. and Shachar-Hill, Y. 2004. What are aquaporins for? ***Journal of Membrane Biology***, 197(1): 1-32.

Hirsch, J.G. and Fedorko, M.E. 1968. Ultrastructure of human leukocytes after simultaneous fixation with glutaraldehyde and osmium tetroxide and "postfixation" in uranyl acetate. ***J. Cell. Biol.***, 38(3): 615-627.

Hoare, C. A. 1972. ***The Trypanosomes of Mammals. A Zoological Monograph***. Oxford and Edinburgh: Blackwell Scientific Publications.

Huizenga, H., Lof, J., Stroom, J.C., Leer, J.W., Brahme, A. and Huizenga, J.R. 2002. Determination of arterial blood ammonia in uremic patients before and after hemodialysis using three different ammonia methods.[comment]. ***International Journal of Radiation Oncology, Biology, Physics***, 52(1): 236-253.

Ikeda, M., Beitz, E., Kozono, D., Guggino, W. B., Agre, P. and Yasui, M. 2002. Characterization of aquaporin-6 as a nitrate channel in mammalian cells. Requirement of pore-lining residue threonine 63. ***Journal of Biological Chemistry***, 277(42): 39873-39879.

Inoue, Y., Tsujimoto, Y. and Kimura, A. 1998. Expression of the glyoxalase I gene of Saccharomyces cerevisiae is regulated by high osmolarity glycerol mitogen-activated protein kinase pathway in osmotic stress response. ***Journal of Biological Chemistry***, 273(5): 2977-2983.

Ishibashi, K., Kuwahara, M., Gu, Y., Kageyama, Y., Tohsaka, A., Suzuki, F., Marumo, F. and Sasaki, S. 1997. Cloning and functional expression of a new water channel abundantly expressed in the testis permeable to water, glycerol, and urea. ***Journal of Biological Chemistry***, 272(33): 20782-20786.

Ishibashi, K., Morinaga, T., Kuwahara, M., Sasaki, S. and Imai, M. 2002. Cloning and identification of a new member of water channel (AQP10) as an aquaglyceroporin. ***Biochimica et Biophysica Acta***, 1576(3): 335-340.

Ishibashi, K., Sasaki, S., Fushimi, K., Uchida, S., Kuwahara, M., Saito, H., Furukawa, T., Nakajima, K., Yamaguchi, Y., Gojobori, T., et al. 1994. Molecular cloning and expression of a member of the aquaporin family with permeability to glycerol and urea in addition to water expressed at the basolateral membrane of kidney collecting duct cells. ***Proceedings of the National Academy of Sciences of the United States of America***, 91(14): 6269-6273.

Itoh, T., Rai, T., Kuwahara, M., Ko, S.B., Uchida, S., Sasaki, S. and Ishibashi, K. 2005. Identification of a novel aquaporin, AQP12, expressed in pancreatic acinar cells. ***Biochemical & Biophysical Research Communications***, 330(3): 832-838.

Ivy, J.L. 1998. Effect of pyruvate and dihydroxyacetone on metabolism and aerobic endurance capacity. ***Medicine & Science in Sports & Exercise***, 30(6): 837-843.

Jahn, T., Moller, A., Zeuthen T., Holm, L., Klerke, D., Mohsin, B., Kühlbrandt, W. and Schjoerring, J. 2004. Aquaporin homologes in plants and mammals transport ammonia. ***FEBS Letters***, 574:31-36.

Jin, R.Z., Forage, R.G. and Lin, E.C. 1982. Glycerol kinase as a substitute for dihydroxyacetone kinase in a mutant of Klebsiella pneumoniae. ***Journal of Bacteriology***, 152(3): 1303-1307.

Johanson, U., Karlsson, M., Johansson, I., Gustavsson, S., Sjovall, S., Fraysse, L., Weig, A.R. and Kjellbom, P. 2001. The complete set of genes encoding major intrinsic proteins in Arabidopsis provides a framework for a new nomenclature for major intrinsic proteins in plants. ***Plant Physiology***, 126(4): 1358-1369.

Jungwirth, H., Bergler H. and Hoegenauer G. 2001. Diazaborine Treatment of Baker's Yeast Results in Stabilization of Aberrant mRNAs. ***The Journal of Biological Chemistry***, 276: 36419–36424.

Kleydman, Y., Yarlett, N. and Gorrell, T.E. 2004. Production of ammonia by Tritrichomonas foetus and Trichomonas vaginalis. ***Microbiology***, 150: 1139-1145.

Kozono, D., Yasui, M., King, L. and Agre, P. 2002. Aquaporin water channels: atomic structure and molecular dynamics meet clinical medicine. ***Journal of Clinical Investigation***, 109: 1395–1399.

Králová, I., Rigden, D, Opperdoes, F and Michels, P. 2000. Glycerol kinase of *Trypanosoma brucei*. Cloning, molecular characterization and mutagenesis. ***European Journal of Biochemistry***, 267: 2323-2333.

Laemmli, U.K. 1970. Cleavage of structural proteins during the assembly of the head of bacteriophage T4. ***Nature***, 227(5259): 680-685.

Lagree, V., Froger, A., Deschamps, S., Hubert, J.F., Delamarche, C., Bonnec, G., Thomas, D., Gouranton, J. and Pellerin, I. 1999. Switch from an aquaporin to a glycerol channel by two amino acids substitution. ***Journal of Biological Chemistry***, 274(11): 6817-6819.

Langreth, S.G. and Balber, A.E. 1975. Protein uptake and digestion in bloodstream and culture forms of Trypanosoma brucei. ***Journal of Protozoology***, 22(40-52).

Lanham, S. M. and Godfrey, D.G. 1970. Isolation of salivarian trypanosomes from man and other mammals using DEAE-cellulose. ***Experimental Parasitology***, 28(3): 521-534.

Lee, J.K., Khademi, S., Harries, W., Savage, D., Miercke, L. and Stroud, R.M. 2004. Water and glycerol permeation through the glycerol channel GlpF and the aquaporin family. ***Journal of Synchrotron Radiation***, 11(Pt 1): 86-88.

Levine, N.D., Corliss, J.O., Cox, F.E., Deroux, G., Grain, J., Honigberg, B.M., Leedale, G. F., Loeblich, A. R., Lom, J., Lynn, D., Merinfeld, E.G., Page, F.C., Poljansky, G., Sprague, V., Vavra, J. and Wallace, F.G. 1980. A newly revised classification of the protozoa. ***Journal of Protozoology***, 27(1): 37-58.

Lewis, P.R. and Knight, D.P. 1977. ***Practical methods in electron microscopy: Staining methods for sectioned material*** (Glauert, A. M., ed. ed.). Amsterdam: North-Holland Biomedical Press.

Lisenbee, C.S., Karnik, S.K. and Trelease, R.N. 2003. Overexpression and mislocalization of a tail-anchored GFP redefines the identity of peroxisomal ER. ***Traffic***, 4(7): 491-501.

List, A., Beran, M., DiPersio, J., Slack, J., Vey, N., Rosenfeld, C.S. and Greenberg, P. 2003. Opportunities for Trisenox (arsenic trioxide) in the treatment of myelodysplastic syndromes. ***Leukemia***, 17(8): 1499-1507.

Liu, K., Kozono, D., Kato, Y., Agre, P., Hazama, A. and Yasui, M. 2005. Conversion of aquaporin 6 from an anion channel to a water-selective channel by a single amino acid substitution. ***Proceedings of the National Academy of Sciences of the United States of America***, 102(6): 2192-2197.

Louassini, M., Foulquie, M.R., Benitez, R. and Adroher, F.J. 1999. Activity of key enzymes in glucose catabolism during the growth and metacyclogenesis of Leishmania infantum. ***Parasitology Research***, 85(4): 300-306.

Luft, J.H. 1961. Improvements in epoxy resin embedding methods. ***The Journal of Biophysical and Biochemical Cytology***, 9: 409-414.

Luyten, K., Albertyn , J., Skkibe,W., Prior, B., Ramos,J., Thevelien, J., Hohmann, S. 1995. Fps1, a yeast member of the MIP family of channel protein, is a facilitator for glycerol uptake and efflux and is inactive under osmotic stress. ***EMBO Journal***, 14: 1360-1371.

Ma, T., Frigeri, A., Hasegawa, H., Verkman, A.S. 1994. Cloning of a water channel homolog expressed in brain meningeal cells and kidney collecting duct that functions as a stilbene-sensitive glycerol transporter. ***Journal of Biological Chemistry***, 269(34): 21845-21849.

Marchesini, N., Bollo, M., Hernandez, G., Garrido, M.N. and Machado-Domenech, E.E. 2002. Cellular signalling in Trypanosoma cruzi: biphasic behaviour of inositol phosphate cycle components evoked by carbachol. ***Molecular & Biochemical Parasitology***, 120(1): 83-91.

Marini, A.M., Soussi-Boudekou, S., Vissers, S. and Andre, B. 1997. A family of ammonium transporters in Saccharomyces cerevisiae. ***Molecular & Cellular Biology***, 17(8): 4282-4293.

McCarter, L.L., Cascio, D., Sawaya, M.R., Gingery, M. and Schroder, I. 2005. Polar flagellar motility of the Vibrionaceae. ***Structure***, 13(4): 637-648.

Meng, Y.L., Liu, Z. and Rosen, B.P. 2004. As(III) and Sb(III) uptake by GlpF and efflux by ArsB in Escherichia coli. ***Journal of Biological Chemistry***, 279(18): 18334-18341.

Meyrial, V., Laize, V., Gobin, R., Ripoche, P., Hohmann, S. and Tacnet, F. 2001. Existence of a tightly regulated water channel in Saccharomyces cerevisiae. ***European Journal of Biochemistry***, 268(2): 334-343.

Michels, P.A., Hannaert, V. and Bringaud, F. 2000. Metabolic aspects of glycosomes in trypanosomatidae - new data and views. ***Parasitology Today***, 16(11): 482-489.

Mobasheri, A., Shakibaei, M. and Marples, D. 2004. Immunohistochemical localization of aquaporin 10 in the apical membranes of the human ileum: a potential pathway for luminal water and small solute absorption. ***Histochemistry & Cell Biology***, 121(6): 463-471.

Molin, M., Norbeck, J. and Blomberg, A. 2003. Dihydroxyacetone Kinases in *Saccharomyces cerevisiae* are involved in Detoxification of Dihydroxyacetone. ***The Journal of Biological Chemistry***, 278: 1415-1423.

Montalvetti, A., Rohloff, P. and Docampo, R. 2004. A functional aquaporin co-localizes with the vacuolar proton pyrophosphatase to acidocalcisomes and the contractile vacuole complex of Trypanosoma cruzi. ***Journal of Biological Chemistry***, 279(37): 38673-38682.

Morgan, G.W., Hall, B. S., Denny, P.W., Carrington, M. and Field, M.C. 2002a. The kinetoplastida endocytic apparatus. Part I: a dynamic system for nutrition and evasion of host defences. ***Trends in Parasitology***, 18(11): 491-496.

Morgan, G.W., Hall, B.S., Denny, P.W., Field, M.C. and Carrington, M. 2002b. The endocytic apparatus of the kinetoplastida. Part II: machinery and components of the system. ***Trends in Parasitology***, 18(12): 540-546.

Morishita, Y., Matsuzaki, T., Hara-chikuma, M., Andoo, A., Shimono, M., Matsuki, A., Kobayashi, K., Ikeda, M., Yamamoto, T., Verkman, A., Kusano, E., Ookawara, S., Takata, K., Sasaki, S. and Ishibashi, K. 2005. Disruption of aquaporin-11 produces polycystic kidneys following vacuolization of the proximal tubule. ***Molecular & Cellular Biology***, 25(17): 7770-7779.

Morita, Y.S., Acosta-Serrano, A., Buxbaum, L.U. and Englund, P.T. 2000. Glycosyl phosphatidylinositol myristoylation in African trypanosomes. New intermediates in the pathway for fatty acid remodeling. ***Journal of Biological Chemistry***, 275(19): 14147-14154.

Mumberg, D., Muller, R. and Funk, M. 1994. Regulatable promoters of Saccharomyces cerevisiae: comparison of transcriptional activity and their use for heterologous expression. ***Nucleic Acids Research***, 22(25): 5767-5768.

Murata, K., Mitsuoka, K., Hirai, T., Walz, T., Agre, P., Heymann, J.B., Engel, A. and Fujiyoshi, Y. 2000. Structural determinants of water permeation through aquaporin-1. ***Nature***, 407(6804): 599-605.

Nasser, M.I. and Landfear, S.M. 2004. Sequences required for the flagellar targeting of an integral membrane protein. ***Molecular & Biochemical Parasitology***, 135(1): 89-100.

Nelson , D. and Cox., M. 2000. Biological Membranes and Transport, ***Lehninger Principles of Biochemistry***, 3 edition ed.: 410-411: Worth Publishers.

Nevoigt, E. and Stahl, U. 1997. Osmoregulation and glycerol metabolism in the yeast *Saccharomyces cerevisiae*. ***FEMS Microbiology Reviews***, 21: 231-241.

Nicoletti, I., Migliorati, G., Pagliacci, M. C., Grignani, F. and Riccardi, C. 1991. A rapid and simple method for measuring thymocyte apoptosis by propidium iodide staining and flow cytometry. ***J. Immunol. Methods***, 139(2): 271-279.

Nielsen, S. 2002. Renal aquaporins: an overview. ***BJU International***, 90 Suppl 3: 1-6.

Nielsen, S., Frokiaer, J., Marples, D., Kwon, T.H., Agre, P. and Knepper, M.A. 2002. Aquaporins in the kidney: from molecules to medicine. ***Physiological Reviews***, 82(1): 205-244.

Niknahad, H. and Ghelichkhani, E. 2002. Antagonism of cyanide poisoning by dihydroxyacetone. ***Toxicology Letters***, 132(2): 95-100.

Norbeck, J. and Blomberg, A. 1997. Metabolic and regulatory changes associated with growth of Saccharomyces cerevisiae in 1.4 M NaCl. Evidence for osmotic induction of glycerol dissimilation via the dihydroxyacetone pathway. ***Journal of Biological Chemistry***, 272(9): 5544-5554.

Opperdoes, F. and Borst, P. 1977. Localization of nine glycolytic enzymes in a microbody like organelle in *Trypanosoma brucei*:The glycosome. ***FEBS letters***, 80: 360-364.

Overath, P., Czichos, J. and Haas, C. 1986. The effect of citrate/cis-aconitate on oxidative metabolism during transformation of Trypanosoma brucei. ***European Journal o Biochemistry***, 160: 175-182.

Pavlovic-Djuranovic, S., Schultz, E. and Beitz, E. 2003. A single aquaporin gene encodes a water/glycerol/urea facilitator in *Toxoplasma gondii* with similarity to plant tonoplast intrinsic proteins. ***FEBS Letters***, 555: 500-504.

Pavlovic-Djuranovic, S., Kun, J.F., Schultz, J.E. and Beitz, E. 2006. Dihydroxyacetone and methylglyoxal as permeants of the Plasmodium aquaglyceroporin inhibit parasite proliferation. ***Biochimica et Biophysica Acta***, Jan 4; [Epub ahead of print].

Pentreath, V.W., Alafiatayo, R.A., Crawley, B., Doua, F. and Oppenheim, B.A. 1996. Endotoxins in the blood and cerebrospinal fluid of patients with African sleeping sickness. ***Parasitology***, 112(Pt 1): 67-73.

Perez-Morga, D., Vanhollebeke, B., Paturiaux-Hanocq, F., Nolan, D.P., Lins, L., Homble, F., Vanhamme, L., Tebabi, P., Pays, A., Poelvoorde, P., Jacquet, A., Brasseur, R. and Pays, E. 2005. Apolipoprotein L-I promotes trypanosome lysis by forming pores in lysosomal membranes. ***Science***, 309(5733): 469-472.

Petersen, A.B., Wulf, H.C., Gniadecki, R. and Gajkowska, B. 2004. Dihydroxyacetone, the active browning ingredient in sunless tanning lotions, induces DNA damage, cell-cycle block and apoptosis in cultured HaCaT keratinocytes. ***Mutation Research***, 560(2): 173-186.

Preston, G., Carrol, T., Guggino, B. and Agre, P. 1992. Appearance of water channels in Xenopus oocytes expressing red cell CHIP28 protein. ***Science***, 256: 385–387.

Preston, G.M., Jung, J.S., Guggino, W.B. and Agre, P. 1993. The mercury-sensitive residue at cysteine 189 in the CHIP28 water channel. ***Journal of Biological Chemistry***, 268(1): 17-20.

Quigley, F., Rosenberg, J., Shachar-Hill, Y. and Bohnert, H. 2001. From genome to function: the *Arabidopsis* aquaporins. ***Genome Biology***, l 3: 1-17.

Ramirez-Solis, A., Mukopadhyay, R., Rosen, B.P. and Stemmler, T.L. 2004. Experimental and theoretical characterization of arsenite in water: insights into the coordination environment of As-O. ***Inorganical Chemistry***, 43(9): 2954-2959.

Rohloff, P., Montalvetti, A. and Docampo, R. 2004. Acidocalcisomes and the contractile vacuole complex are involved in osmoregulation in Trypanosoma cruzi. ***Journal of Biological Chemistry***, 279(50): 52270-52281.

Rout, M.P. and Field, M.C. 2001. Isolation and characterization of subnuclear compartments from Trypanosoma brucei. Identification of a major repetitive nuclear lamina component. ***Journal of Biological Chemistry***, 276(41): 38261-38271.

Sanders, O.I., Rensing, C., Kuroda, M., Mitra, B. and Rosen, B.P. 1997. Antimonite is accumulated by the glycerol facilitator GlpF in Escherichia coli. ***Journal of Bacteriology***, 179(10): 3365-3367.

Savage, D.F., Egea, P.F., Robles-Colmenares, Y., O'Connell, J.D. and Stroud, R.M. 2003. Architecture and selectivity in aquaporins: 2.5 a X-ray structure of aquaporin Z. ***Plos Biology***, 1(3): E72.

Schmid, C., Nkunku, S., Merolle, A., Vounatsou, P. and Burri, C. 2004. Efficacy of 10-day melarsoprol schedule 2 years after treatment for late-stage gambiense sleeping sickness. ***Lancet***, 364(9436): 789-790.

Shen, Z.X., Chen, G.Q., Ni, J.H., Li, X.S., Xiong, S.M., Qiu, Q.Y., Zhu, J., Tang, W., Sun, G.L., Yang, K.Q., Chen, Y., Zhou, L., Fang, Z.W., Wang, Y.T., Ma, J., Zhang, P., Zhang, T.D., Chen, S.J., Chen, Z. and Wang, Z.Y. 1997. Use of arsenic trioxide (As2O3) in the treatment of acute promyelocytic leukemia (APL): II. Clinical efficacy and pharmacokinetics in relapsed patients. ***Blood***, 89(9): 3354-3360.

Siebold, C., Garcia-Alles LF, Erni, B. and Baumann, U. 2003. A mechanism of covalent substrate binding in the x-ray structure of subunit K of the Escherichia coli dihydroxyacetone kinase. ***Proceedings of the National Academy of Sciences of the United States of America***, 100: 8188–8192.

Sikorski, R.S. and Hieter, P. 1989. A system of shuttle vectors and yeast host strains designed for efficient manipulation of DNA in Saccharomyces cerevisiae. ***Genetics***, 122(1): 19-27.

Soignet, S.L., Maslak, P., Wang, Z.G., Jhanwar, S., Calleja, E., Dardashti, L.J., Corso, D., DeBlasio, A., Gabrilove, J., Scheinberg, D.A., Pandolfi, P.P. and Warrell, R.P. 1998. Complete remission after treatment of acute promyelocytic leukemia with arsenic trioxide. ***The New England Journal of Medicine***, 339(19): 1341-1348.

Stanko, R.T., Reynolds, H.R., Lonchar, K. D. and Arch, J.E. 1992. Plasma lipid concentrations in hyperlipidemic patients consuming a high-fat diet supplemented with pyruvate for 6 wk. ***American Journal of Clinical Nutrition***, 56(5): 950-954.

Steinborn, K., Szallies, A., Mecke, D. and Duzsenko, M. 2000. Cloning, heterologous expression and kinetics analysis of glycerol kinase (TbGLK1) from *Trypanosoma brucei*. ***Biological chemistry***, 381: 1071-1077.

Stroud, R. M., Nollert, P. and Miercke, L. 2003. The glycerol facilitator GlpF its aquaporin family of channels, and their selectivity. ***Advances in Protein Chemistry***, 63: 291-316.

Sun, J., van den Heuvel, J., Soucaille, P., Qu, Y. and Zeng, A.P. 2003. Comparative genomic analysis of dha regulon and related genes for anaerobic glycerol metabolism in bacteria. ***Biotechnology Progress***, 19(2): 263-272.

Taguchi, T., Suzuki, I., Balis, J.U. and Yuri, K. 2002. Glyceraldehyde metabolism in human erythrocytes in comparison with that of glucose and dihydroxyacetone. ***Environmental Research***, 89(2): 138-145.

Tajkhorshid, E., Schulten, K. and Jensen, M. O. 2002. Energetics of glycerol conduction through aquaglyceroporin GlpF. ***Biophysical Journal***, 83(1): 154-160.

Takata, K., Matsuzaki, T. and Tajika, Y. 2004. Aquaporins: water channel proteins of the cell membrane. ***Progress in Histochemistry & Cytochemistry***, 39(1): 1-83.

Tamas, M., Luyten, K., Sutherland, F., Hernandez, A., Albertyn, J., Valadi, H., Li, H., Prior, B., Kilian S., Ramos, J., Gustafsson, L., Thevelein, J. and Hohmann, S. 1999. Fps1p controls the accumulation and release of the compatible solute glycerol in yeast osmoregulation. ***Molecular Microbiology***, 31: 1087-1104.

Tang, J., St Martin, E.J. and Lin, E.C. 1982. Derepression of an NAD-Linked Dehydrogenase That Serves an Escherichia coli Mutant for Growth on Glycerol. ***Journal of Bacteriology***, 152: 1001-1007.

Thar, R. and Kuhl, M. 2003. Bacteria are not too small for spatial sensing of chemical gradients: an experimental evidence. ***Proceedings of the National Academy of Sciences of the United States of America***, 100(10): 5748-5753.

Tsukaguchi, H., Shayakul, C., Berger, U.V., Mackenzie, B., Devidas, S., Guggino, W.B., van Hoek, A.N. and Hediger, M.A. 1998. Molecular characterization of a broad selectivity neutral solute channel. ***Journal of Biological Chemistry***, 273(38): 24737-24743.

Tyerman, S., Niemietz,C. and Bramley,H. 2002. Plant aquaporins: multifunctional water and solute channels with expanding roles. ***Plant, Cell and Environment***, 25: 173–194.

Unger, V.M. 2000. Fraternal twins: AQP1 and GlpF. ***Nature Structural Biology***, 7(12): 1082-1084.

Vassella, E., Den Abbeele, J.V., Butikofer, P., Renggli, C.K., Furger, A., Brun, R. and Roditi, I. 2000. A major surface glycoprotein of trypanosoma brucei is expressed

transiently during development and can be regulated post-transcriptionally by glycerol or hypoxia. ***Genes & Development***, 14(5): 615-626.

Verkman, A. 1989. Mechanisms and regulation of water permeability in renal epithelia. ***American Journal of Physiology***, 257(5 Pt 1):: 837-850.

Verkman, A. S. 2000. Physiological importance of aquaporins: lessons from knockout mice. ***Current Opinion in Nephrology & Hypertension***, 9(5): 517-522.

Verkman, A. S. 2002. Aquaporin water channels and endothelial cell function. ***Journal of Anatomy***, 200(6): 617-627.

Vickers, T.J., Greig, N. and Fairlamb, A.H. 2004. A trypanothione-dependent glyoxalase I with a prokaryotic ancestry in Leishmania major. ***Proceedings of the National Academy of Sciences of the United States of America***, 101(36): 13186-13191.

Wagner, C.A., Friedrich, B., Setiawan, I., Lang, F. and Broer, S. 2000. The use of *Xenopus laevis* oocytes for the functional characterization of heterologously expressed membrane proteins. ***Cellular Physiology and Biochemistry***, 10: 1-12.

Wallace, I.S. and Roberts, D.M. 2004. Homology modeling of representative subfamilies of Arabidopsis major intrinsic proteins. Classification based on the aromatic/arginine selectivity filter. ***Plant Physiology***, 135(2): 1059-1068.

Walsh, M., Smits, H., Scholte, M. and van Dam, K. 1994. Affinity of glucose transport in *Saccharomyces cerevisiae* is modulated during growth on glucose. ***Journal of Bacteriology***, 176(4): 953-958.

Wang, J.Y. and Cho, S.K. 2004. Coordination of repair, checkpoint, and cell death responses to DNA damage. ***Advances in Protein Chemistry***, 69: 101-135.

Wang, Y., Schulten, K. and Tajkhorshid, E. 2005. What makes an aquaporin a glycerol channel? A comparative study of AqpZ and GlpF. ***Structure***, 13(8): 1107-1118.

Webster, J., Urban, C., Berbaum, K., Loske, C., Alpar, A., Gartner, U., de Arriba, S.G., Arendt, T. and Munch, G. 2005. The carbonyl scavengers aminoguanidine and tenilsetam protect against the neurotoxic effects of methylglyoxal. ***Neurotoxicity Research***, 7(1-2): 95-101.

WHO. 2001. African trypanosomiasis or sleeping sickness.,(Fact sheet N°259).

Wiemer, E.A., Michels, P.A. and Opperdoes, F.R. 1995. The inhibition of pyruvate transport across the plasma membrane of the bloodstream form of Trypanosoma brucei and its metabolic implications. ***Biochemical Journal***, 312: 479-484.

Wille, U., Schade, B. and Duszenko, M. 1998. Characterization of glycerol uptake in bloodstream and procyclic forms of *Trypanosoma Brucei*, ***European Journal of Biochemistry***, 256: 245-250.

Wysocki, R., Chery, C.C., Wawrzycka, D., Van Hulle, M., Cornelis, R., Thevelein, J.M. and Tamas, M.J. 2001. The glycerol channel Fps1p mediates the uptake of arsenite and antimonite in Saccharomyces cerevisiae. ***Molecular Microbiology***, 40(6): 1391-1401.

Xu, C., Zhou, T., Kuroda, M. and Rosen, B.P. 1998. Metalloid resistance mechanisms in prokaryotes. ***Journal of Biochemistry***, 123(1): 16-23.

Yang, B., Ma, T. and Verkman, A.S. 2001. Erythrocyte water permeability and renal function in double knockout mice lacking aquaporin-1 and aquaporin-3. ***Journal of Biological Chemistry***, 276(1): 624-628.

Yasui, M. 2004. Molecular Mechanisms and Drug Development in Aquaporin Water Channel Diseases: Structure and Function of Aquaporins. ***Journal of Pharmacological Sciences***, 96: 260 – 263.

Yasui, M., Kwon, T. H., Knepper, M. A., Nielsen, S. and Agre, P. 2000. Aquaporin-6: An intracellular vesicle water channel protein in renal epithelia. ***Journal of the American Society of Nephrology***, 11(4): 764-777.

Zardoya, R. 2005. Phylogeny and evolution of the major intrinsic protein family. ***Biology of the Cell***, 97(6): 397-414.

Zardoya, R., Ding, X., Kitagawa, Y. and Chrispeels, M. J. 2002. Origin of plant glycerol transporters by horizontal gene transfer and functional recruitment. ***Proceedings of the National Academy of Sciences of the United States of America***, 99(23): 14893-14896.

Zardoya, R. and Villalba, S. 2001. A phylogenetic framework for the aquaporin family in eukaryotes. ***Journal of Molecular Evolution***, 52(5): 391-404.

My academic teachers

Rafael Briceño

Juan L Concepcion

Michael Duszenko

Pablo Djabayan

Victor Jiménez Cid

Dieter Mecke

Teresa Meza

Beatriz Nieves

Samuel Segnini

Dario Simarro

Lebenslauf

Angaben zur Person:

Name:	Néstor Luis Uzcátegui Araujo
Geburtsdatum:	27. November 1969, in Barquisimeto
Familienstand:	verheiratet
Staatsangehörigkeit:	Venezolaner

Schule und Studium:

1987	Abschluss-Abitur, Instituto Diocesano Barquisimeto, Barquisimeto-Venezuela
10/1988-02/1994	Studium an der Universidad de los Andes [ULA] (Licenciado en Bioánalisis), Mérida-Venezuela
01/1993-01/1994	Diplomarbeit an der Universidad de los Andes, Facultad de ciencias. Prof. Juan L. Concepción
Seit 01/1995	Lehrtätigkeit am Universidad Central de Venezuela, Caracas-Venezuela
10/2001-03/2002	Vorbereitung auf die Deutsche Sprach Prüfung für den Hochschulzugang (DSH) am Goethe Institut, Mannheim. (bestanden)
Seit 04/2002	Promotion am Interfakultären Institut für Biochemie der Universität Tübingen, AG molekulare Parasitologie, Prof. Dr. Michael Duszenko „Aquaglyceroporins of *Trypanosoma brucei* a potential target for chemotherapy: Cloning, heterologous expression, biochemical characterization and localization".
10/2002	Prüfung zur Anerkennung als Diplom Biochemiker bei den Professoren D. Mecke und H. Probst

Veröffentlichungen:

Figarella K, **Uzcátegui N**, García N, Silva N, Camacho N, Ponte-Sucre A. Molecular pharmacology of chemo-resistant Leishmania, Archivos Venezolanos de Farmacología y Terapeutica ISSN 0798-0264, 22(1), 2003.

Uzcátegui NL, Szallies A, Pavlovic-Djuranovic S, Palmada M, Figarella K, Boehmer C, Lang F, Beitz E, Duszenko M. Cloning, heterologous expression and characterization of three aquaglyceroporins from Trypanosoma brucei. Journal of Biological Chemistry, 279(41): 42669-42676, 2004.

Figarella K, Rawer M, **Uzcátegui NL**, Kubata B, Lauber K, Madeo F, Wesselborg S and Duszenko M. Prostaglandin D_2 induces programmed cell death in Trypanosoma brucei bloodstream form. Cell Death and Differentiation, 12(4):335-346, 2005.

Uzcátegui NL/ Figarella K (Joint first authors), Camacho A and Ponte-Sucre A. Substrate preferences and glucose uptake in glibenclamide-resistant Leishmania parasites. Comparative Biochemistry and Physiology, 140:395-402, 2005.

Meza N, Rossi N, Galeazzi T, Sanchez N, Colmenares F, Medina O, **Uzcátegui NL**, Alfonzo N, Arango C, Urdaneta H. Prevalence of Cysticercosis in Chronic psychiatric inpatients from a Venezuelan community. American Journal of Tropical Medicine and Hygiene, 73:504-9, 2005.

Figarella K, **Uzcátegui NL**, Beck A, Schoenfeld C, Kubata BK, Lang F, and Duszenko M. Caspase-independent programmed cell death in *Trypanosoma brucei* by prostaglandins of J series involves oxidative stress**.** Cell Death and Differentiation, feb 3 (Epub ahead of print) 2006.

Uzcátegui NL, Duszenko M. Structure and Function of Aquaglyceroporins from Trypanosoma brucei: possible target for chemotherapy. In: Protein Structure Function Relationship, Proc. 8th International Symposium, and University of Karachi, Pakistan, in Press. 2006

Zeuthen T, Wu B, Pavlovic-Djuranovic S,Holm L H, **Uzcátegui NL**, Duszenko M, Kun JF, Schultz JE, Beitz E. Protozoan parasite aquaglyceroporins from *Plasmodium falciparum, Toxoplasma gondii* and *Trypansoma brucei* pass ammonia. Accepted for publication in Molecular Microbiology.

Uzcátegui NL, Bassarak, B, Figarella K, Lang F, Mukhopadhyay R, Duszenko M. As(III) and Sb(III) uptake by Aquaglyceroporins from *Trypanosoma brucei*. Manuscript in preparation.

Uzcátegui NL, Carmona-Gutiérrez D, Lang F, Figarella K, Duszenko M. Dihydroxyacetone inhibits proliferation of *Trypanosoma brucei* bloodstream form via G2/M cell cycle arrest. Manuscript in preparation.